1-1-2019

Effect Of Sulfobutyl Ether **B**-Cyclodextrins On Oral And Dermal Pharmacokinetics Of Drugs

Vijay Kumar Shankar

EFFECT OF SULFOBUTYL ETHER β-CYCLODEXTRINS ON ORAL AND DERMAL PHARMACOKINETICS OF DRUGS

A Dissertation
submitted in partial fulfillment of requirements
for the Doctor of Philosophy degree in pharmaceutical sciences
in the Department of Pharmaceutics and drug delivery
The University of Mississippi

By
Vijay Kumar Shankar
December 2019

ABSTRACT

In drug discovery, demand for drug candidates with increased potency has led to synthesis of lipophilic molecules to enhance their binding to target. This has resulted in approvals of large number of drugs having poor biopharmaceutical properties. Aqueous solubility of drugs can be increased by various techniques, the simple and most commonly employed technique is by preparation of inclusion complex using cyclodextrins. The Sulfobutyl ether β-cyclodextrin (SBE-β-CD) was used to enhance the aqueous solubility of progesterone and silymarin.

Progesterone is a female sex hormone, and it is crucial to maintain a basal level of 10-20 ng/mL to treat luteal phase deficiency or estrogen dominance and to maintain normal physiological functions of progesterone. The clinical trials of available oral progesterone products have shown high interpatient and intrapatient variability, attributed to progesterone's low aqueous solubility and resulting in sub-optimal or excessive plasma levels. The solubility of progesterone in water was enhanced by SBE-β-CD, progesterone in 100 mM SBE-β-CD was ~2000-fold more soluble than its intrinsic solubility. The optimized SBE-β-CD formulation increased *ex-vivo* rat intestinal permeation of progesterone and rat oral bioavailability of progesterone in SD rats compared to progesterone API.

Silymarin is an extract of Milk Thistle, major constituents are taxifolin, silychristin, silydianin, silybin A, silybin B, isosilybin A and isosilybin B. The *in vitro*, preclinical and clinical studies have demonstrated silymarin possesses hepatoprotective, anticancer, hypocholesterolemic, cardioprotective effect and dermatological beneficial effect (treatment of UV induced erythema,

melanoma, non-melanoma skin cancer, rosacea, melasma, vitiligo and psoriasis) both individually and collectively. Solubility enhancement of silymarin constituent is utmost important to increase bioavailability and to improve drug developability property. The solubility of silymarin in water was enhanced by SBE-β-CD by conventional and heating method, heating method was found to be more efficient with less time consuming. The oral bioavailability and tissue exposure of silymarin constituents were increased on oral administration of SBE-β-CD–silymarin complex compared to silymarin suspension. To treat dermal ailments SBE-β-CD–silymarin cream was developed and optimized to stabilize the cream and increase the skin penetration and permeation of all silymarin constituents across the skin.

DEDICATION

Dedicated to my parents and siblings

LIST OF ABBREVIATIONS

β-CD	β-cyclodextrin
A_L	Linear phase solubility curve
A_N	Negative deviation from linear phase solubility curve
API	Active pharmaceutical ingredient;
ATR	Attenuated total reflectance;
AUC	Area under the curve
BCS	Biopharmaceutical classification system
CE	Complexation efficiency
$C_{max,}$	Maximum plasma concentration
CMC	Critical micellar concentration
CSA 50	Cetostearyl alcohol 50
CSA 70	Cetostearyl alcohol 70

DMSO-d_6	Deuterated dimethyl sulfoxide
DSC	Differential scanning calorimetry
EDTA	Ethylene diamine tetra acetic acid
F_{abs}	Absolute bioavailability
FASSGF	Fasted state simulated gastric fluid
FASSIF	Fasted state simulated intestinal fluid
FESSGF	Fed state simulated gastric fluid;
FESSIF	Fed state simulated intestinal fluid
FTIR	Fourier transform infrared spectroscopy
GI	Gastrointestinal
GMS	Glycerol monostearate
$^{1}H/^{13}C$ NMR	Proton/carbon nuclear magnetic resonance
HP-β-CD	Hydroxy-2-propyl-β-cyclodextrin
HPLC	High performance liquid chromatography

HQC	High quality control
IDR	Initial dissolution rate
i.p.	Intraperitoneal
IS	Internal standard
ISA	Isosilybin A
ISB	Isosilybin B
IV	Intravenous
$K_{1:1}$	Stability constants
Ke	Elimination rate constant
LLMOD	Large-scale low-mode method
Log P	Partition coefficient
Log D	Distribution coefficient
LPD	Luteal phase deficiency
LQC	Low quality control

M-β-CD	Methyl-β-cyclodextrin
MCS	Macrocycle conformational sampling
MCSE	Macrogol cetostearyl ether 20
MD	Molecular dynamics
MDT	Mean dissolution time
MDR	Mean dissolution rate
MM-GBSA	Molecular mechanics-generalized Born surface area
MQC	Medium quality control
NADPH	Nicotinamide adenine dinucleotide phosphate
NCE	New chemical entities
NOAEL	No observed adverse effect levels
NVT	Constant number of particles volume and temperature
NPT	Constant number of particles pressure and temperature
O/W	Oil in water

OD	Octyldodecanol
OPLS	Optimized potential for liquid simulations
P_{app}	Apparent permeability coefficient
PAMPA	Parallel artificial membrane permeability assay
PDB	Protein Data Bank
PEG	Polyethylene glycol
PG	Propylene glycol
PRCG	Polak-Ribière conjugate gradient
PO	Per os (oral administration)
QC	Quality control
RMSD	Root-mean-square deviation
S_0	Drug solubility in deionized water
SA	Silybin A
SB	Silybin B

SBE-β-CD	Sulfobutyl-ether-β-cyclodextrin aka CAPTISOL®
SC	Silychristin
SD	Silydianin
SD rats	Sprague Dawley rats
SGF	Simulated gastric fluid
SIF	Simulated intestinal fluid
Sint	Intercept of phase solubility curve
SP	Standard precision
pKa	Dissociation constant
TIP3P	Three-site transferrable intermolecular potential
$T_{max,}$	Time of peak concentration
TPGS	D-α-tocopheryl polyethylene glycol succinate
TX	Taxifolin
U_{CD}	Cyclodextrin utility number

UPDGA	Uridine diphosphate glucuronic acid
ZnSe	Zinc selenide

ACKNOWLEDGEMENTS

I would like to express my deep and sincere gratitude to my advisor, Dr. S. Narasimha Murthy for his support, patience and encouragement throughout my research work. His motivation and support at all the time during my research helped me learn many aspects required to achieve my research goals. I am ever grateful for all his kind support.

I would like to take this opportunity to express my sincere thanks to Dr. Michael A. Repka, Dr. Seongbong Jo and Dr. Samir Ross for accepting my request, and providing valuable suggestions during my prospectus that I believe have improved my overall work. It was kind of Ms. Debbie P. King for helping me with all the departmental procedures and making sure that the things necessary for the projects are provided on time.

I owe a great thanks to Anitha and Srinivas for their valuable suggestions and helping me in completion of various projects successfully. I would like to acknowledge my senior lab members Dr. Avadhesh, Dr. Abhijeet and Dr. Murali for assisting me to learn research basics in our lab and their continuing support throughout my projects. I also thank my group members Purnendu, Dr. Srinath Rangappa, Dr. Srinatha Anegundha, Marey, Apoorva, Abhishek and all graduate students of pharmaceutics and drug delivery department for their support in various projects.

I would like to acknowledge the help of Dr. Robert Doerksen, Dr. Pankaj Pandey, Dr. Mika Jeakabsons, Dr. H. N. Shivakumar (Institute for Drug Delivery and Biomedical Research, Bangalore, India), Dr. Suresh Bhandari, Dr. Vo, Sandeep Sarabu, Nagireddy, Bhavani Prasad

Vinjamuri, and Dr. RK for their assistance and support to conduct my various projects successfully.

I would like to thank Vimal, Nagi, Anitha, Sushmitha, Neeraja, Tahir, Tabish, Adal, Kuldeep, Abhisheak, Abhsihek, Srinivas, Sandeep, Raman, Karthik, Narender, Suresh, Preet, Dr. Vish, Rama Aunty, Dinesh and Praveen for making Oxford life lovable and cherishing.

Above all, I owe my loving thanks to my father (Shankar), mother (Gurumani), brother (Manju) and sister (Roopa) for their support and encouragement at every moment of life. My special gratitude to brother-in-law (Murali), sister-in-law (Keerthi), nephew (Sarvesh and Lohith), and niece (Dhiya and Jishna) for their loving and unconditional support.

I gratefully acknowledge Ligand Pharmaceuticals (San Diego, CA) and other funding sources that made my PhD work possible.

TABLE OF CONTENTS

LIST OF TABLES

Chapter-2

LIST OF FIGURES

Chapter-2

Chapter-3

Chapter-4

CHAPTER 1

Introduction

In drug discovery, demand for drug candidates with increased potency has led to synthesis of lipophilic molecules to enhance their binding to targets (1). This has resulted in approvals of large number of drugs having poor biopharmaceutical properties. Approximately 90% of the drug in developmental stages and over 40% of approved drugs have poor aqueous solubility (2). Drug solubility in GI fluid and permeation across GI barrier are two crucial factors governing the oral bioavailability of a drug, drugs as to be dissolved in GI fluid to permeate across the GI membrane (3). Drugs with poor aqueous solubility are variably absorbed leading to erratic bioequivalence (4). The Biopharmaceutical Classification System (BCS) categorizes drugs intended for oral administration based on their solubility and permeability. The drugs are classified into four classes class I (high solubility and permeability), class II (low solubility and low permeability), class III (high solubility and low permeability) and class IV (low solubility and permeability) drugs (5). Solubility enhancement of BCS class II drug is utmost important to increase bioavailability (4) and to improve drug developability property(3).

The aqueous solubility of lipophilic drugs is increased by employing different techniques like particle size reduction (micronization, nanosuspension), solid dispersion, super critical fluid processing, salt formation, micellar solubilization, solubilizers, hydrotrophy and cyclodextrin inclusion complex preparation (3). In recent years, β-cyclodextrins have been widely used for increasing aqueous solubility of lipophilic drugs (6,7).

Cyclodextrins are macrocyclic oligosaccharides which take on a well-defined shape containing a lipophilic cavity and hydrophilic groups on the outer surface. The lipophilic cavity can accommodate a lipophilic drug and because of the solubilizing capability of the hydrophilic groups the cyclodextrin can significantly enhance the aqueous solubility of otherwise insoluble drugs (1).

There are three main types of cyclodextrins categorized based on number of α-(1,4)-linked glycosyl units. The α-cylodextrin, β-cyclodextrin (β-CD) and γ-cyclodextrin are composed of six, seven and eight α-(1,4)-linked glycosyl units, respectively (8). β-CD is less toxic and have higher aqueous solubility compared to α-cylodextrin and γ-cyclodextrin, respectively. β-CD bind to and partially surround lipophilic drugs and hence increase their aqueous solubility. The native and modified β-CD are most extensively used to enhance aqueous solubility of drugs. Whereas β-CD itself is relatively poorly water soluble, the modified β-CD such as methyl-β-cyclodextrins (M-β-CD), hydroxy-2-propyl-β-cyclodextrins (HP-β-CD) and sulfobutyl-ether-β-cyclodextrins (SBE-β-CD, known as Captisol^{TM}) have very high solubility (7,8). β-CD and M-β-CD upon intravenous dosing are reported to cause nephrotoxicity (8,9). Due to safety concerns, the use of M-β-CD (<10%) is limited to nasal and pulmonary drug delivery systems. The NOEL (no observed adverse effect levels) reported for HP-β-CD and SBE-β-CD on oral administration in rats are up to 500 and 3600 mg/kg/day, respectively (9,10). The NOAEL of SBE-β-CD in rats is 7.2 times greater than NOAEL of HP-β-CD. Hence, SBE-β-CD effects on oral and dermal pharmacokinetics of BCS class II drugs were evaluated.

CHAPTER 2

Optimization of Sulfobutyl-Ether-β-Cyclodextrin Levels in Oral Formulations to Enhance Progesterone Bioavailability

1. Introduction

Progesterone is a female sex hormone produced by the adrenal gland and corpus luteum (during the luteal phase)(11). Luteal phase deficiency (LPD) is a state of deficient progesterone levels in which the patient is unable to maintain and regulate a normal menstrual cycle, pregnancy and embryogenesis (12). It is essential to maintain a basal level of 10-20 ng/mL (11) of progesterone to treat LPD and estrogen dominance (12). Progesterone is prescribed for assisted reproductive technology cycles (*in vitro* fertilization), to support implantation in early pregnancy, to control anovulatory bleeding, to prevent recurrent pregnancy loss and for treatment of secondary amenorrhea (13). Progesterone is also used in prevention of endometrial hyperplasia in non-hysterectomized postmenopausal women on hormone replacement therapy receiving conjugated estrogen tablets (14).

Progesterone is a BCS class II steroidal drug (6) with a reported aqueous solubility of 0.007 mg/mL and low oral bioavailability (13). Most marketed oral progesterone products are micronized and suspended in peanut oil base (e.g., Prometrium®) to increase intestinal absorption, and consequently bioavailability and efficacy (15). The clinical trials of Prometrium® showed high interpatient and intrapatient variability in C_{max} and $AUC_{(0\text{-}10h)}$, indicating variation in oral drug

absorption resulting in sub-optimal or excessive plasma levels of progesterone (13). The most common alternative for progesterone is synthetic progestins (medroxyprogesterone acetate), but these are associated with adverse effects (like fluid retention, acne, rashes, weight gain and depression) due to their affinity to bind glucocorticoid, androgen, and mineralocorticoid receptors (16). An alternate approach to enhance the potential efficacy of progesterone with increased oral bioavailability and having low interpatient and intrapatient variability is to develop a formulation to enhance its aqueous solubility (13).

Native and modified β-cyclodextrins are most commonly used because of their large cavity size compared to α-cyclodextrins, which enable them to bind to and partially surround lipophilic drugs and hence increase their aqueous solubility. β-CD and M-β-CD upon intravenous dosing are reported to cause nephrotoxicity(8,9). Due to safety concerns, the use of M-β-CD (<10%) is limited to nasal and pulmonary drug delivery systems. The no observed adverse effect levels (NOAEL) reported for HP-β-CD and SBE-β-CD on oral administration in rats are up to 500 and 3600 mg/kg/day, respectively(9,10). Hence, HP-β-CD and SBE-β-CD are the cyclodextrin derivatives most extensively evaluated for solubility enhancement of active pharmaceutical ingredients for oral administration.

There are previously reported phase solubility studies of progesterone in SBE-β-CD (17) and HP-β-CD (17,18), in which the solubility of progesterone was found to be 9.9 and ~7 mg/mL in 100 mM of SBE-β-CD and 60 mM of HP-β-CD, respectively (17). The studies on evaluating the solubility/permeability interplay of progesterone with cyclodextrins have shown that higher concentrations of HP-β-CD in the formulation decrease the permeability of progesterone across Caco2 cell monolayers, in PAMPA, in the rat jejunal model (6) and in the single pass intestinal perfusion rat model (19). Studies in rat intestine have shown that sodium taurocholate and lecithin

displace progesterone from HP-β-CD–progesterone complexes (19). The present study is designed to evaluate the influence of gastric fluid contents on the SBE-β-CD–progesterone complex and to study the effect of SBE-β-CD levels on *ex vivo* rat intestinal permeability and rat oral bioavailability of the lipophilic drug progesterone.

The SBE-β-CD–progesterone equilibrium complex mixtures were prepared and isolated, and then characterized by differential scanning calorimetry (DSC), Fourier transform infrared spectroscopy (FTIR), proton and carbon nuclear magnetic resonance (NMR) spectroscopy and computational methods. The isolated SBE-β-CD–progesterone complex mixture solubility in simulated gastrointestinal fluid and displacement of progesterone by bile salts in water were evaluated. The optimal levels of SBE-β-CD required to prevent displacement of progesterone by the contents present in fasted state simulated intestinal fluid (FASSIF) and fed state simulated intestinal fluid (FESSIF) were determined by employing a simple *in vitro* experiment. *Ex vivo* permeation studies were performed to evaluate permeation of progesterone across rat intestine and the effect of excess SBE-β-CD on the permeation. The oral bioavailability of progesterone, the isolated SBE-β-CD–progesterone complex mixture, and the isolated SBE-β-CD–progesterone complex mixture with excess SBE-β-CD was evaluated in Sprague Dawley rats. To evaluate the potential utility of this isolated SBE-β-CD–progesterone complex mixture in human, *in vitro* dissolution of progesterone API and the isolated SBE-β-CD–progesterone complex mixture filled into capsules were evaluated in water, simulated gastric fluid (SGF) and simulated intestinal fluid (SIF).

2. Materials and Methods

2.1 Chemicals and reagents

Progesterone, pepsin, phosphate buffered saline and L-α-phosphatidylcholine (lecithin) were purchased from Sigma Aldrich, Inc., USA. SBE-β-CD (Captisol®) was provided by Ligand Pharmaceuticals, Inc, USA, who in part funded the study. Sodium taurocholate was purchased from Alfa Aesar, USA. Euthasol® (pentobarbital sodium and phenytoin sodium) solution was procured from Virbac, USA. Methocel E15 Premium EL (hydroxypropyl methyl cellulose) was purchased from the Dow Chemical company, USA. The HPLC grade solvents acetonitrile, methanol, dibasic potassium phosphate, dibasic sodium phosphate, glacial acetic acid, hydrochloric acid, sodium hydroxide, sodium chloride, sodium acetate, ortho-phosphoric acid and Milli Q water were of research grade and were used without further purification.

2.2 Phase solubility studies

The solubility enhancement of progesterone by complexation with SBE-β-CD was evaluated by adding excess amounts of progesterone to different concentrations of SBE-β-CD (10, 20, 40, 60, 80 and 100 mM) in Milli-Q® water (Higuchi and Connors method) (20). Samples were kept shaking at 25 °C for 3 days and at equilibrium samples were filtered using a Millipore (0.45 μm) syringe filter. The filtrate was analyzed using HPLC to evaluate the saturation solubility of progesterone in SBE-β-CD. Phase solubility study curves were used to calculate complexation efficiency (CE) and stability constants ($K_{1:1}$).

2.3 Characterization of the isolated SBE-β-CD–progesterone equilibrium complex mixture

The complex was prepared by adding excess progesterone (~35 to 40 mg/mL) to 100 mM SBE-β-CD in Milli-Q® water. Samples were kept shaking at 25 °C for 3 days and at equilibrium samples were filtered using a Millipore (0.45 μm) syringe filter. These samples were lyophilized and characterized using DSC, FTIR and NMR. The complex was also studied by computational methods.

2.3.1 Differential scanning calorimetry

The isolated SBE-β-CD–progesterone complex mixtures were characterized with a DSC 25 Series, TA instrument equipped with Pyris software (Shelton, CT, USA). Approximately 3-3.5 mg of progesterone API, of a physical mixture of SBE-β-CD and progesterone, and of the lyophilized complex mixture were hermetically sealed in a crimped aluminum pan and heated from 25 °C to ~200 °C, at a heating rate of 10 °C/min to obtain a DSC thermogram.

2.3.2 Fourier transform infrared spectroscopy

FTIR studies were conducted on an Agilent Technologies Cary 660 (Santa Clara, CA.). The bench was equipped with an ATR (Attenuated Total Reflectance MIRacle™, Pike Technologies, Madison, WI) which was equipped with a single bounce diamond coated ZnSe internal reflection element. FTIR spectroscopic analysis was performed on the prepared complex by scanning over the range from 400 to 4000 cm^{-1} (21).

2.3.3 Nuclear Magnetic Resonance studies

The ^{1}H-NMR spectrum of progesterone, the isolated SBE-β-CD–progesterone complex mixture, the physical mixture of SBE-β-CD and progesterone, and pure SBE-β-CD dissolved in DMSO-d_6:D_2O (2:1) were recorded on a Bruker Advance DRX 500 MHz FT NMR instrument at 298 K. The ^{13}C NMR spectra of progesterone and of the isolated SBE-β-CD–progesterone complex mixture dissolved in DMSO-d_6 were also obtained. The spectra were processed with software Topspin 3.2.

2.3.4 Molecular modeling

The computational study utilized the Maestro 10.5 program from the Schrödinger Software Suite. The 3D X-ray structure of β-CD was retrieved from the Protein Data Bank (PDB ID:1JL8) (22), and was modified to produce four models of cyclodextrin isomers for SBE-β-CD, in an approach similar to that reported by Jain *et al.* (2011) (23) to represent the possible structural arrangements of sulfobutyl ether groups in the SBE-β-CD structure (Fig. 1). Isomer 1 was prepared by placing all of its sulfobutyl ether groups on the positions of primary hydroxyl groups (6-OH on the glucose subunits) of β-CD whereas Isomers 2 and 3 were prepared by attaching three sulfobutyl ether groups to primary hydroxyl groups and four to secondary hydroxyl groups (2-OH on the glucose subunits) of β-CD. The final Isomer 4 was constructed by placing one sulfobutyl ether group on a primary hydroxyl group (6-OH), three on secondary 2-OH hydroxyl groups, and three on secondary 3-OH hydroxyl groups (3-OH) on the glucose subunits of β-CD. This isomer is representative of a general overall distribution found for Captisol (22). The sulfobutyl group was used in its ionized form. We followed similar procedures for conformational search and for docking as reported in our previous publication (23). A conformational search of modified SBE-

β-CD (for all four isomers) was done separately using MacroModel's Macrocycle Conformational Sampling (MCS) (24) tool (Schrödinger), employing the OPLS2005 force field. During the MCS, the large-scale low-mode (LLMOD) method was used with the generalized Born model [GB/SA] solvent treatment. Redundant conformers were eliminated using an RMSD cutoff of 0.75 Å. The energy window for saving structures was set to 10 kcal/mol and the enhanced torsional sampling option was used. The resulting conformers were minimized in the gas phase using the Polak-Ribière Conjugate Gradient (PRCG) method with the OPLS2005 force field. Progesterone was sketched in Maestro (25) and energy-minimized using the LigPrep (26) module of Schrödinger, using the OPLS2005 force field at pH 7.4. Those conformers within an energy window of 7.5 kcal/mol were selected for docking of progesterone, which was done using Glide (Schrödinger) (27), with Standard Precision and flexible ligand sampling. Docking grids were prepared for each conformer of each SBE-β-CD model in such a manner as to ensure that the whole SBE-β-CD structure was labeled as the active site. The binding free energies were calculated on the representative complex after MD simulation using Prime MM-GBSA (28) considering refinement of polar hydrogens only, applying the variable dielectric generalized Born (VSGB) water model. The 2D structures of SBE-β-CD isomers and progesterone are shown in Figs. 1 and 2, respectively.

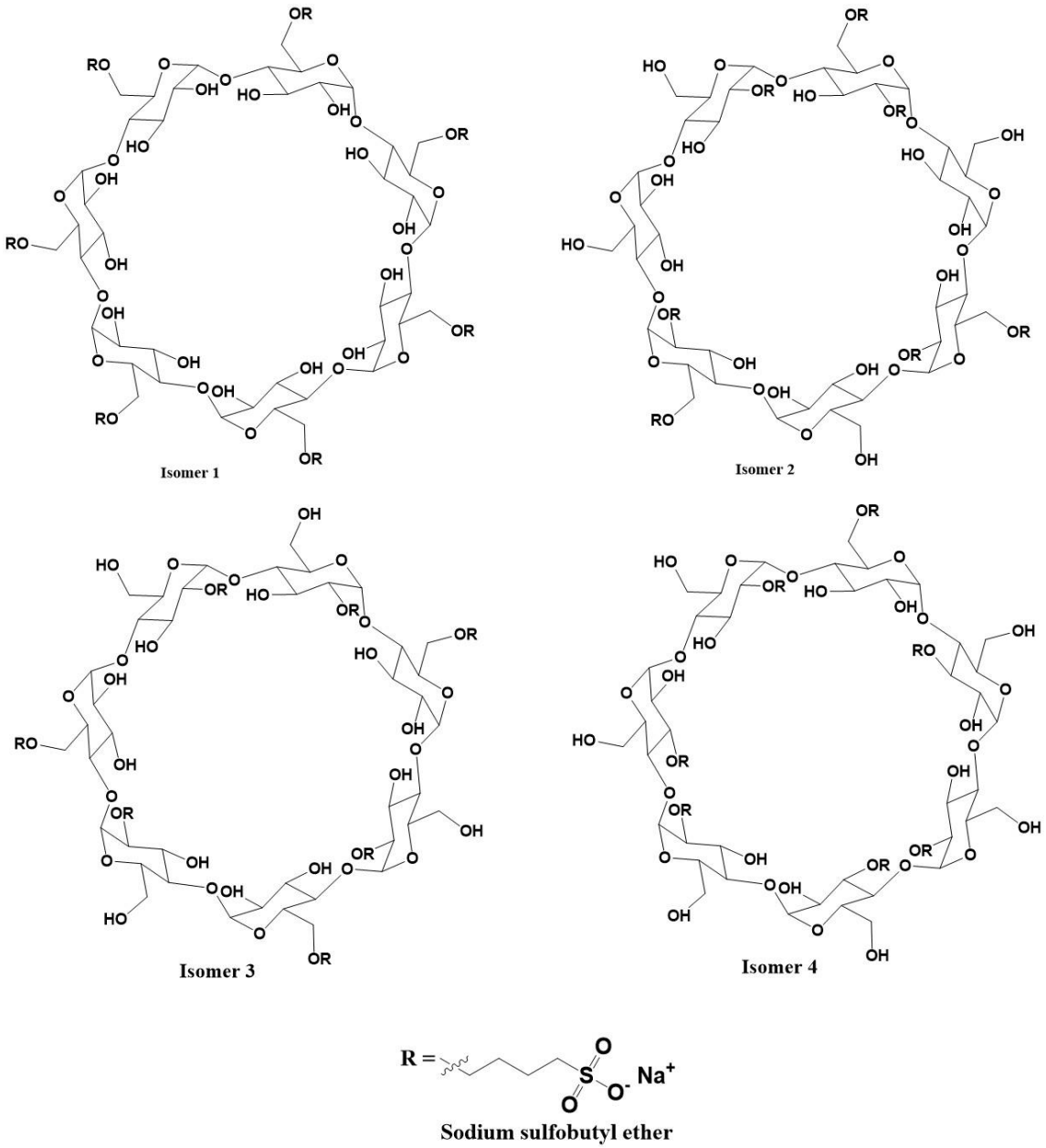

Figure 1. 2D structures of the four different isomeric forms of SBE-β-CD used for computational study.

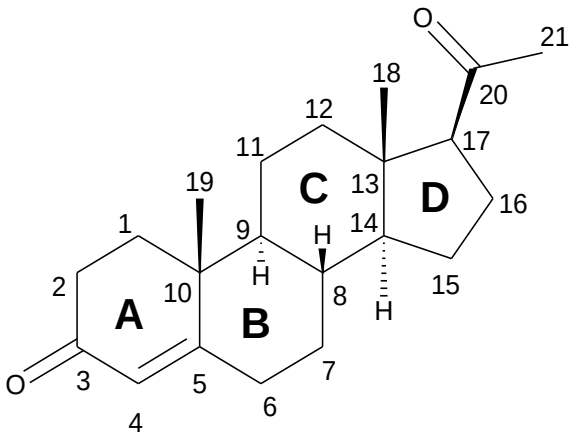

Figure 2. 2D structure of progesterone with atom and ring numbering.

2.3.5 Molecular dynamics simulations

MD simulations for the best complexes of progesterone and SBE-β-CD were carried out using the Desmond (29,30) program. The best complex of each isomer with progesterone (SBE-β-CD–progesterone complex) was solvated with TIP3P (31) waters in a cubic box of side length 10 Å with periodic boundary conditions. The solvated complex was neutralized by adding 7 Na^+ ions, yielding a salt concentration (NaCl) of 0.15 M. The constructed system was simulated with the modified NPT relaxation protocol in Desmond. The protocol involved an initial minimization of the solvent while keeping restraints on the solute, followed by short MD simulations of 12–24 ps in sequential NVT and NPT ensembles with the Langevin thermostat and barostat, respectively. The temperature was maintained at 300 K throughout the production run using the Langevin algorithm and the pressure was isotropically restrained to 1 bar with the Langevin barostat (32). The short-range Coulombic interactions were set to a cut-off value of 9.0 Å using the short-range method, while the smooth particle mesh Ewald method was used for handling long-range Coulombic interactions. After completion of the relaxation protocol, the final production run of 5 ns was carried out on the solvated complex, to avoid any structural artifacts

introduced during system buildup and equilibrium steps. During the simulation, the trajectories were sampled at an interval of 4.8 ps. The structural stability of the complexes was analyzed based on the root-mean-square deviation (RMSD), for which the first frame was used as a reference. The number of intermolecular hydrogen bonds between progesterone and SBE-β-CD was also calculated. Representative complexes were subjected to binding free-energy calculations using Prime MM-GBSA.

2.4 Solubility of progesterone and SBE-β-CD-progesterone complex

The solubility studies were performed in water, fasted state simulated gastric fluid (FASSGF) at pH 1.6, fed state simulated gastric fluid (FESSGF) at pH 5.0, FASSIF at pH 6.5 and FESSIF at pH 5.8. The above mentioned gastrointestinal simulated fluids were prepared using previously published protocols (33). The solubility was evaluated by adding excess progesterone API and 25 mg of isolated SBE-β-CD–progesterone complex mixture in water and simulated gastrointestinal fluids. Samples were kept shaking at 37 °C for 8 h at 100 rpm in a Bio-shaker and samples were filtered using a Millipore (0.45 μm) syringe filter. The filtrate was analyzed using HPLC to evaluate the solubility of progesterone. Note: the filter was determined not to interfere in the determination.

2.5 Effect of sodium taurocholate on SBE-β-CD–progesterone complex

The effect of sodium taurocholate on the solubility of the isolated SBE-β-CD–progesterone complex mixture was evaluated by adding 25 mg of lyophilized complex to different concentrations (2, 4, 6, 8, 10, 12, 14, 16, 18, 20, 30, 40 and 50 mM) of sodium taurocholate. The above samples were kept shaking at 37 °C for 8 h at 100 rpm in a Bio-shaker and samples were

filtered using a Millipore (0.45 μm) syringe filter. The filtrate was analyzed using HPLC to evaluate the solubility of progesterone in the presence of sodium taurocholate.

2.6 Effect of excess SBE-β-CD on sodium taurocholate displacement of progesterone from SBE-β-CD–progesterone complex

The effect of excess SBE-β-CD on sodium taurocholate displacement of progesterone from the isolated SBE-β-CD–progesterone complex mixture was evaluated by adding 25 mg of lyophilized complex to different concentrations (0, 5, 10, 20, 30, 40 and 50 mM) of SBE-β-CD in a solution containing 20 mM sodium taurocholate. The above samples were kept shaking at 37 °C for 8 h at 100 rpm in a Bio-shaker and samples were filtered using a Millipore (0.45 μm) syringe filter. The filtrate was analyzed using HPLC to evaluate the solubility of progesterone in the presence of excess SBE-β-CD and sodium taurocholate.

2.7 *In vitro* simulation to evaluate effect of excess SBE-β-CD on displacement of progesterone from SBE-β-CD–progesterone complex in FASSIF and FESSIF

The effect of excess SBE-β-CD on the solubility of the SBE-β-CD–progesterone complex in FASSIF and FESSIF was simulated *in vitro*. 25 mg of the lyophilized complex and different concentrations of excess SBE-β-CD were added to FESSIF (2.5, 5, 7.5,10, 15 and 20 mM of SBE-β-CD) and FASSIF (1, 2, 3, 4, 5, 7.5 and 10 mM of SBE-β-CD), respectively. The above samples were kept shaking at 37 °C for 8 h at 100 rpm in a Bio-shaker and samples were filtered using a Millipore (0.45 μm) syringe filter. The filtrate was analyzed using HPLC after appropriate dilution to evaluate quantities of solubilized progesterone in samples.

2.8 Stability studies

Lyophilized powder was packed in screw capped HDPE bottles and liquid equilibrium complex mixture were packed in glass vials and stored in a stability chamber under two conditions, at 40 °C and 75% RH and at 25 °C and 60% RH. The stability was assessed by evaluating drug content in samples after 3 and 6 months using HPLC.

2.9 Animal studies

The animal studies were conducted at University of Mississippi, School of Pharmacy, as per the protocol #14-021, approved by the Institutional Animal Care and Use Committee and Animal Welfare Assurance # A3356-01. On arrival, rats were housed in cages at the Animal Care Facility in a temperature and humidity controlled room with a 12:12 h light:dark cycle, and they were provided free access to food and water for one week before use in the experiments.

2.9.1 *Ex vivo* rat intestinal permeation studies

Three male rats (225-250 g) fasted overnight the day before the experiment but had free access to water. On the day of the experiment, the rats were removed from the animal care facility and brought to the procedure lab. The rats were euthanized using an intraperitoneal (i.p.) dose of Euthasol® (150 mg/kg body weight). The abdomen was cut open using an incision of 4-5 cm and the proximal small intestine segment was isolated. The isolated small intestine was slowly flushed with phosphate buffered saline (PBS) at pH 7.4 to remove the intestinal content. The freshly harvested small intestine was cut open to expose the mucosal layer and cleaned by a gentle flow of PBS at pH 7.4 on the mucous surface. Fresh rat intestine was sandwiched between two chambers of a Franz diffusion cell with an active diffusion area of 0.64 cm^2, and the mucosal layer was

exposed to the donor chambers. The resistance across rat intestine was measured using a wave form generator to ensure the integrity of the small intestine segment used for the permeation study. Rat intestine with resistance of ≥3 KΩ.cm^2 was used for permeation studies. To the donor compartment, 500 µL of complex dissolved in water (200 µg), FASSIF (203 µg), FESSIF (213 µg), FASSIF (219 µg) (with excess 5 mM SBE-β-CD), FESSIF 228 µg (with excess 15 mM SBE-β-CD) and the positive control (51 µg) of progesterone dissolved in 0.5% of Brij S20 were used for permeation studies. The receiver chamber was filled with 5 ml of 0.5% of Brij S20, which was stirred at 600 rpm with a 3 mm magnetic stir bar and the temperature was maintained at 37 °C with a circulating water bath. 200 µL samples were withdrawn from the receiver compartment at different time intervals (0, 0.25, 0.5, 1, 2, 4, 6 and 8 h) and each time an equal volume of fresh receiver media was used to replace what was withdrawn. The above samples were transferred into vials and subjected to HPLC analysis.

2.9.2 *In vivo* pharmacokinetic studies

The 16 jugular vein cannulated male rats were used for pharmacokinetic studies. These animals fasted overnight and had free access to water on the day before the experiment. On the day of the experiment, the rats were removed from the animal care facility and brought to the procedure lab. Animals were randomly divided into four different groups of 4 animals each (Group I: PO isolated SBE-β-CD–progesterone complex mixture; Group II: PO progesterone API; Group III: PO isolated SBE-β-CD–progesterone complex mixture with excess SBE-β-CD; and Group IV: progesterone IV). Each oral dose was weighed and filled in Tropac® Capsule 9el (gelatin). The capsules to animals of Groups I, II and III were administered by placing the capsule in the Torpac® capsule gavage needle attached to a dosing syringe. The delivery tube of the dosing syringe was

placed in the mouth and advanced along the lower palate as far as the esophagus for administration. After administration of capsules, 1 mL of water was administered to Group I and II animals, and to Group III animals 1 mL of water containing 15 mM of SBE-β-CD was administered. The dose to Group IV was administered by slow bolus intravenous injection into the tail vein (dosing volume: 2 mL/kg body weight). Approximately 200 µL of blood was drawn into heparin-coated tubes at pre-dose, 0.08, 0.17, 0.33, 0.5, 0.75, 1, 1.5 and 2 h through jugular vein catheter. Plasma was harvested by centrifuging the blood at 4000 rpm for 5 min and stored frozen at 80 ± 10 °C until analysis.

2.10 *In vitro* dissolution studies

The dissolution studies were carried out for progesterone API and the isolated SBE-β-CD–progesterone complex mixture filled in capsules containing the dose equivalent to 100 mg of progesterone. The drug profile was evaluated using a USP dissolution apparatus-I (Hanson SR8, Chatsworth, CA) maintained at 37 ± 0.5 °C and having a shaft rotation speed of 100 rpm. The dissolution test was performed using 900 mL of water, simulated gastric fluid (pH 1.2) and simulated intestinal fluid phosphate buffer (pH 6.8). The samples were withdrawn at 5, 10, 15, 20, 30, 45, 60, 90 and 120 min intervals and the filtrate was analyzed using HPLC after appropriate dilution. The *in vitro* dissolution profile was used to calculate dissolution parameters including mean dissolution time (MDT), mean dissolution rate (MDR) and initial dissolution rate (IDR) (34).

2.11 HPLC analysis

The HPLC method was developed using a Shimadzu UFLC system, equipped with prominence SPD-M20A (Diode array detector). The chromatographic separation of progesterone and the

internal standard (IS) (fenofibrate) was achieved on a Waters XTerra® RP18 5 µm column with dimensions 4.6 mm x 150 mm, which was maintained at ambient room temperature. The binary mobile phase system consisted of methanol:0.1% formic acid in water [80:20 v/v] at a flow rate of 1.2 mL/min. All solubility, *in vitro* and *ex vivo* samples were subjected to HPLC analysis without any further extraction procedure.

2.11.1 *In vivo* sample preparation

A simple protein precipitation method was followed for extraction of progesterone from *in vivo* study samples. To an aliquot of 50 µL of rat plasma sample, an internal standard solution (5 µL of fenofibrate 5 µg/mL) was added and the mixture was vortexed, after which 200 µL of acidified acetonitrile was added and the mixture was again vortexed. The sample was centrifuged at 4 °C for 10 min at 14,000 rpm on a Centrifuge 5430R (Eppendorf, Germany) and the supernatant was transferred to a vial for HPLC analysis. The UV detection wavelength was 242 nm. The compound eluted at 3.9 min and the internal standard eluted at 5.5 min with a total run time of 8 min.

3. Results and Discussion

Progesterone is a BCS Class II drug (6), and hence its oral absorption is limited due to low aqueous solubility. It is crucial to enhance the solubility/dissolution of the drug to overcome its poor and variable bioavailability issues.

3.1 Phase solubility

The phase solubility curve (Fig. 3) demonstrates a linear solubility increase of progesterone as a function of increase in concentration of SBE-β-CD, indicating an A_L type curve (35). The aqueous solubility of progesterone increased 1972 ± 77.8-fold in the presence of 100 mM of SBE-β-CD compared to the intrinsic solubility of progesterone in water (Table 1). The affinity (stability) constants ($K_{1:1}$) Eq. (1) and complexation efficiencies (CE) Eq. (2) of SBE-β-CD–progesterone were calculated based on the parameters of the phase solubility plot.

Equation 1. Stability constant ($K_{1:1}$)

$$\boldsymbol{K_{1:1} = \frac{m}{S_0(1-m)}}$$

Equation 2. Complexation efficiency (CE)

$$\boldsymbol{CE = \frac{m}{(1-m)}}$$

where *m* is the slope of the curve obtained by plotting the drug solubility versus cyclodextrin concentration, determined by linear regression. The *CE* and $K_{1:1}$ of the SBE-β-CD–progesterone complex were 1.65 ± 0.21 and 52,670 ± 4914 M^{-1}, respectively, considering the intrinsic solubility (0.031 mM) for the stability constant calculation. By contrast, the stability constant was determined to be 983 ± 320 M^{-1}, based on the intercept. This huge variation of stability constant could be due to the non-ideality of water as solvent. Poorly soluble drugs show a negative intercept deviation, i.e., S_{int} (intercept of phase solubility curve) < S_0 (drug solubility in deionized water), which leads to overestimation of $K_{1:1}$ when determined from the slope and intercept (18).

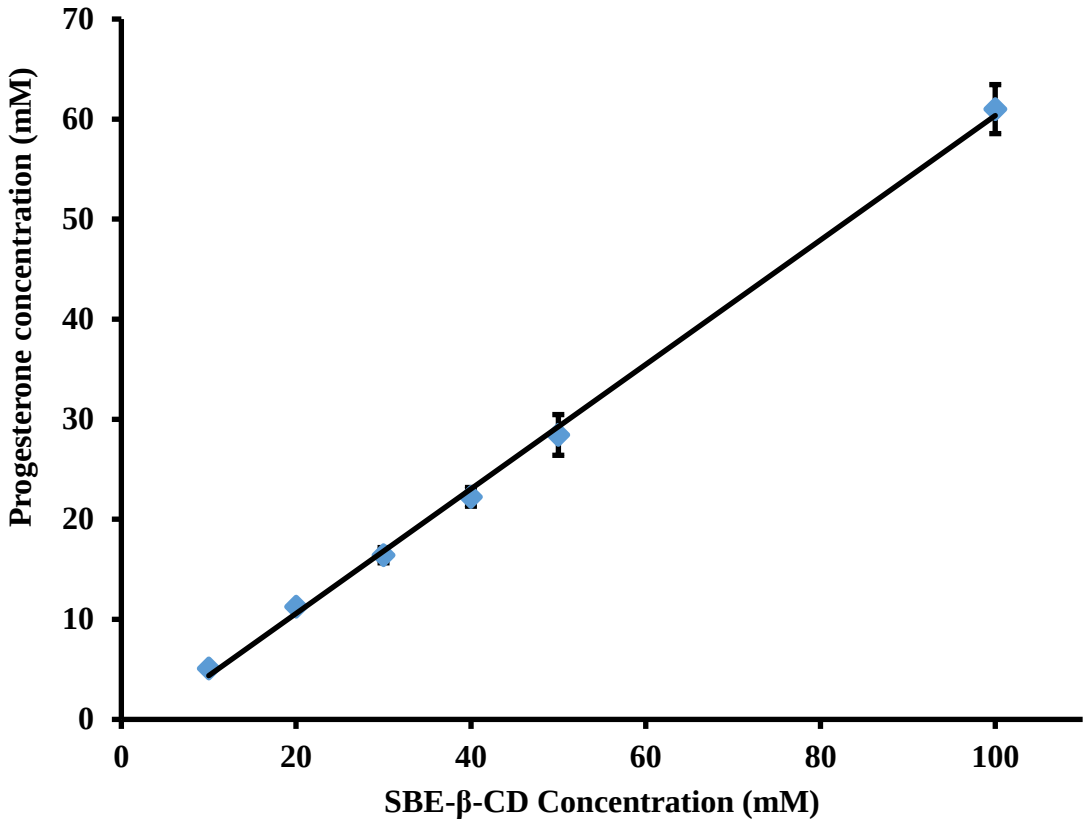

Figure 3. Phase solubility profile of progesterone in SBE-β-CD ($R^2 = 0.9986$).

Table 1. Progesterone solubility enhancement by SBE-β-CD. Each point represents mean ± SD of triplicate values.

SBE-β-CD (mM)	Progesterone (mM ± S.D.)	Number of fold increase in solubility
0	0.03 ± 0.001	1.00 ± 0.00
10	5.08 ± 0.11	161 ± 3.47
20	11.3 ± 0.20	358 ± 6.33
30	16.4 ± 0.76	522 ± 24.1
40	22.2 ± 0.93	734 ± 29.7
50	28.4 ± 2.04	904 ± 64.7
100	61.0 ± 2.45	1972 ± 77.8

3.2 Characterization of SBE-β-CD–progesterone complex

3.2.1 Differential scanning calorimetry

DSC thermograms of progesterone, SBE-β-CD, physical mixtures of progesterone with SBE-β-CD and the SBE-β-CD–progesterone complex are represented in Fig. 4. SBE-β-CD demonstrates no crystallinity. Progesterone API exhibited a sharp melting endotherm at 132 °C confirming its inherent crystalline property. The endothermic peak (melting peak) of progesterone was reduced in the physical mixture but completely disappeared in the complex, indicating interactions between drug and cyclodextrin resulting in the loss of crystallinity (36,37) of progesterone.

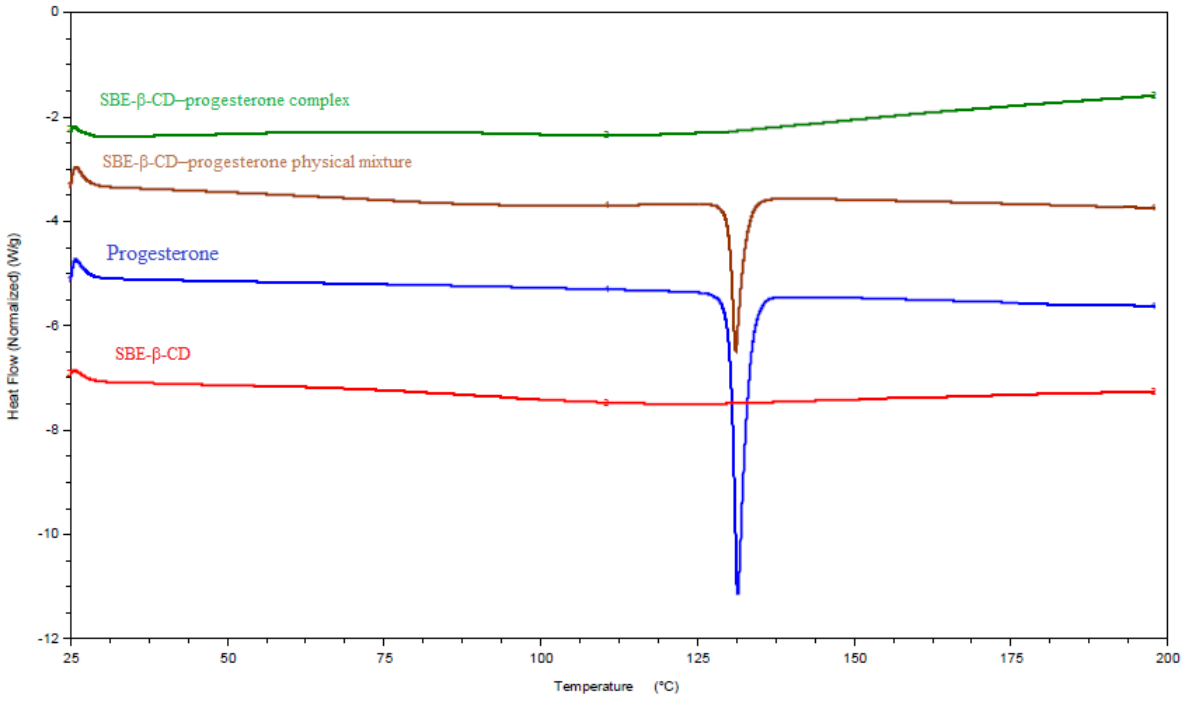

Figure 4. DSC thermograms of SBE-β-CD–progesterone complex, SBE-β-CD, physical mixture and progesterone API.

3.2.2 Fourier Transform Infrared (FTIR) spectroscopy

FTIR has been extensively used to analyze the interaction between cyclodextrins and guest molecules in the solid state. In general, the spectra of inclusion complexes exhibit significant broadening of bands, indicating the formation of inclusion complexes. The FTIR bands of progesterone that correspond to ketone stretches at 1697 (at C3 position) and 1660 (at C20 position) cm^{-1} were disappeared and broadened, respectively in the SBE-β-CD–progesterone complex (Fig. 5). The disappearance of the ketone stretching bands at 1697 may indicate formation of inclusion complexes in which a C3 position participates in a hydrogen bond between SBE-β-CD and progesterone. There were no other significant changes observed in the spectral pattern of SBE-β-CD or progesterone compared to the complex, signifying that there were no other chemical changes involved in the formation of the inclusion complex.

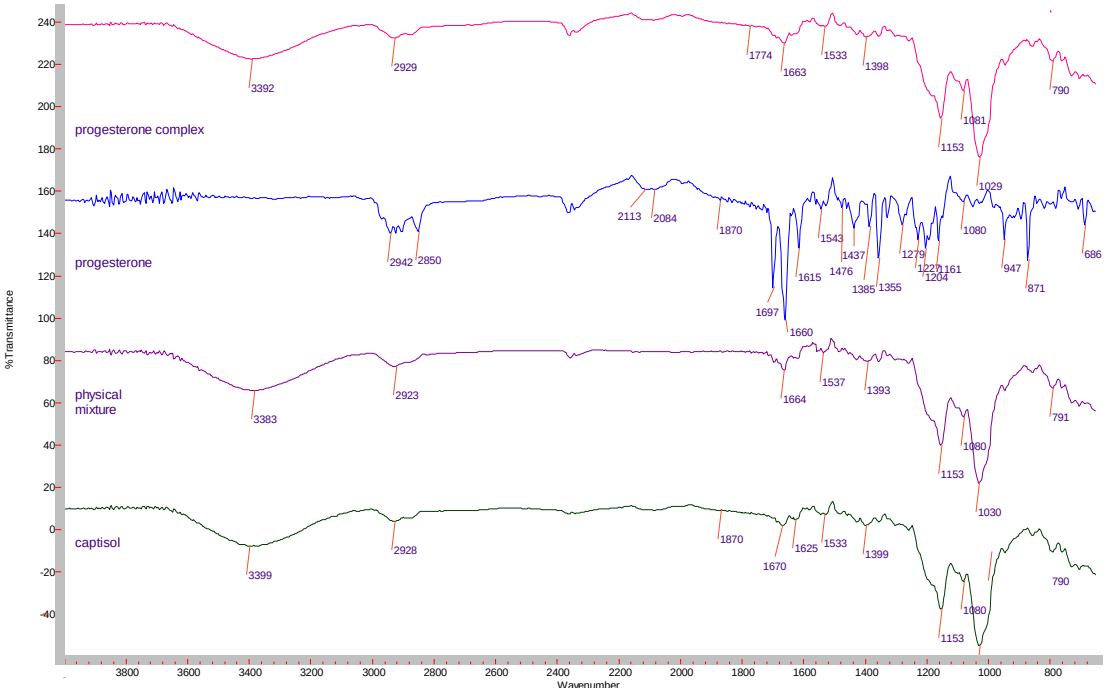

Figure 5. FTIR spectra of SBE-β-CD (Captisol™), progesterone, SBE-β-CD–progesterone physical mixture and SBE-β-CD–progesterone complex.

3.2.3 NMR studies

The ^{1}H NMR spectra of progesterone, SBE-β-CD and its complexes (physical and inclusion complexes) were recorded to gain deeper insight into the interaction of the drug with cyclodextrin. The ^{1}H NMR spectra of progesterone and the SBE-β-CD–progesterone complex with important protons (most affected by complexation) of progesterone are shown in Fig. 6. The ^{13}C NMR spectra of progesterone and the SBE-β-CD–progesterone complex with important carbons of progesterone are shown in Fig. 7. The chemical shifts observed for progesterone are given in Tables 2 and 3.

3.2.3.1 Proton (^{1}H) and carbon (^{13}C) nuclear magnetic resonance

^{1}H and ^{13}C NMR are effective tools that can be used to confirm complexation and also provide insight into the mode of inclusion of a guest into the host cavity. The changes in the chemical shift patterns of the complex, relative to those for the isolated drug, are indicative of host–guest interaction. Selected proton signals of progesterone and the SBE-β-CD–progesterone complex in DMSO-d_6:D2O are summarized in Table 2. Similarly, selected carbon data of progesterone and its inclusion complex are shown in Table 3. Due to the structural complexity of SBE-β-CD, it was difficult to assign the protons and carbons of the cyclodextrin itself by ^{1}H and ^{13}C NMR; therefore, we only monitored the changes in the spectrum of progesterone in the inclusion complex. The differences found in the chemical shifts of progesterone in the SBE-β-CD–progesterone complex indicate that Ring A and Ring D of progesterone each have the possibility to be included within the SBE-β-CD cavity.

Table 2. Selected ^{1}H NMR chemical shifts of progesterone and the SBE7-β-CD–progesterone complex**.**

Progesterone protons (atom numbering)	Free progesterone (ppm)	SBE-β-CD–progesterone complex (ppm)	Difference (ppm)
H4	6.02	6.11	0.09
H17	2.61	2.67	0.06
H18	0.91	1.01	0.10
H21	2.45	2.37	−0.08

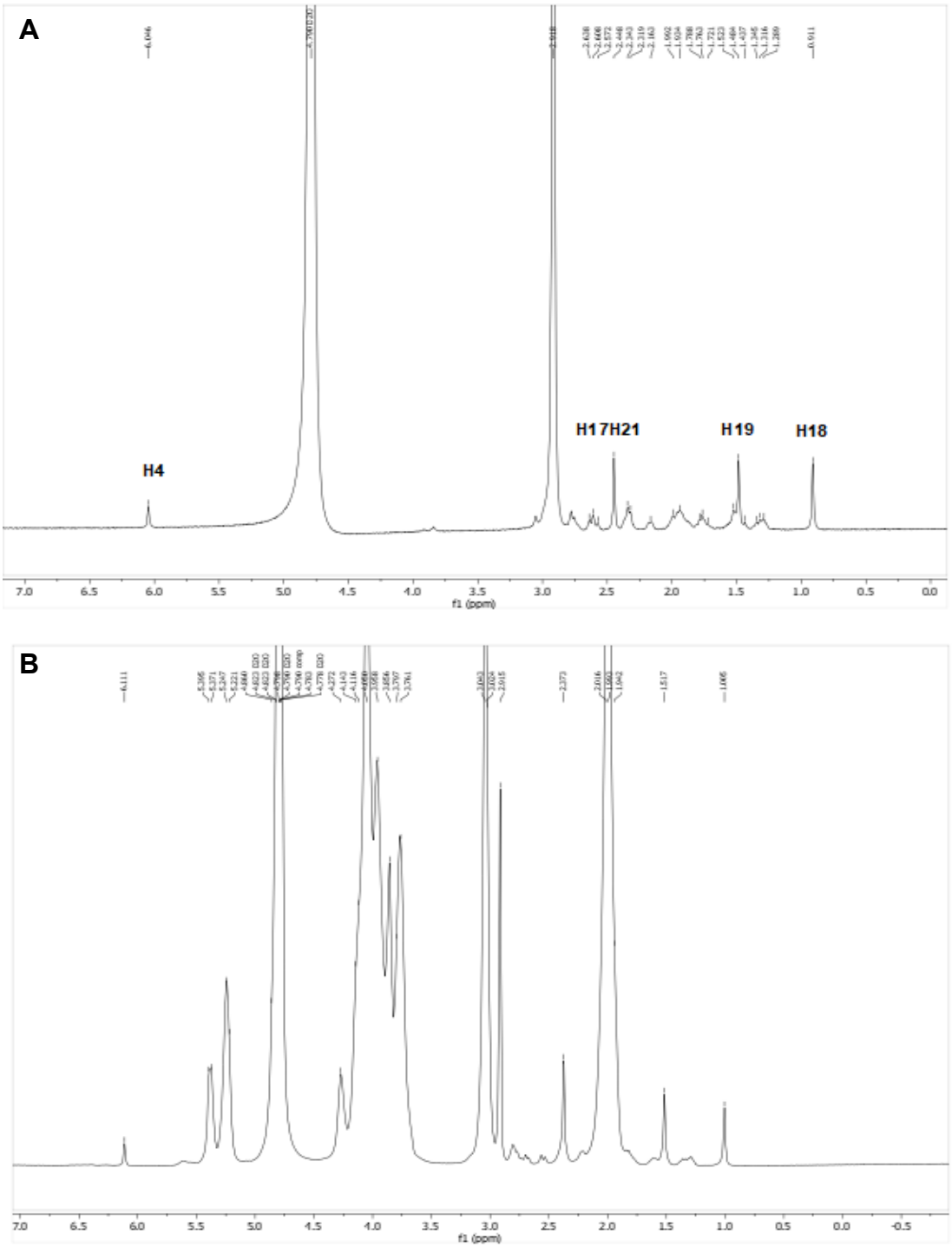

Figure 6. ^{1}H NMR spectra of (A) progesterone and (B) SBE-β-CD–progesterone complex in DMSO-d_6-D_2O (2:1).

Table 3. Selected ^{13}C chemical shifts of progesterone and the SBE-β-CD–progesterone complex

Progesterone protons (atom numbering)	Free progesterone (ppm)	SBE-β-CD–progesterone complex (ppm)	Difference (ppm)
C3	197.912	198.246	0.334
C4	123.187	123.271	0.084
C5	170.727	171.090	0.363
C17	62.468	62.577	0.109
C20	208.398	208.727	0.329
C21	31.144	31.292	0.148

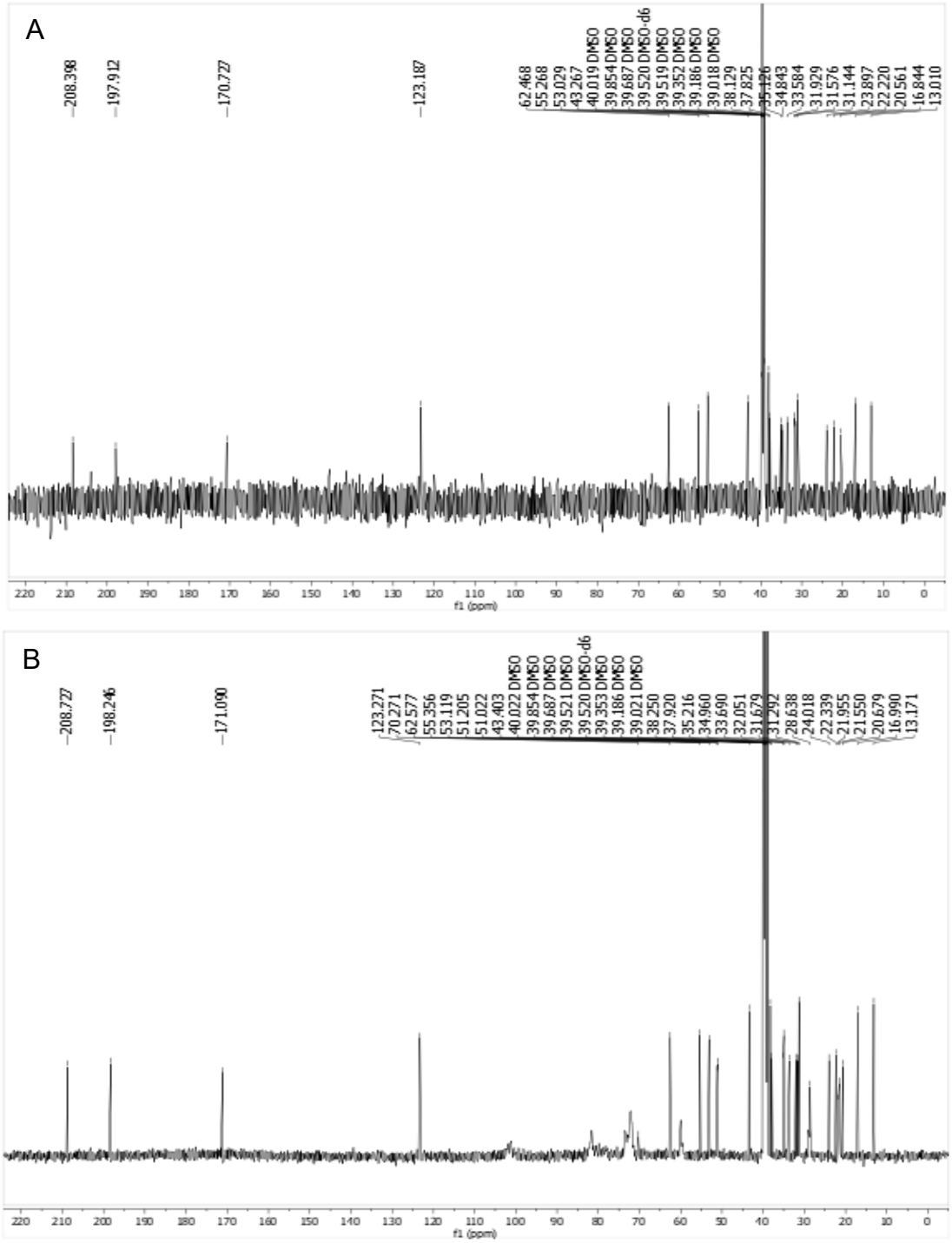

Figure 7. ^{13}C NMR spectra of (A) progesterone and (B) SBE-β-CD–progesterone complex in DMSO-d_6-D_2O (2:1).

3.2.4 Molecular modeling

3.2.4.1 Conformational search

A total of 968, 970, 971 and 669 conformers of SBE-β-CD were generated using the MCS tool within a cutoff window of 10 kcal/mol, for Isomers 1, 2, 3, and 4, respectively. We selected 10, 8, 15, and 10 conformers for Isomers 1, 2, 3, and 4 respectively, which matched the criteria of having a slightly open cavity (suitable for docking).

3.2.4.2 Docking and molecular dynamics of SBE-β-CD–progesterone complex

The progesterone molecule was docked into the four isomers of SBE-β-CD using the Glide standard precision (SP) method implemented in the Schrödinger software with flexible ligand sampling. The docking and scoring of progesterone into the generated grids of each low energy conformer of each isomer resulted in the most favorable SBE-β-CD–progesterone complexes (Table 4). The best docking complex of each isomer was subjected to a 5 ns MD simulation to help understand the stability and binding orientation of the complexes.

The representative complexes of progesterone with the four different SBE-β-CD isomers from the MD simulations are shown in Fig. 8. Since the H4 and H21 protons (located on opposite ends of progesterone) in the ^{1}H NMR of progesterone (Fig. 6, Table 2) were downshifted and upshifted, respectively, in the SBE-β-CD–progesterone complex, we interpreted that to show that progesterone forms inclusion complexes with SBE-β-CD in two different orientations (pose A: C3, and pose B:C20 carbonyl facing the hydroxyl of SBE-β-CD). To get more insight into the structure of the inclusion complexes, we also performed ^{13}C NMR for SBE-β-CD–progesterone. The chemical shifts of progesterone at C3, C5, C17, C20, and C21 showed significant changes after formation of the inclusion complex with SBE-β-CD. These data further supported that

progesterone interacts with SBE-β-CD in two different orientations. In our MD simulations we explored both such orientations. In Fig. 8, progesterone was seen to interact with SBE-β-CD on the secondary face in all of the isomers, using the starting point as Pose A, in which the carbonyl at C3 of Ring A formed an H-bond with the hydroxyl of SBE-β-CD (Fig. 8). Meanwhile we ran alternate MD simulations starting with the alternative pose (Pose B) of progesterone having the C20 carbonyl of progesterone H-bonded with the hydroxyl of SBE-β-CD for Isomers 1 and 4 (Table 4 and Fig. 9) and that stable pose was well maintained during the simulation. The pose B for isomer 2 and 3 was not considered for molecular dynamics simulation, due to very poor docking scores and orientation/pose of progesterone was not found inside the cavity of SBE-7-CD. The details of the interactions between progesterone and the protein in the different simulations clearly illustrate how the change occurs in the pattern of the NMR signals of the protons (H4 and H21) and carbons (C3, C20) of progesterone (Figs. 6 and 7) in the progesterone–SBE-β-CD complex. The binding free energies from the MD simulations (Table 4) revealed that there is a more favorable interaction of progesterone with SBE-β-CD when the C3 carbonyl group of Ring A is embedded in the cavity of SBE-β-CD (Pose A). Overall, all four possible isomers of SBE-β-CD showed H-bonds with progesterone at the C3 or at the C20 carbonyl group with progesterone partially embedded in the SBE-β-CD cavity, and thus either Ring A or Ring D lies within the SBE-β-CD cavity. This matches well with the experimental (^{1}H NMR and ^{13}C NMR) data (Figs. 6 and 7, and Tables 2 and 3) and helps to confirm the formation of the inclusion complex of progesterone with SBE-β-CD.

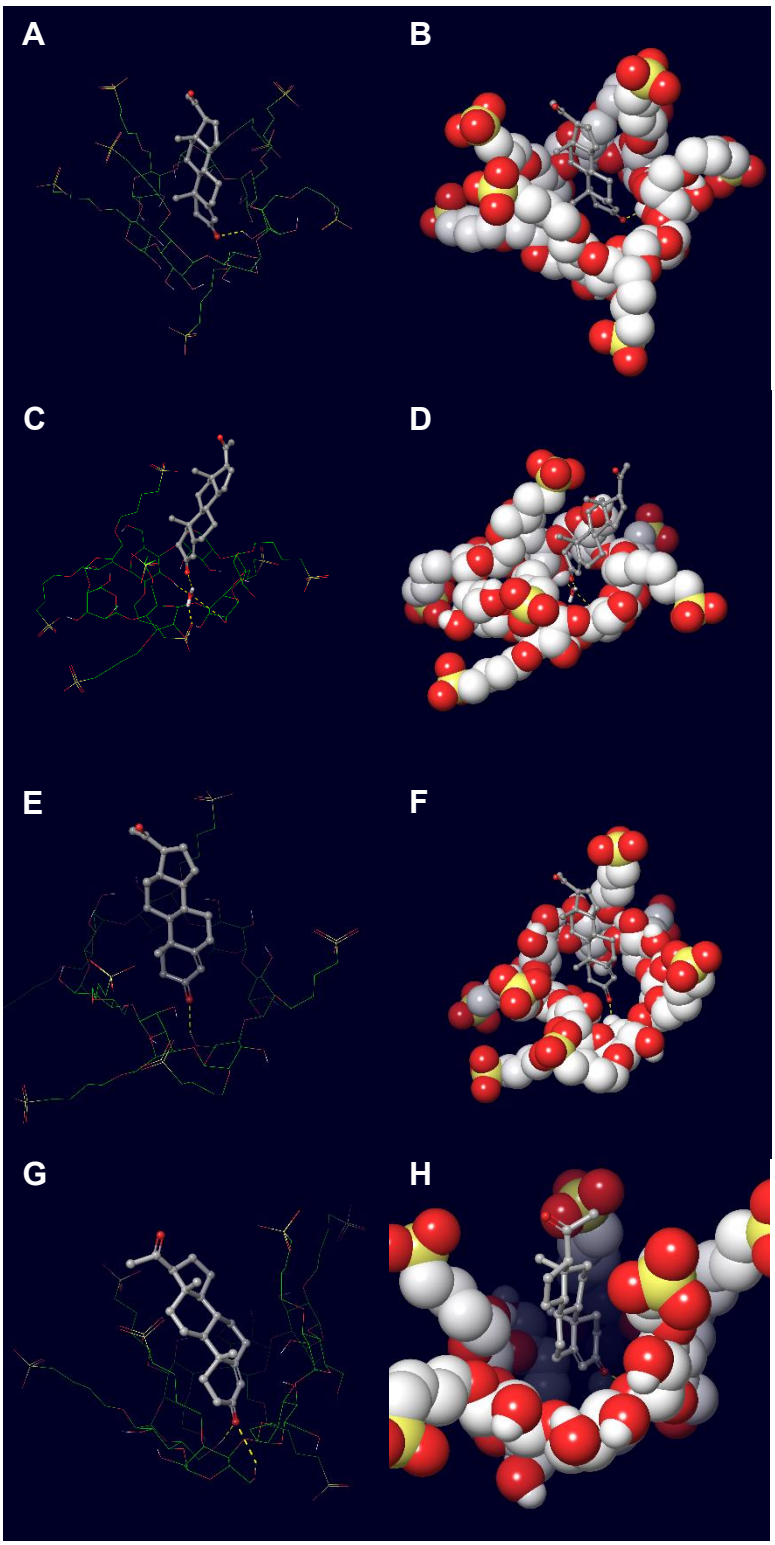

Figure 8. Binding poses (Pose A) after 5 ns molecular dynamics simulations of representative complexes of progesterone (ball and stick model) with Isomer **1** (A and B); Isomer **2** (C and D); Isomer **3** (E and F) and Isomer 4 (G and H) of SBE-β-CD (line representation, left images; CPK model, right images). Hydrogen bonds are shown in yellow dashes.

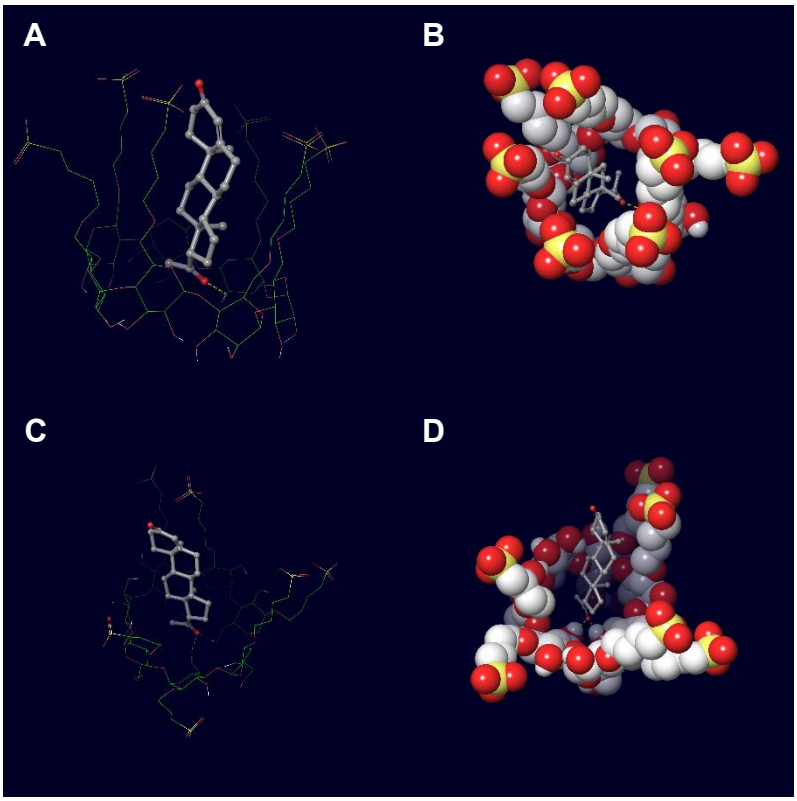

Figure 9. Binding pose (Pose B) of a representative complex of progesterone (ball and stick model) with Isomer 1 (A and B) and Isomer 4 (C and D) of SBE-β-CD (line representation, left images; CPK model, right images). A hydrogen bond is shown with yellow dashes.

Table 4. The energetic profile of the most favorable inclusion complexes of progesterone with SBE-β-CD models (Captisol®) before molecular dynamics simulations, in Pose A (Ring A downward) or Pose B (Ring A upward) and computed Binding Free Energies for the four SBE-β-CD–Progesterone Complexes after MD Simulations.

Complex	**SBE-β-CD–progesterone complex**					
	Pose A				**Pose B**	
Isomer	**1**	**2**	**3**	**4**	**1**	**4**
Conformer Number	8	5	5	1	2	3
Docking Score (kcal/mol)	–4.384	–4.422	–5.187	–5.288	–3.805	–4.936
$\mathbf{E_{model}}$	–30.476	–28.836	–36.023	–41.387	–26.338	–37.661
ΔG (kcal/mol)	–51.410	–40.136	–45.544	–57.930	–48.632	–45.860

The Pose A MD trajectories revealed persistent intermolecular hydrogen bonds (Fig. 10 and Supplementary Fig. S1) between the carbonyl group (at the C3 position) of progesterone and the 2/3-OH of the glucose unit of SBE-β-CD in complexes with Isomers 1, 3 and 4 (Fig. 10 and Fig. 11). In contrast, in the complex with Isomer 2, only a few instances of hydrogen bonding occurred between the carbonyl group of progesterone and the 2/3-OH of the glucose unit of SBE-β-CD. Interestingly, in Isomer 2, we observed that the carbonyl at the C3 position of Ring A formed water-mediated hydrogen bonding instead of direct hydrogen bonding with 2-OH or 3-OH of the glucose unit of SBE-β-CD during the 5 ns simulation (Fig. 10 and 11). During the Pose A simulations of all four of the isomers, the carbonyl at the C3 position of Ring A was almost always deeply embedded into SBE-β-CD. In addition, in the Pose B simulations with Isomers 1 and 4 of SBE-β-CD, there were persistent H-bonds during the simulations (Fig. 10 and 11). The RMSD analysis revealed that the SBE-β-CD–progesterone complex of all four of the isomers with both orientations were stable during the entire simulation period. The RMSDs computed with respect to the initial structure of SBE-β-CD fluctuated between 2.7 and 4.0 Å (Fig. 12 and 13). The RMSD of progesterone into the four isomeric models of SBE-β-CD fluctuated only between 0.4 to 1.2 Å (Fig. 12 and 13). The most significant deviations in RMSD were a result of the flexible motion of the sulfobutyl ether arms.

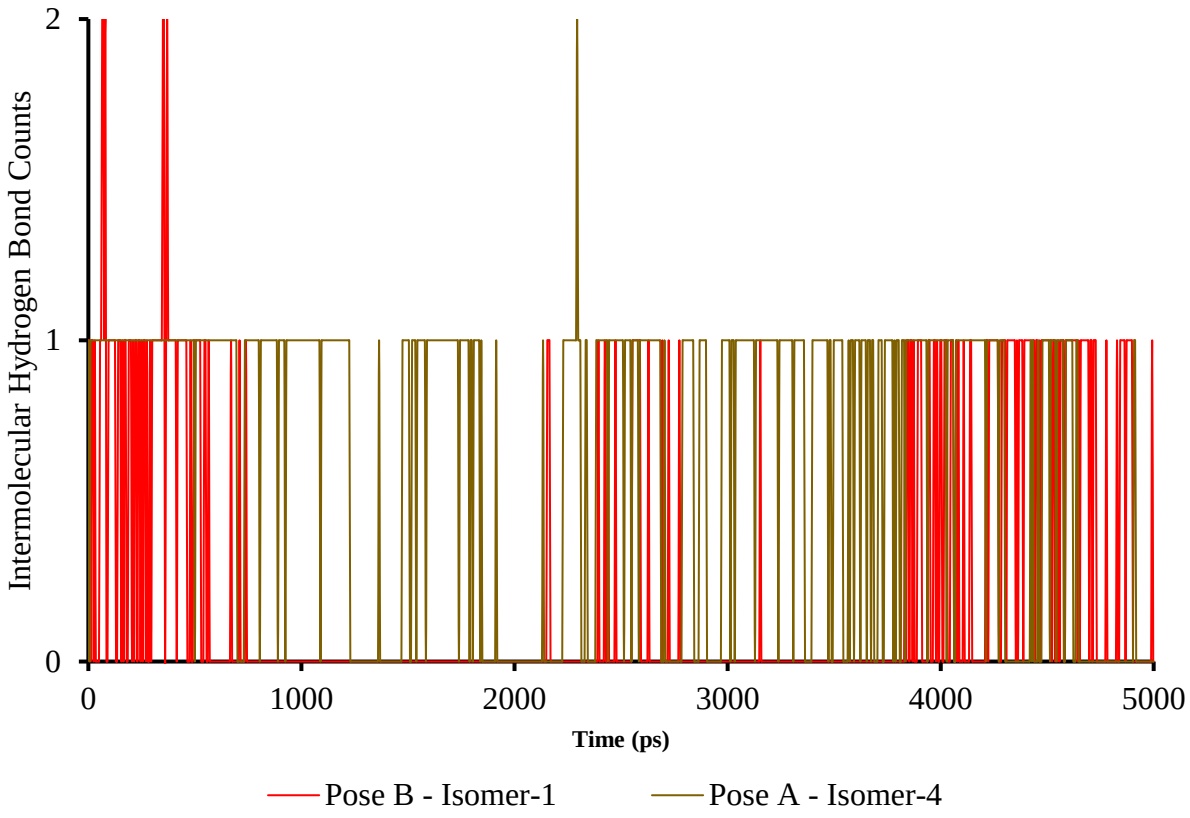

Figure 10. An intermolecular hydrogen bond (H-bond) graph for the best complexes between progesterone and SBE-β-CD (Isomers 1 and 4) observed for 5 ns MD simulation.

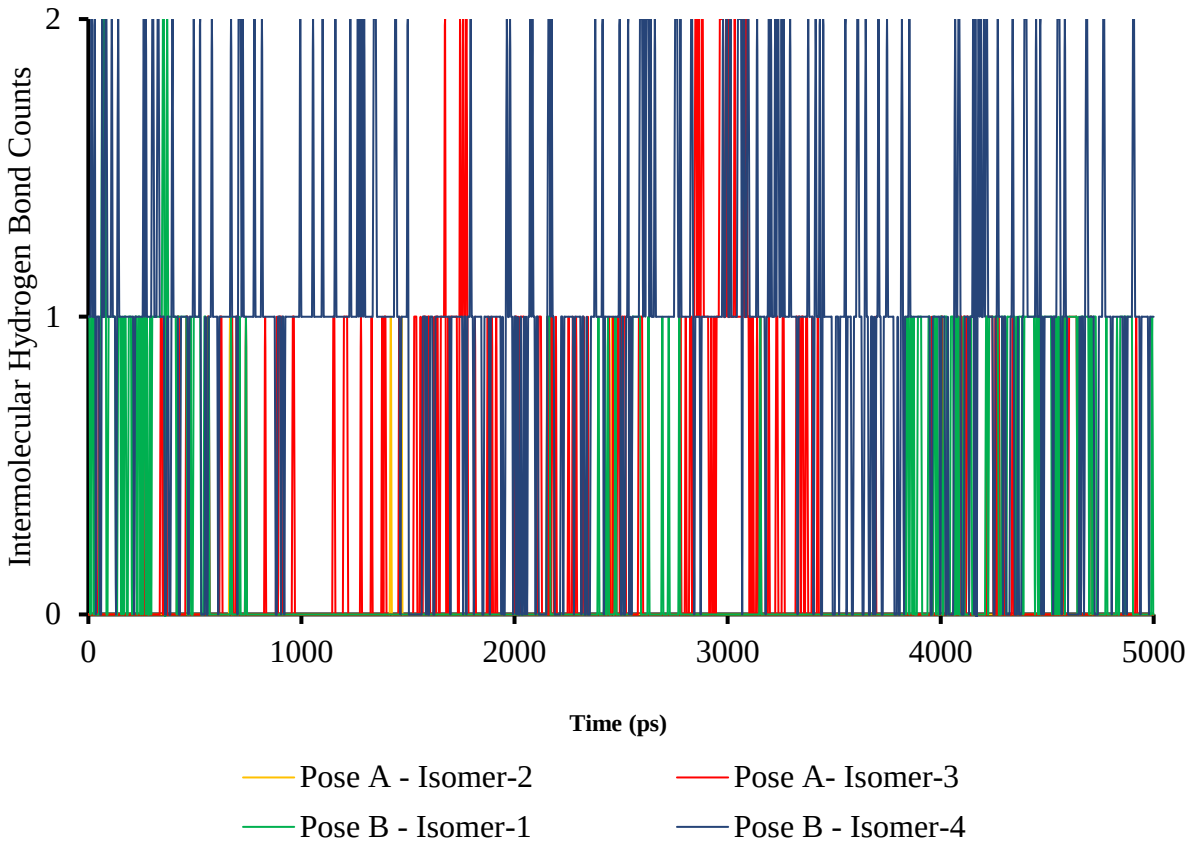

Figure 11. An intermolecular hydrogen bond (H-bond) graph between progesterone and SBE-β-CD complexes (for each of the four isomers) observed for 5 ns MD simulation.

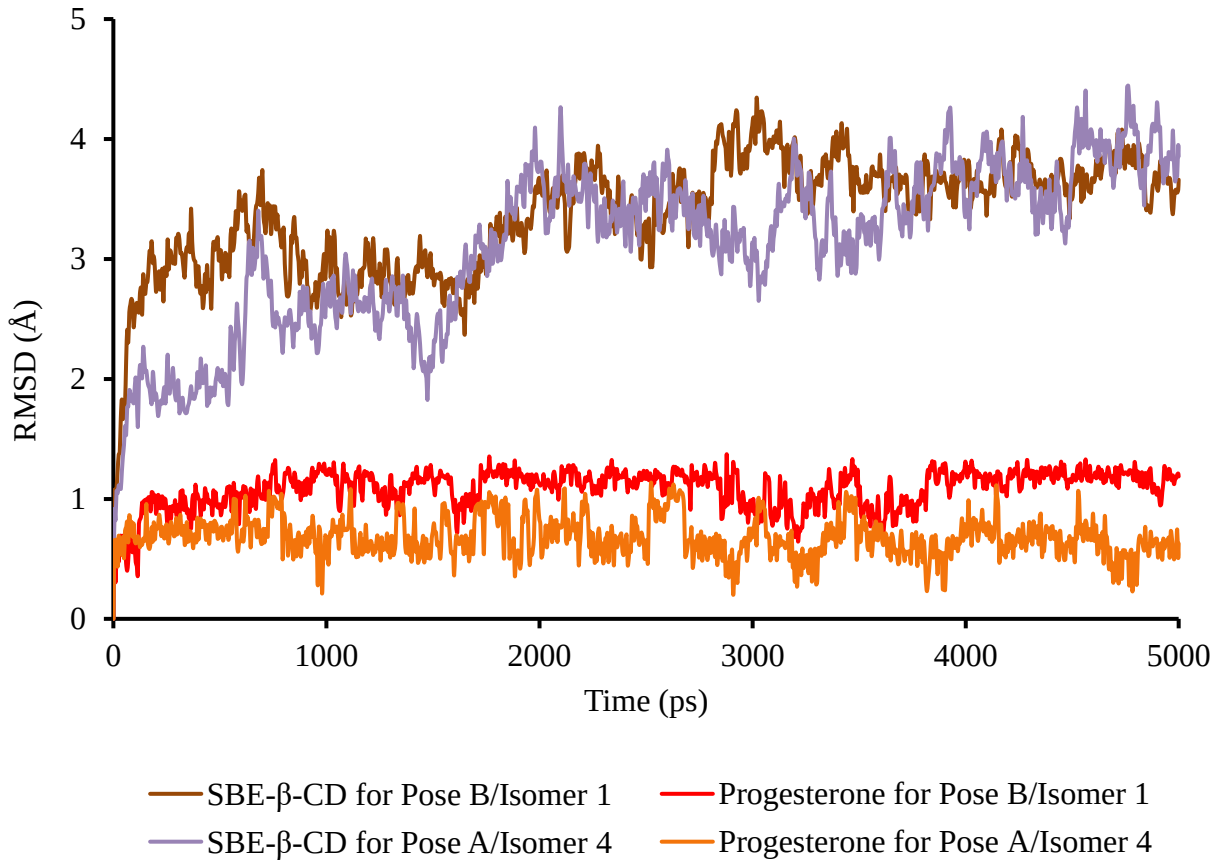

Figure 12. RMSD (for all non-hydrogen atoms) plot for the MD simulation (5 ns) of the best complexes formed between progesterone and SBE-β-CD (Isomers 1 and 4). The brown and purple lines indicate the RMSD of SBE-β-CD for Isomers 1 (Pose B) and 4 (Pose A), respectively. The RMSD of progesterone for Isomer 1 (Pose B) and Isomer 4 (Pose A) are represented by red and orange lines, respectively.

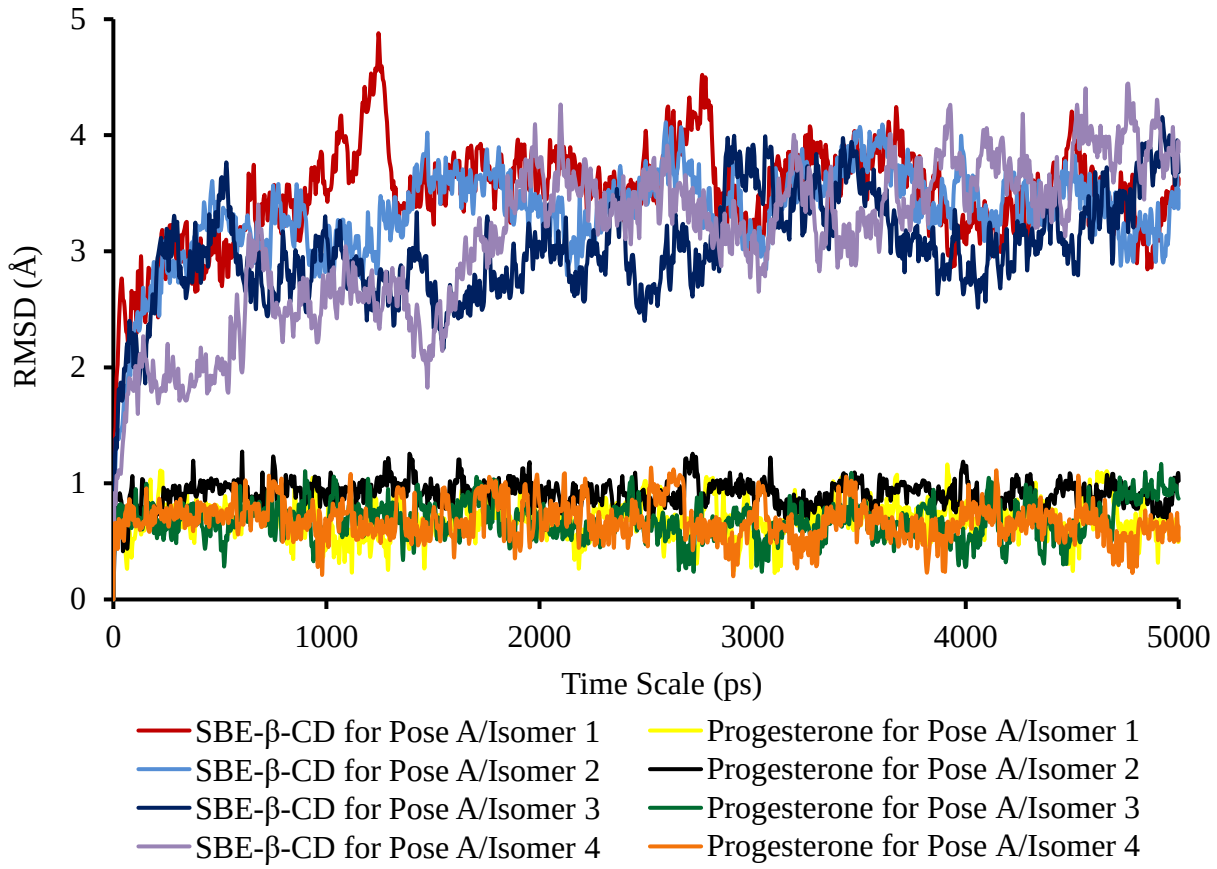

Figure 13. RMSD (for all non-hydrogen atoms) plot for the MD simulation (5 ns) of the best complexes formed between progesterone and the four isomeric states of SBE-β-CD (Isomers 1-4). The red, blue, dark blue and purple lines indicate the RMSD of SBE-β-CD for Isomer 1 (Pose A), Isomer 2 (Pose A), Isomer 3 (Pose A) and 4 (Pose A), respectively. The RMSD of progesterone for Isomer 1 (Pose A), Isomer 2 (Pose A), Isomer 3 (Pose A) and Isomer 4 (Pose A) are represented by yellow, black, green and orange lines, respectively.

3.3 Solubility of progesterone and SBE-β-CD–progesterone complex

The results in Table 5 demonstrate that the solubility of progesterone was decreased compared to its intrinsic solubility in FASSGF, similar to its intrinsic solubility in FESSGF, but increased 2-fold and 4-fold compared to its intrinsic solubility in FASSIF and FESSIF, respectively. The main factors influencing oral bioavailability of a drug are solubility of the drug in gastrointestinal fluid and permeation across the GI barrier. The prerequisite for a drug to permeate the GI membrane is drug dissolution in GI fluid (3). The drug solubility in GI fluid depends on the pH and content of the media, but drug pKa and particle size also influence aqueous solubility. Solubility of weakly basic drugs (e.g., carvedilol) (38) increases in FASSGF, whereas the solubility of weakly acidic drugs increases in higher pH solvents (FESSGF, FASSIF and FESSIF) (3). Also, increasing the ionic strength of the buffer increases the solubility of drugs in GI fluids (38). Progesterone is a neutral compound, so the pH of the GI fluid will only marginally influence solubility. By comparison, sodium taurocholate and lecithin in FASSIF and FESSIF form self-aggregates to assist in solubilizing progesterone (39).

Lowering the pH and ionic strength of FASSGF and FESSGF had no effect on the solubility of the SBE-β-CD–progesterone complex, whereas only 75% and 25% of the SBE-β-CD–progesterone complex dissolved in FASSIF and FESSIF, respectively. Various studies have reported that bile salts present in intestinal fluid displace drug molecules from cyclodextrin cavities leading to precipitation of the drug in the intestinal lumen (9,40,41).

Table 5. Solubility of progesterone and of the SBE-β-CD–progesterone complex in water and in simulated gastrointestinal fluid. Each point represents the mean ± SD of triplicate values.

Medium	**Progesterone (mM)**	
	Progesterone API (mM ± S.D.**)**	**SBE-β-CD–Progesterone Complex (mM** ± S.D.**)**
Water	0.03 ± 0.001	4.998 ± 0.021
FASSGF (pH 1.2)	0.020 ± 0.002	4.869 ± 0.015
FESSGF (pH 5.0)	0.039 ± 0.018	4.299 ± 0.097
FASSIF (pH 6.8)	0.075 ± 0.036	3.311 ± 0.078
FESSIF (pH 6.5)	0.205 ± 0.003	1.020 ± 0.053

3.4 Effect of sodium taurocholate on the isolated SBE-β-CD–progesterone complex mixture

The isolated SBE-β-CD–progesterone complex mixture solubility decreased linearly from 4.94 ± 0.30 mM to 1.64 ± 0.04 mM with linear increase of sodium taurocholate concentration up to 18 mM, which indicates displacement of progesterone from the cavity of SBE-β-CD (Fig. 14 and Table 6). The progesterone displacement was found to saturate beyond a concentration of 18 mM, which could be the result of formation of sodium taurocholate aggregates (micelles). The size of sodium taurocholate micelles must be very large to form a complex with SBE-β-CD (42). A few studies have reported the critical micellar concentration (CMC) of sodium taurocholate to be 8-12 mM or 3-5 mM (43). The CMC of surfactants depends on factors like pH, temperature and ionic strength of the solvent used (44).

A drug can form a complex with cyclodextrin through non-covalent interactions to form an inclusion complex. Association and dissociation of drug and cyclodextrin in solvent is rapid. Upon oral administration of the cyclodextrin–drug complex, the primary mechanism of drug release from the cyclodextrin cavity is dilution (41). Another mechanism involved in drug release is the displacement of the drug by certain contents of the GI tract that have a relatively higher

affinity than the drug to cyclodextrin (41). In the small intestine, displacement of the drug from the cyclodextrin cavity is reported to be largely by bile salts (40) and to a negligible amount by lecithin (45).

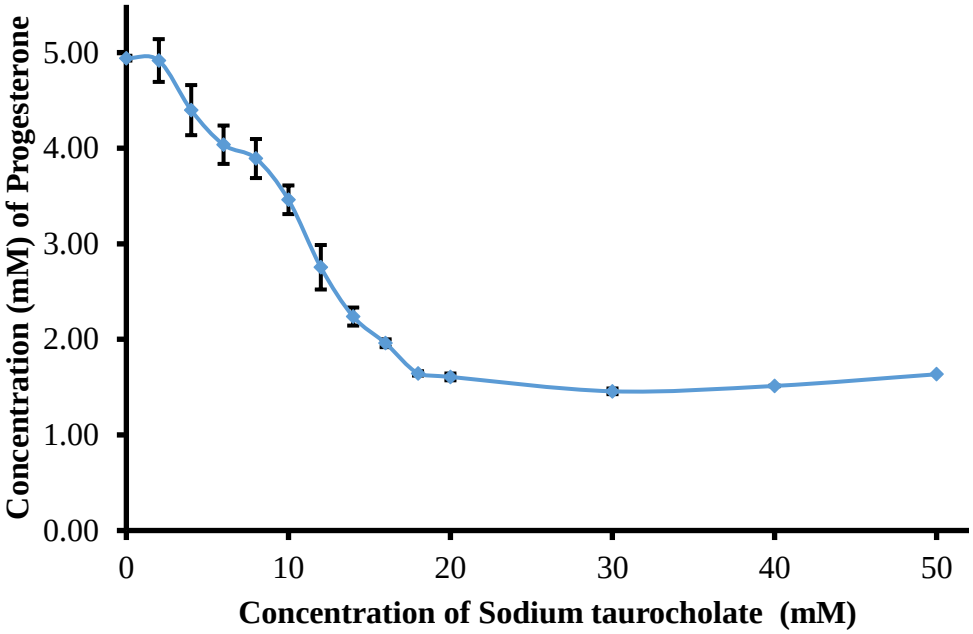

Figure 14. Progesterone displacement from the inclusion complex by sodium taurocholate.

Table 6. Percentage progesterone displacement from the SBE-β-CD–progesterone complex by sodium taurocholate. Each point represents mean ± SD of triplicate values.

Sodium Taurocholate (mM)	Progesterone (%) Mean ± S.D.
0	1.27 ± 0.48
2	1.60 ± 0.49
4	12.0 ± 4.48
6	22.2 ± 4.02
8	19.3 ± 5.24
10	22.2 ± 4.02
12	30.8 ± 4.08
14	44.9 ± 2.99
16	55.2 ± 4.65
18	60.8 ± 1.89
20	67.1 ± 0.81
30	67.9 ± 0.45
40	70.9 ± 0.71
50	69.7 ± 0.59

3.5 Effect of excess SBE-β-CD on sodium taurocholate displacement of progesterone from SBE-β-CD cavity

The results in Fig. 15 and Table 7 demonstrate that addition of excess SBE-β-CD prevents the precipitation of progesterone and approximately 40 mM of excess SBE-β-CD is required to completely counteract displacement of progesterone from cyclodextrin cavities in water. This indicates that an amount of free SBE-β-CD adequate to form inclusion complexes with bile salts would prevent precipitation or displacement of progesterone from cyclodextrin. The absorption

of a drug is increased if the drug is available in solubilized form at the site of absorption (46). The cyclodextrin utility number (U_{CD}) equation was derived by Rao and Stella, to calculate the concentration of cyclodextrin required for complete solubilization of a drug (47). U_{CD} only holds good for calculating the amount of cyclodextrin required to keep the drug in fully solubilized form in the absence of bile salts. Olessen et al. (2016), developed a model to calculate the optimum amount of cyclodextrin to be incorporated in a formulation to prevent the precipitation of the drug from the cyclodextrin complex in the presence of bile salts (45). This equation does not work well for the SBE-β-CD–progesterone complex, as there was a ~54-fold difference in stability constant calculated using the intercept or intrinsic solubility. Employing one definition or the other might lead to overdosing or underdosing of cyclodextrin. Hence, there is a need to evaluate experimentally the optimum concentration of cyclodextrin required to fully solubilize the drug in the presence of bile salts.

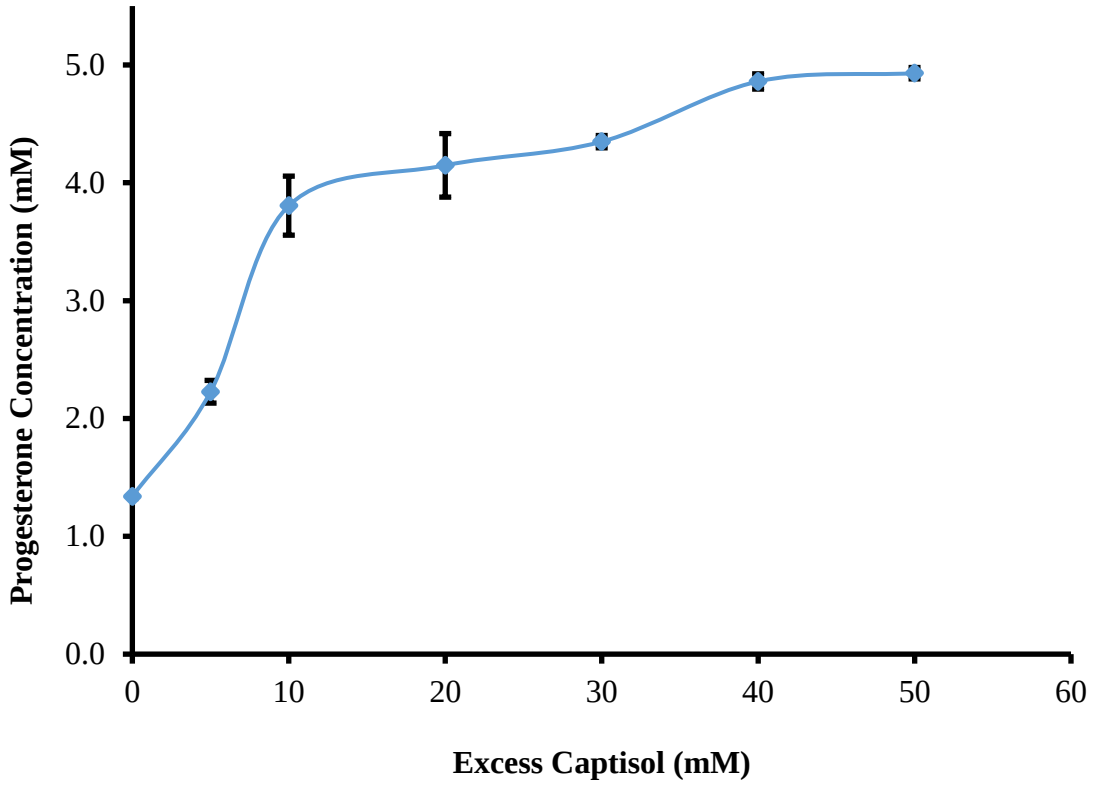

Figure 15. Effect of excess SBE-β-CD (Captisol^{TM}) on progesterone displacement from the SBE-β-CD–progesterone complex by sodium taurocholate. Each point represents mean ± SD of triplicate values.

Table 7. Effect of excess SBE-β-CD on percentage progesterone displacement from the SBE-β-CD–progesterone complex by 20 mM of sodium taurocholate. Each point represents mean ± SD of triplicate values.

SBE-β-CD (mM)	Progesterone (%) Mean ± S.D.
0	73.2 ± 0.38
5	55.5 ± 1.92
10	37.0 ± 5.39
20	33.0 ± 1.04
30	23.9 ± 5.00
40	2.87 ± 0.96
50	1.34 ± 1.29

3.6 *In vitro* simulation to evaluate effect of excess SBE-β-CD on displacement of progesterone from the SBE-β-CD–progesterone complex in FASSIF and FESSIF

The results in Figs. 16 and 17 and Tables 8 and 9 indicate that an increase in free SBE-β-CD in FASSIF and FESSIF prevents displacement of progesterone from the cyclodextrin cavity. This study demonstrates that the formulation of the SBE-β-CD–progesterone complex administered in the fasted state or fed state should contain 5 mM and 15 mM free SBE-β-CD, respectively, to prevent precipitation of progesterone in GI fluids.

The results of section 3.3 indicate that the solubility of the SBE-β-CD–progesterone complex is different in FESSIF and FASSIF. This might be due to differences in the composition of the bile salt, lecithin, salt composition or changes in pH of biorelevant media. The CMC of bile salts depends on the ionic strength and pH of the media (44), hence the CMC of sodium taurocholate in FASSIF and FESSIF would be completely different from its CMC in water. Also,

the bile salts might have a different displacement effect on progesterone from the SBE-β-CD complex depending on if it were in water, FASSIF or FESSIF.

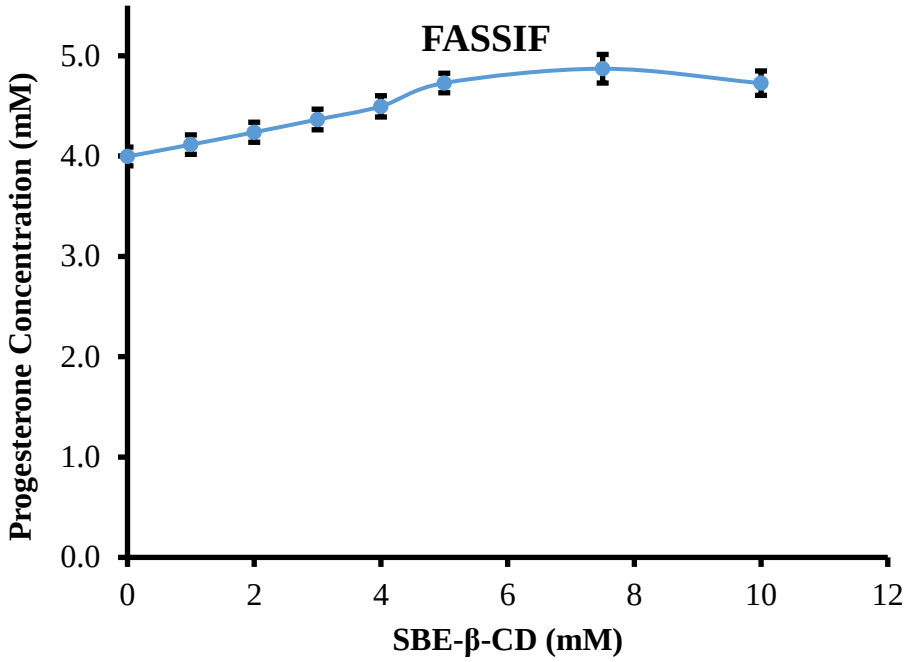

Figure 16. Excess SBE-β-CD effect in FASSIF on the solubility of the SBE-β-CD–progesterone complex. Each point represents mean ± SD of triplicate values.

Table 8. Effect of excess SBE-β-CD on percentage progesterone displacement from SBE-β-CD–progesterone complex in FASSIF. Each point represents mean ± SD of triplicate values.

SBE-β-CD (mM)	**Progesterone (%) Mean ± S.D.**
0	33.4 ± 1.55
1	31.4 ± 1.61
2	29.4 ± 1.66
3	27.2 ± 1.71
4	25.1 ± 1.76
5	21.2 ± 1.62
7.5	18.8 ± 2.37
10	21.2 ± 2.03

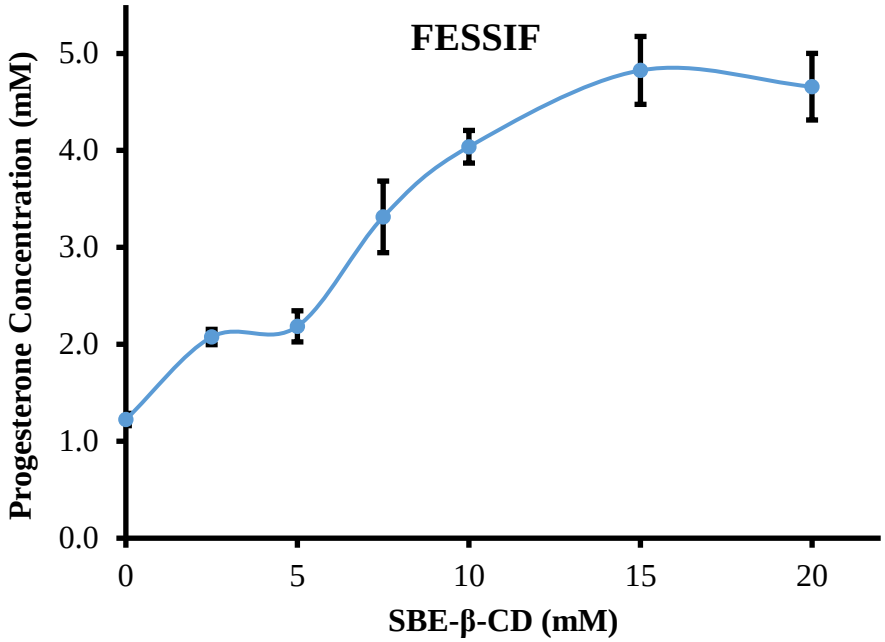

Figure 17. Excess SBE-β-CD effect in FESSIF on the solubility of the SBE-β-CD–progesterone complex. Each point represents mean ± SD of triplicate values.

Table 9. Effect of excess SBE-β-CD on percentage progesterone displacement from SBE-β-CD–progesterone complex in FESSIF. Each point represents mean ± SD of triplicate values.

SBE-β-CD (mM)	**Progesterone (%) Mean ± S.D.**
0	79.6 ± 1.05
2.5	64.5 ± 1.32
5	63.6 ± 2.68
7.5	44.8 ± 6.15
10	32.7 ± 2.81
15	19.6 ± 5.83
20	22.4 ± 5.72

3.7 Stability study

The stability of the SBE-β-CD–progesterone complex in water under two sets of conditions, 25 °C (60% RH) and 40 °C (75% RH), was ≥ 98.0 and ≥ 97.2% for periods of 3 and 6 months, respectively. The stability of the lyophilized SBE-β-CD–progesterone complex under the same conditions was ≥ 99.0 and ≥ 97.7% for periods of 3 and 6 months, respectively. Fig. 18 suggests that the SBE-β-CD–progesterone complex in water or in lyophilized form is stable at 25 °C (60% RH) and 40 °C (75% RH) for periods up to 6 months.

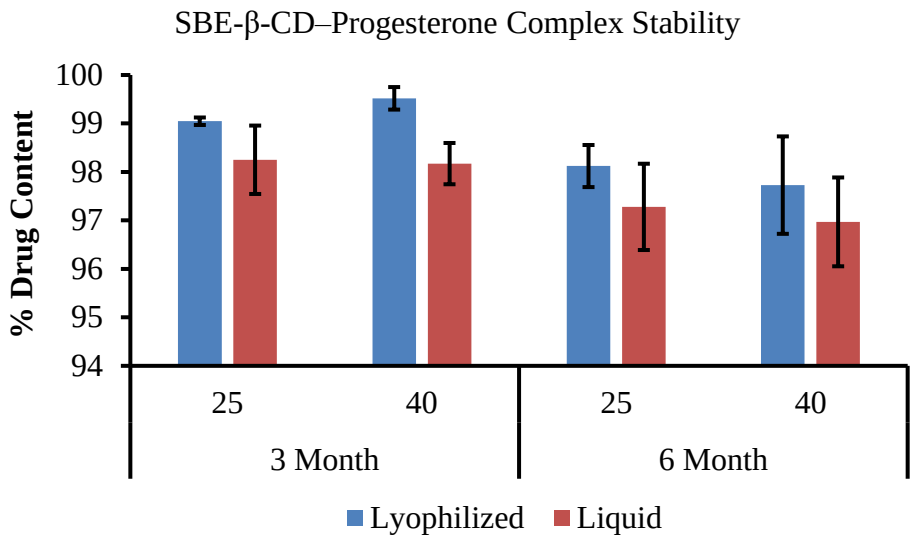

Figure 18. Stability of the SBE-β-CD–progesterone complex (lyophilized and liquid) at 25 °C (60% RH) and 40 °C (75% RH) for periods of 3 and 6 months (n=3) (mean ± S.D.).

3.8 *Ex vivo* intestinal permeability study

The bioavailability of cyclodextrin upon oral administration is poor, and highly hydrophilic cyclodextrins have a negligible permeation across the intestinal barrier (48). Upon oral administration < 3% of SBE-β-CD is absorbed and subsequently it is cleared quickly through renal excretion, and hence it is non-toxic and has a high safety margin (12,14). Various *in vivo* (17) and *in vitro* (5,40,49) studies suggest the optimum concentration of cyclodextrin required to enhance

permeability across the intestine or any biological barriers (40,49). Evaluation of a few *in vitro* data imply that too little or too much cyclodextrin can decrease the permeability and bioavailability of a drug (49).

Niels Erik Olesen et al., derived a biopharmaceutical model to assess the effect of cyclodextrin on intestinal absorption and avoid overdosing of cyclodextrin which could decrease drug absorption across the intestinal barrier (50). This model employs the $K_{1:1}$ constant in its derivation. For poorly soluble drugs the $K_{1:1}$ value determined from a phase solubility curve is not a true value; (35) hence this model was not employed for determination of the optimum concentration of cyclodextrin. Also, simple experimental evaluation of the effect of SBE-β-CD on drug permeation is more reliable compared to the biopharmaceutical model, since the model contains exceptions for certain drugs which cannot be employed for all drugs and therefore there is a risk of an erroneous result.

The *ex vivo* rat intestinal permeation study results shown in Fig. 19 demonstrate that the excess SBE-β-CD used in FASSIF and FESSIF had negligible effects on permeation of progesterone. The intestinal apparent permeability coefficient P_{app} (Fig. 20) of progesterone in different groups appeared in the following order: Complex in water > Complex in FASSIF > Complex in FESSIF with excess SBE-β-CD > Complex in FASSIF with excess SBE-β-CD > Complex in FESSIF and > Progesterone in 0.5% Brij S20. The *ex vivo* intestinal permeability study results depict that if SBE-β-CD is used in the formulation, there is increased permeation of progesterone across the intestinal barrier.

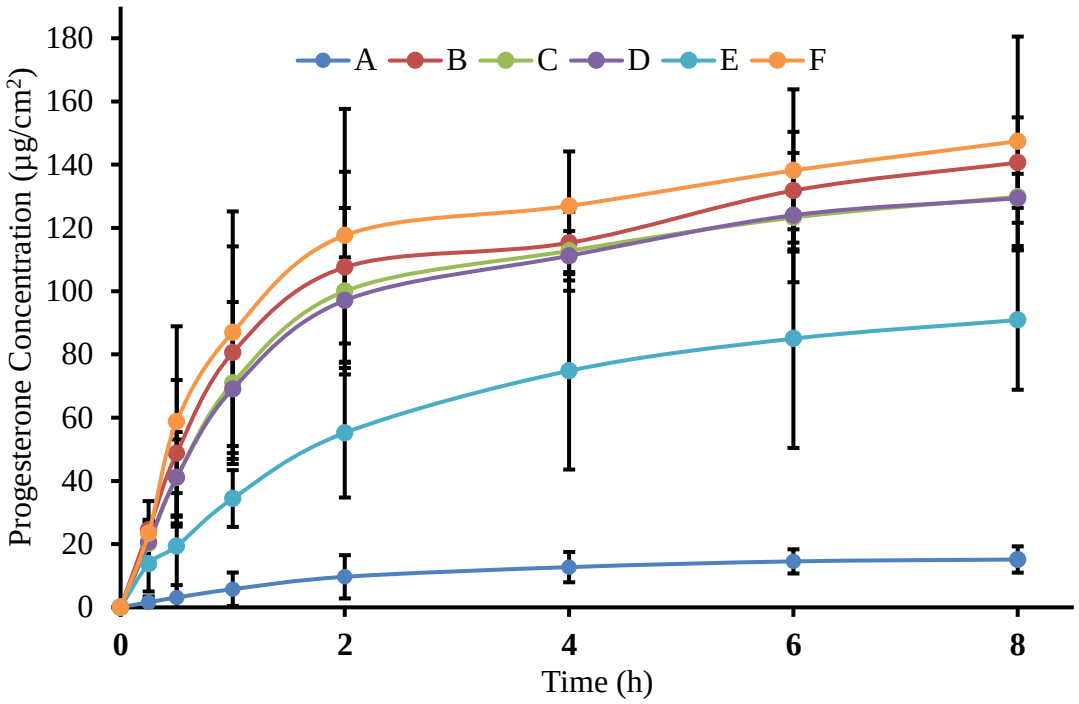

Figure 19. Permeation of progesterone across rat intestine: (A) Progesterone in 0.5% of Brij S20; (B) Complex in water; (C) Complex in FASSIF; (D) Complex in FASSIF with excess SBE-β-CD; (E) Complex in FESSIF; and (F) Complex in FESSIF with excess SBE-β-CD.

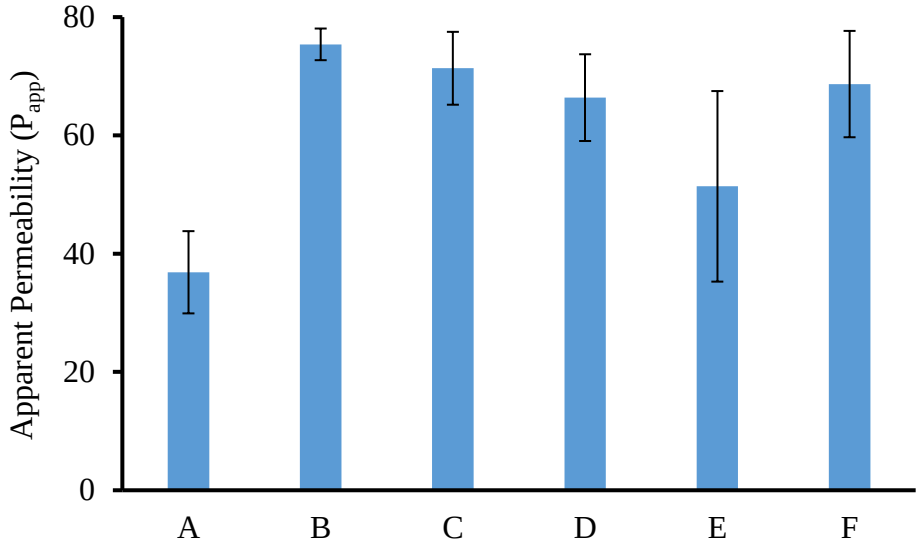

Figure 20. Apparent intestinal permeability of progesterone: (A) Progesterone in 0.5% Brij S20; (B) Complex in water; (C) Complex in FASSIF; (D) Complex in FASSIF with excess SBE-β-CD; (E) Complex in FESSIF; and (F) Complex in FESSIF with excess SBE-β-CD.

3.9 Rat pharmacokinetic study

The mean plasma concentration versus time profiles of oral progesterone API, oral SBE-β-CD–progesterone complex and IV progesterone are shown in Fig. 21. It was evident from the plots that the plasma levels of progesterone were higher when it is administered in the form of the SBE-β-CD–progesterone complex as compared with progesterone API. Table 6 shows AUC_{0-1h}, C_{max}, T_{max} and $\%F_{abs}$ values obtained with oral progesterone API, the oral SBE-β-CD–progesterone complex and IV progesterone dose. The calculated value for AUC_{0-1h} given in Table. 10 showed that the overall oral bioavailability of progesterone was increased 5-fold when administered via the SBE-β-CD–progesterone complex.

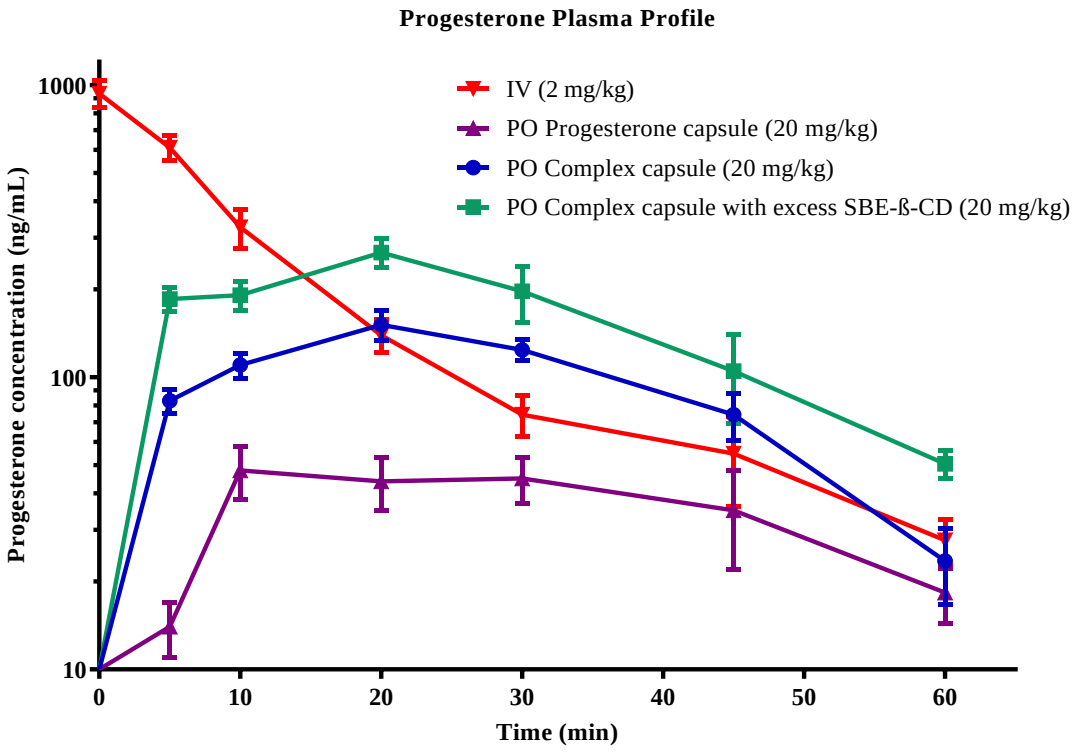

Figure 21. Plasma profile of progesterone upon oral administration of SBE-β-CD–progesterone complex capsule (20 mg/kg), SBE-β-CD–progesterone complex capsule with excess SBE-β-CD (20 mg/kg), progesterone capsule (20 mg/kg), and IV administered progesterone (2 mg/kg).

Table 10. Pharmacokinetic parameters of progesterone upon oral administration of a SBE-β-CD–progesterone complex capsule (20 mg/kg), a SBE-β-CD–progesterone complex capsule with excess SBE-β-CD (20 mg/kg), a progesterone capsule (20 mg/kg), and IV administered progesterone (2 mg/kg) in rats.

Pharmacokinetic Parameters	**Formulation**			
	Progesterone capsule	**SBE-β-CD – progesterone complex capsule**	**SBE-β-CD – progesterone complex capsule (Excess SBE-β-CD)**	**IV progesterone**
Dose (mg/kg)	20	20	20	2
$AUC_{0-1\,h}$ (ng.h/mL)	34.9 ± 15.3	93.1 ± 5.88	157 ± 22.8	147 ± 15.6
T_{max} (min)	10	20	20	5
C_{max} (ng/mL)	52.6 ± 20.4	151 ± 17.5	267 ± 30.6	611 ± 59.7
% F_{abs}	2.36	6.31	10.7	100

3.10 Dissolution studies

The dissolution profiles for progesterone and SBE-β-CD–progesterone complex capsules in water, SGF and SIF are shown in Fig. 22. The SBE-β-CD–progesterone complex capsules in all three media have significant improvement in dissolution characteristics compared to progesterone API capsules. Greater than 95% of progesterone was dissolved in all three media, when testing SBE-β-CD–progesterone complex capsules for 45 min. By contrast, at 120 min, 11.5, 8.08 and 16.9% of progesterone was dissolved from progesterone API capsule for the three media. The dissolution parameters of progesterone are given in Table 11. The SBE-β-CD–progesterone complex capsules had the lowest mean dissolution time (MDT) and highest initial dissolution rate (IDR) and mean dissolution rate (MDR) in SIF compared to SGF with water as dissolution media. The progesterone API capsules had the lowest MDT and highest MDR in SIF compared to other dissolution media (water and SGF), while IDR in water was highest compared to other media (SGF and SIF).

GI dissolution and absorption of solid dosage forms depends on GI transit time along with permeation rates across the GI barrier. These parameters vary in individuals, under disease conditions, and between the fasted and fed state (51). The gastric lag phase (time taken to empty 10% of the contents from the stomach), gastric half emptying and small bowel transit in fasted normal healthy volunteered subjects were approximately 55, 180 and 180 min, respectively (52). In the fed state, gastric half emptying, gastric emptying, small intestine half emptying and transit through colon were approximately 2.5 to 3, 4 to 5, 2.5 to 3 and 30 to 40 h, respectively (53). Progesterone tablets are prescribed to be administered at bed time after meals (13). The dissolution study results imply that SBE-β-CD–progesterone complex capsules would get dissolved in the stomach (>95% in SGF at 45 min) before entering the small intestine.

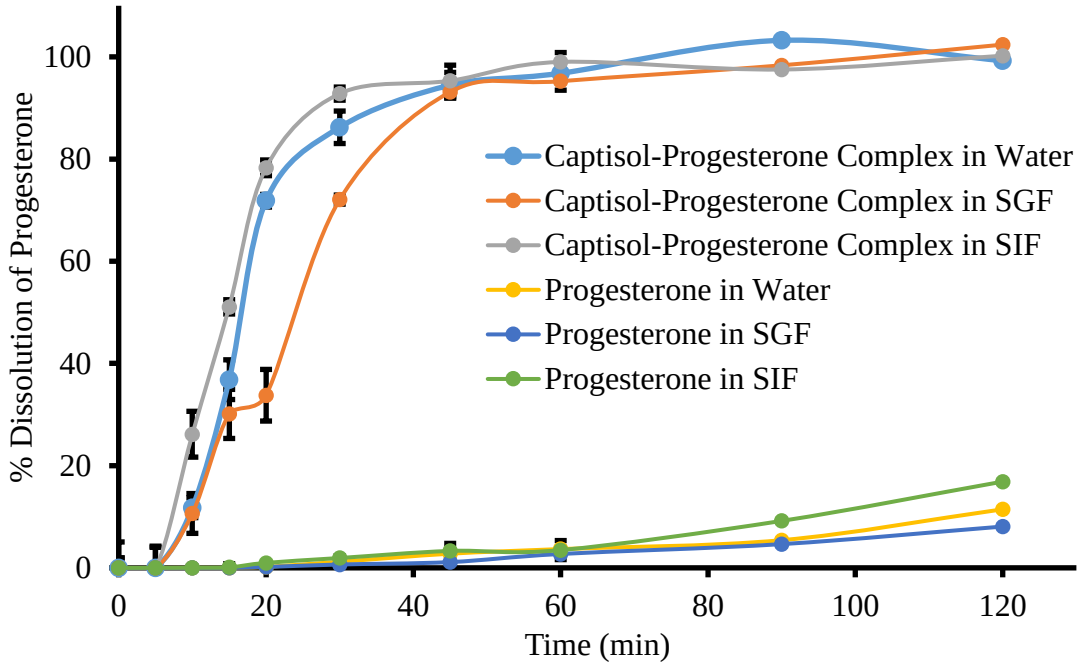

Figure 22. Dissolution of progesterone and of the SBE-β-CD–progesterone complex in water, simulated gastric fluid (pH 1.2) and simulated intestinal fluid (pH 6.8).

Table 11. Progesterone dissolution parameters in water, simulated gastric fluid (SGF, pH = 1.2), and simulated intestinal fluid (SIF, pH = 6.8).

Formulation	Dissolution Media	Dissolution Parameters		
		Mean dissolution rate (min^{-1})	Mean dissolution time (min)	Initial dissolution rate (min^{-1})
Progesterone Capsule	Water	0.023	48.9	0.001
	SGF	0.017	56.0	0.001
	SIF	0.037	57.4	0.002
SBE-β-CD–progesterone Complex Capsule	Water	1.210	31.6	0.780
	SGF	0.970	25.3	0.710
	SIF	1.570	14.9	1.740

4. Conclusion

The solubility of progesterone in water was enhanced by SBE-β-CD resulting in an A_L type phase solubility curve. Experimental techniques such as DSC, FTIR, ^{1}H and ^{13}C NMR, and molecular modeling studies confirmed the formation of a complex between SBE-β-CD and progesterone. *In vitro* experiments were employed to determine the amount of SBE-β-CD required to prevent progesterone displacement from SBE-β-CD cavities and this concentration of SBE-β-CD was used in *ex vivo* intestinal permeation studies. Increased permeation of progesterone across the membrane was observed. The SBE-β-CD–progesterone complex with excess SBE-β-CD increased oral bioavailability 5-fold compared to progesterone API suspension. It is of the utmost importance to consider drug displacement by bile salts in the intestine to avoid underestimation of oral bioavailability of NCE's. Also, it is essential to conduct a simple *in vitro* experiment in early drug discovery to determine the role of bile salts in displacement of the drug from the cyclodextrin cavity. It can be very helpful to administer additional amounts of free cyclodextrin to prevent precipitation of NCE's in the intestines during preclinical studies. However, the dissolution study results indicate that SBE-β-CD–progesterone complex capsules get dissolved in the stomach before entering the small intestine and the addition of excess SBE-β-CD may not be needed, which would decrease the bulk of the formulation. However, to arrive at the most robust performing formulation, it may be necessary evaluating the bioavailability of multiple designs with and without an excess to determine the most advantageous composition.

CHAPTER 3

Influence of Sulfobutyl-Ether- β-Cyclodextrins on oral bioavailability and tissue distribution of silymarin

1. Introduction

Silymarin is an extract of Milk Thistle (Silybum marianum) comprises a mixture of flavonolignans and flavanols. The major constituents of silymarin extracts are taxifolin (TX), silychristin (SC), silydianin (SD), silybin A (SA), silybin B (SB), isosilybin A (ISA) and isosilybin B (ISB) (55). These extracts are used as traditional remedies for centuries to treat hepatitis and cirrhosis and used to protect liver from toxic substances (56,57). In the present-day silymarin is most extensively investigated drug for the treatment of liver disease and conditions (57). Silymarin also exhibits a variety of pharmacological activities like anticancer (against prostate, lung, intestine, colorectal and liver tumors), hypocholesterolemic and cardioprotective effect both individually and collectively (58). Silymarin is available as a dietary supplement and most widely used herbal product in United States (59). Silymarin extracts is considered safe herbal product as there are no severe adverse events reported (60).

The clinical study of silymarin extracts and marketed oral silymarin formulations has reported high variability in its pharmacokinetic profile (55,61,62), this could result in erratic pharmacological effect of silymarin constituents. The variability in silymarin pharmacokinetics is intended to its low aqueous solubility, poor permeation across intestinal barrier and rapid first pass

metabolism on oral administration (61). Several researchers have endeavored to increase the oral bioavailability and subsequent therapeutic effect of silymarin constituents employing different formulation approaches like liposomes (63), phytosomes (64), self microemulsifying drug delivery systems (65), floating tablets (66), micronization, nanoemulsions (67) and solid dispersions (68). Most of these formulation approaches were competent to certain extent in increasing the oral bioavailability of silymarin constituents. However, the commercial feasibility of these formulations is limited as they lack scalability, stability, reproducibility of physicochemical properties and dosage form development. Hence, further investigation of simple appropriate technique to enhance the bioavailability of entire silymarin constituents is essential to avail their beneficial effects (61).

Solubility enhancement of silymarin constituent is utmost important to increase bioavailability and to improve drug developability property (3). Aqueous solubility of drugs can be increased by various techniques, the simple and most commonly employed technique is by preparation of inclusion complex using cyclodextrins. The lipophilic drugs form an inclusion complex with cyclodextrins and increases solubility of lipophilic drugs in water. The native and modified β-cyclodextrin's (β-CD) have a large cavity size compared to α and γ-CD, hence have higher aqueous solubility enhancing potential. The native β-CD's water solubility is low compared to their derivatives methyl-β-cyclodextrins (M-β-CD), hydroxy-2-propyl-β-cyclodextrins (HP-β-CD) and sulfobutyl-ether-β-cyclodextrins (47). The reported studies have demonstrated the utility of β-CD and HP-β-CD (69) in increasing aqueous solubility of silymarin constituent silibinin/silybin. The intravenous safety studies of β-CD and M-β-CD have demonstrated they produce nephrotoxicity in larger doses (10,70). The no observed adverse effect level (NOAEL) for SBE-β-CD on oral administration in rats is 3600 mg/kg/day, which is >7 times than NOAEL (500

mg/kg/day) of HP-β-CD (10). Hence, SBE-β-CD are most appropriate cyclodextrins for evaluating aqueous solubility enhancing potential of active pharmaceutical ingredients intended for oral formulations.

The objective of this study was to enhance the oral bioavailability of silymarin by preparing an inclusion complex of SBE-β-CD–silymarin with a simple, less time consuming and efficient method of complexation. The stability of inclusion complex was evaluated in different simulated gastrointestinal fluids. To ensure silymarin remains in solubilized form to facilitate its absorption across intestinal barrier on oral administration of SBE-β-CD–silymarin complex. *Ex vivo* permeation studies were performed to evaluate the influence of SBE-β-CD on permeation of silymarin across porcine intestine. The oral bioavailability of silymarin and its metabolites on oral administration of SBE-β-CD–silymarin and silymarin complex were evaluated in Sprague Dawley (SD) rat. The influence of SBE-β-CD on tissue distribution of silymarin on oral administration was evaluated in SD rats.

2. Materials and Methods

2.1 Chemicals and reagents

Isosilybin and silychristin was purchased from Tractus Company Limited, England. Silydianin was purchased from ChromaDex Inc. USA. Taxifolin was purchased from Enzo Life Sciences Inc. USA. Silymarin extract, pepsin, phosphate buffered saline, β-glucuronidase, sulfatase and L-α-phosphatidylcholine (lecithin) were purchased from Sigma-Aldrich (St. Louis, MO), USA. SBE-β-CD was a gift sample obtained from Ligand Pharmaceuticals, Inc., USA. Sodium taurocholate was purchased from Alfa Aesar, USA. Euthasol® (pentobarbital sodium and phenytoin sodium) solution was procured from Virbac, USA. Methocel E15 Premium EL (hydroxypropyl methyl cellulose) was a gift sample from Dow Chemical company, USA. The

HPLC grade solvents acetonitrile, methanol, dibasic potassium phosphate, dibasic sodium phosphate, glacial acetic acid, hydrochloric acid, sodium hydroxide, sodium chloride, sodium acetate, ortho-phosphoric acid and Milli Q water were of research grade used without further purification.

2.2 Estimation of silymarin constituents in silymarin extract

Silymairn is collective term used for main constituents present in extract, structure of silymarin constituents are depicted in Figure 1. The silymarin extract was weighed and dissolved in dimethyl sulfoxide (DMSO). These solutions were diluted appropriately using DMSO and the amount of individual constituents present in each milligram of silymarin extract was estimated by HPLC method using calibration curve of individual reference standards.

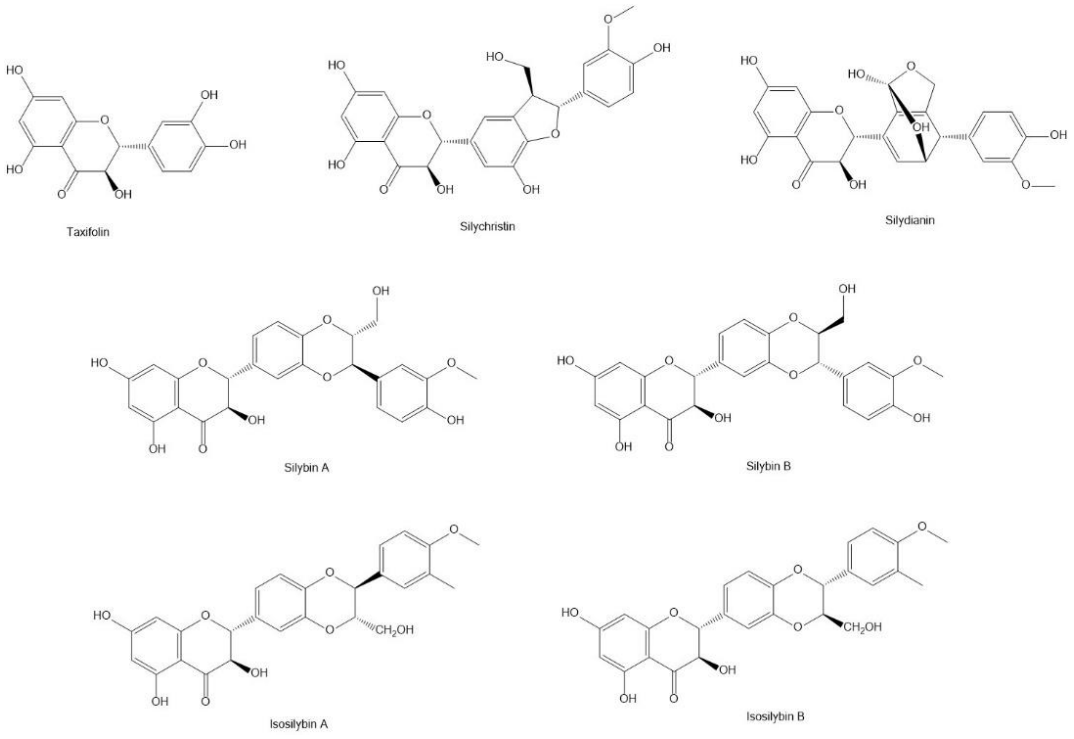

Figure 1. structure of Silymarin constituents.

2.3 Physicochemical properties of Silymarin constituents

2.3.1 Solubility of Silymarin constituents

The solubility of silymarin constituents were estimated by adding excess amounts of silymarin extract in Milli-Q® water, fasted state simulated gastric fluid (FASSGF) at pH 1.6, fed state simulated gastric fluid (FESSGF) at pH 5.0, fasted state simulated intestinal fluid (FASSIF) at pH 6.5 and fed state simulated intestinal fluid (FESSIF) at pH 5.8. These gastrointestinal simulated fluids were prepared by using reported method (34). Samples were kept shaking at 25 °C for 3 days and at equilibrium samples were filtered using a Millipore (0.45 μm) syringe filter. The filtrate was analyzed using HPLC to evaluate the saturation solubility of individual constituents of silymarin in water and simulated gastrointestinal fluids.

2.3.2 Simultaneous determination of Log P, Log D and pKa of Silymarin constituents

The Log P, Log D and pKa of silymarin constituents were determined simultaneously by employing previously published method (71). The 12 buffers between pH ranges of 1.0 to 12 were prepared using universal buffer stock containing 25 mM hydrochloric acid, 25 mM citric acid, 25 mM phosphoric acid, 30 mM boric acid and 20 mM sodium chloride. To microcentrifuge tubes 500 µL of pre-saturated buffers (1 to 12 pH) with octanol and 500 µL of pre-saturated octanol with buffers (1 to 12 pH) were added. To above tubes 10 µL of 10 mM DMSO stock solutions of TX, SC, SD, silybin and isosilybin were added. These mixtures were vortexed for 5 min and kept shaking at room temperature for 16 h, after specified time these tubes were centrifuged at 10,000 RPM for 30 minutes. After centrifugation buffer and octanol phases were separated, both the phases were diluted with acetonitrile (1:1) and subjected to HPLC analysis.

2.4 Phase solubility studies

2.4.1 Conventional Method

SBE-β-CD–silymarin constituents complex were prepared by adding excess of silymarin extract to different concentrations of SBE-β-CD (10, 20, 40, 60, 80 and 100 mM) in Milli-Q® water (Higuchi and Connors method) (20). Samples were kept shaking at 25 °C for 3 days and at equilibrium samples were filtered using a Millipore (0.45 μm) syringe filter. The filtrate was analyzed using HPLC to evaluate the saturation solubility of silymarin constituents in SBE-β-CD. Phase solubility study curves were used to calculate complexation efficiency (CE) and stability constants ($K_{1:1}$).

2.4.2 Heating Method

SBE-β-CD–silymarin constituents complex were prepared by adding excess of silymarin extract to different concentrations of SBE-β-CD (10, 20, 40, 60, 80 and 100 mM) in Milli-Q® water. Samples were kept shaking at 25 °C for 15 minutes and samples were placed on hot plate stirrer for 60 min at 75 °C temperature. After specified time the samples were cooled at room temperature and was filtered using a Millipore (0.45 μm) syringe filter. The filtrate was analyzed using HPLC to evaluate the saturation solubility of silymarin in SBE-β-CD. Phase solubility study curves were used to calculate complexation efficiency (CE) and stability constants ($K_{1:1}$).

2.5 Stability of SBE-β-CD–silymarin complex in simulated gastric fluids

The lyophilized SBE-β-CD–silymarin complex (25 mg) were dissolved in water, FASSGF, FESSGF, FASSIF and FESSIF. Samples were kept shaking at 37 °C for 8 h at 100 rpm in a Bio-shaker and samples were filtered using a Millipore (0.45 μm) syringe filter. The filtrate was analyzed using HPLC and concentrations of 0 h samples were compared with 8 h samples.

2.6 Stability studies

The lyophilized SBE-β-CD–silymarin complex prepared by heating and conventional method were stored in a stability chamber under two different conditions, at 40 °C and 75% RH and at 25 °C and 60% RH. The stability was assessed by evaluating drug content in samples after 3 and 6, 12 months using HPLC.

2.7 *Ex vivo* porcine intestinal permeation studies

The freshly harvested porcine intestine was obtained from slaughter house and cut open to expose the mucosal layer and cleaned with PBS pH 7.4. The intestine was sandwiched between donor and receiver chambers of a franz diffusion cell with an active diffusion area of 0.64 cm^2. The resistance across porcine intestine was measured using a wave form generator to ensure the integrity of the small intestine segment used for permeation study. The intestinal membrane with resistance of ≥2.5 $K\Omega.cm^2$ was used for permeation studies. The donor chamber was filled with 0.5 ml of SBE-β-CD–silymarin complex and silymarin in phosphate buffered saline containing 0.5% of Brij S20 used as a positive control. The receiver chamber was filled with 5 ml of PBS (pH 7.4), which was stirred at 600 rpm with a 3 mm magnetic stir bar and the temperature was maintained at 37 °C with a circulating water bath. 200 μL samples were withdrawn from the

receiver compartment at different time intervals (0, 1, 2, 4, 6 and 8 h) and each time an equal volume of fresh receiver media was used to replace withdrawn media. The above samples were transferred into vials and subjected to HPLC analysis.

2.8 *In vivo* studies

The animal studies were conducted at University of Mississippi, School of Pharmacy, as per the protocol #14-021, approved by the institutional animal ethical committee and animal welfare assurance # A3356-01. On arrival, rats were housed in cages at the animal care facility in a temperature and humidity controlled room with a 12:12 h light:dark cycle, and they had a free access to food and water for one week to acclimatize animals before use in the experiments.

2.8.1 Silymarin pharmacokinetic studies in SD rats

Twelve jugular vein cannulated male rats were used for pharmacokinetic studies. These animals fasted overnight and had free access to water on the day before the experiment. On the day of the experiment, the rats were removed from the animal care facility and brought to the procedure lab. Animals were randomly divided into three different groups of 4 animals each (Group I: PO SBE-β-CD–Silymarin complex; Group II: PO Silymarin API suspension and Group III: Silymarin intravenous). Dose to animals of group-I and II were administered using rat oral gavage (fixed to dosing syringe), placed in the mouth and advanced along the lower palate as far as the esophagus (dosing volume: 10 mL/kg body weight). The dose to group III was administered by slow bolus intravenous injection into the tail vein (dosing volume: 2 mL/kg body weight). The dose of individual silymarin constituents administered to animals of different groups are presented in Table 1. Approximately 200 µL of blood was drawn into heparin-coated tubes at pre-dose, 0.08,

0.17, 0.33, 0.5, 0.75, 1, 1.5, 2, 4 and 8 h through jugular vein catheter. Plasma was harvested by centrifuging the blood at 4000 rpm for 5 min and stored frozen at 80 ± 10 °C until analysis. Silymarin constituents in plasma samples were estimated using HPLC.

Table 1. The dose of individual silymarin constituents administered to animals of different groups.

Silymarin Constituents	Oral SBE-β-CD–silymarin complex	Oral silymarin suspension 1000 mg/kg	Intravenous SBE-β-CD–silymarin complex
Taxifolin	26.2	11.1	5.24
Silychristin	52.5	57.1	10.5
Silydianin	77.1	19.0	15.4
Silybin A	22.4	21.4	4.48
Silybin B	44.0	35.8	8.8
Isosilybin A	27.5	28.2	5.5
Isosilybin B	7.9	7.81	1.58

2.8.2 Estimation of silymarin metabolites in oral pharmacokinetic plasma samples

The silymarin metabolites in plasma were estimated by incubating the plasma samples with enzymes β-glucuronidase and sulfatase. The β-glucuronidase enzyme was dissolved in 0.1 M sodium phosphate buffer pH 6.8 to prepare a stock solution containing 2000 units/mL of glucuronidase. The sulfatase enzyme was dissolved in 0.1 M sodium acetate buffer pH 5.0 to prepare a stock solution containing 200 units/mL of sulfatase. 25 µL of stock solution of β-glucuronidase and sulfatase were added to 2 different 25 µL aliquots of plasma and vortex mixed for 2 min. These mixtures were incubated at 37 °C for 4 h and after incubation period the enzyme

activity was terminated by addition of acetonitrile and silymarin constituents were determined using HPLC.

2.8.3 Silymarin Tissue distribution studies

Male SD rats were used for tissue distribution studies. The animals were fasted overnight and had free access to water on the day before the experiment. On the day of the experiment, the rats were removed from the animal care facility and brought to the procedure lab. Animals were randomly divided into two different groups of 4 animals each (Group I: PO SBE-β-CD–Silymarin complex and Group II: PO Silymarin API suspension). Dose to animals were administered using rat oral gavage (fixed to dosing syringe), placed in the mouth and advanced along the lower palate as far as the esophagus (dosing volume: 10 mL/kg body weight). After 30 min of administration of oral dose, rats were euthanized using an intraperitoneal (i.p.) dose of Euthasol® (150 mg/kg body weight). Approximately 200 µL of blood was drawn into heparin-coated tubes and, liver, lungs, kidney, spleen, heart, ocular and brain tissue were isolated. Plasma was harvested by centrifuging the blood at 4000 rpm for 5 min. Plasma and tissue samples were stored at 70 ± 10 °C until analysis along. Silymarin constituents in plasma and tissue samples were determined uisng HPLC.

2.9 HPLC analysis

The HPLC method was developed using a Shimadzu UFLC system, equipped with prominence SPD-M20A (Diode array detector). The chromatographic separation of silymarin constituents and the internal standard (IS) dapsone was achieved on a Symmetry Shield RP18 column (150 x 4.6 mm, 5 µm); which was maintained at ambient room temperature. The binary

mobile phase system reservoir A (Methanol : 10mM Ammonium acetate pH 5 [65:35 v/v]) and reservoir B (10 mM ammonium acetate pH 5) were run as per gradient program (0-1.9 min: 25% A and 75% B; 2.0-14.9 min: 80 % A and 20 % B and 15-37.9 min: 80 % A and 20% B and 38-40 min: 25 % A and 75 % B) at a flow rate of 1 mL/min was used throughout the analytical run of 40 min. Samples of solubility, *in vitro* and *ex vivo* samples were subjected to HPLC analysis without any further extraction procedure.

Silybin purchased from Sigma-Aldrich is mixture of SA and SB. The percentage contents of SA and SB in silybin mixture were analyzed by HPLC and found to be 47.7 and 52.3%, respectively. Isosilybin purchased from Tractus Company Limited, England is mixture of ISA and ISB. The percentage contents of ISA and ISB in isosilybin mixture were analyzed by HPLC and found to be 68.4 and 31.6%, respectively. The measured ratios of SA and SB in silybin and ISA and ISB in isosilybin were used for the quantitative analysis.

2.10 Recovery

A simple protein precipitation method was employed for extraction of silymarin constituents from *in vivo* study samples. The extraction recovery of TX, SC, SD, SA, SB, ISA and ISB was determined by comparing the peak-area ratios of the analytes from LQC, MQC and HQC levels spiked in rat plasma, liver, brain, spleen, lungs, kidney, heart and ocular tissue homogenate (n=3) with the responses of analytes of LQC, MQC and HQC concentrations in acetonitrile.

2.11 *In vivo* sample preparation

To an aliquot of 50 µL of rat plasma/enzyme treated samples/tissue homogenate, 5 µL of dapsone (5 µg/mL) and 200 µL of acetonitrile was added and mixture was vortexed. These samples were centrifuged at 4 °C for 10 min at 14,000 rpm on a centrifuge 5430R (Eppendorf, Germany) and the supernatant was transferred to a vial for HPLC analysis. The eluate was monitored by setting UV detection wavelength at 288 nm. The silymarin constituents and IS was eluted at 7.90, 16.1, 19.1, 20.1, 25.3, 27.0, 32.2 and 34.1 min for IS, TX, SC, SD, SA, SB, ISA and ISB, respectively.

3. Results and Discussion

Silymarin constituents are low aqueous soluble drugs, and hence its low oral bioavailability is attributed to low absorption of silymarin across the intestinal barrier. It is important to enhance the solubility/dissolution of the drug to overcome its poor bioavailability issues and avail beneficial effects of silymarin constituents.

3.1 Estimation of silymarin constituents in silymarin extract

The silymarin extract is obtained from plant source and different methods are employed to extract the silymarin. The constituents from the different source consists different proportion of silymarin constituents. Hence, it is essential to estimate the exact amount of silymarin constituents present in extract, prior to using the extract for any *in vitro* or *in vivo* studies. The amount of silymarin constituents present in extract is presented in Table 2, SC is the major constituent present in the silymarin extract. The order of concentrations of silymarin constituents present in silymarin extract are SC > SA > SB > ISA > SD > TX > ISB.

Table 2. The amount of silymarin constituents present in each milligram of silymarin extract. Each point represents mean ± SD of triplicate values.

Silymarin Constituents	(µg/mg) Mean ± S.D (n=3)
Taxifolin	11.1 ± 0.36
Silychristin	57.1 ± 1.18
Silydianin	19.0 ± 0.57
Silybin A	21.4 ± 0.74
Silybin B	35.8 ± 1.08
Isosilybin A	28.2 ± 0.86
Isosilybin B	7.81 ± 0.26

3.2 Physicochemical properties of Silymarin constituents

3.2.1 Solubility of silymarin constituents in water and simulated gastrointestinal fluids

The solubility of silymarin in water is presented in Table 3, SC have higher and ISB lowest solubility in water compared to other silymarin constituents. The intrinsic solubility of silymarin in water was in following order of SC > TX > SD > SB > ISA > SA > ISB. Although silymarin constituents are derivatives of quercetin (Fig. 1), the solubility of silymarin constituents in water differs from 1.52 to 145 µg/mL. This indicates the ring other than A, B and C and spatial arrangements of functional groups attached to E ring of silybin and isosilybin influence the solubility of silymarin constituents in water (Fig. 1).

The drug solubility in GI fluid depends on physical and chemical properties of drug and GI fluid. GI fluid's ionic strength and content of the media influence solubility of drug (39). Drug solubility in GI fluid and permeation across GI barrier are two crucial factors governing the oral

bioavailability of a drug, drugs as to be dissolved in GI fluid to permeate across the GI membrane (3). The solubility of drug in water might not be an indicative of their solubility in GI fluids. Hence, it's essential to determine the solubility of drug molecule in GI simulated fluids intended for oral administration. The ionized form of drug has higher solubility in water compared to their unionized counterparts. The weakly basic drugs are predominantly ionized and solubilized in FASSGF, whereas weakly acidic salts are predominantly ionized and solubilized in FESSGF, FASSIF and FESSIF (3).

The solubility of TX in FASSIF was decreased by ~20%, whereas solubility of TX in other simulated gastrointestinal fluids (SGIF) was unchanged (Table 3). The percentage solubility of SC, SD, SA, SB, ISA and ISB in FASSGF decreased to 65.2, 66.9, 9.86, 10.6, 14.3 and 10.5% of water solubility, respectively (Table 3). The percentage solubility of SC, SD, SA, SB, ISA and ISB in FASSIF decreased to 69.6, 72.4, 62.6, 30.7, 41.5 and 57.2% of water solubility, respectively (Table 3). The decrease in the solubility of SC, SD, SA, SB, ISA and ISB in FASSGF, FESSGF and FASSIF could be due to pH of the media (39). The solubility of SC, SD, SA, SB, ISA and ISB were increased in FESSGF by 1.24, 1.65, 9.04, 6.31, 10.6, 13.9 fold compared to water solubility, respectively (Table 3). Increase in FESSGF solubility might be due to presence of bile salt and lecithin in FESSGF media (39).

Table 3. The solubility of silymarin constituents (µg/mL) in Milli-Q® water and simulated gastrointestinal fluids. Each point represents mean ± SD of triplicate values.

Silymarin Constituents	Milli-Q® water	FASSGF (pH 1.6)	FESSGF (pH 5.0)	FASSIF (pH 6.5)	FESSIF (pH 5.8)
Taxifolin	135 ± 3.31	123 ± 8.30	129 ± 7.35	97.7 ± 2.63	125 ± 4.23
Silychristin	145 ± 9.87	94.6 ± 5.31	101 ± 4.65	71.3 ± 6.18	181 ± 13.4
Silydianin	55.9 ± 1.56	37.4 ± 0.29	40.5 ± 2.39	27.3 ± 1.13	92.2 ± 2.55
Silybin A	3.45 ± 0.45	0.34 ± 0.04	2.16 ± 0.17	1.37 ± 0.04	31.2 ± 0.69
Silybin B	11.0 ± 0.24	1.17 ± 0.06	3.38 ± 0.02	4.78 ± 0.20	69.4 ± 1.68
Isosilybin A	7.29 ± 0.20	1.04 ± 0.05	3.03 ± 0.22	2.79 ± 0.15	77.0 ± 2.84
Isosilybin B	1.52 ± 0.03	0.16 ± 0.00	0.87 ± 0.05	0.67 ± 0.03	21.2 ± 0.39

3.2.2 Simultaneous determination of Log P, Log D and pKa of Silymarin constituents

Despite silymarin is most extensively studied for various *in vitro* and *in vivo* pharmacological activities, the physicochemical properties of individual constituents are yet to be determined experimentally. Lipophilicity (Log P and Log D) and dissociation constant (pKa) is an intrinsic property of a molecule, which are most important factors influencing absorption, distribution, metabolism and excretion of a drug. These factors are used in early discovery to predict the *in vivo* pharmacokinetics and to facilitate formulation development (71). The Log D is logarithmic ratio of drug concentration in octanol to drug concentration in buffer of particular pH. The Log P is the logarithmic ratio of drug concentration in octanol to drug concentration in aqueous phase, as the unionized form. The pKa of silymarin constituents were calculated by plotting the measured Log D (pH) as a function of apparent pH described by Po-Chang Chiang et al (71).

The results in Table 4 demonstrates Log P and Log D (pH 7.4) of silymarin constituents are in following order ISB > ISB > SB = SA > SD > SC > TX and ISA ≥ ISB ≥ SA ≥ SB > SC >

TX ≥ SD, respectively. The pKa of all silymarin constituents were in range of 5.57 to 6.10 (Table 4). The plot of Log D (pH) vs pH in Figure 2 depicts all silymarin constituents are weakly acidic drugs and they remain unionized in entire pH range of GI tract and consequently, decrease in the solubility of SC, SD, SA, SB, ISA and ISB in FASSGF, FESSGF and FESSIF (Table 3). This plot indicates, if silymarin constituents are administered in solubilized form their absorption would be rapid in entire GI tract.

Table 4. The Log P, Log D and pKa of silymarin constituents. Each point represents mean ± SD of triplicate values.

Silymarin Constituents	**Log P**	**Log D (pH 7.4)**	**pKa**
Taxifolin	1.06 ± 0.06	0.19 ± 0.01	5.79 ± 0.02
Silychristin	1.51 ± 0.01	1.06 ± 0.01	5.82 ± 0.11
Silydianin	1.16 ± 0.05	0.14 ± 0.08	5.57 ± 0.13
Silybin A	2.29 ± 0.03	1.77 ± 0.01	6.03 ± 0.03
Silybin B	2.26 ± 0.07	1.80 ± 0.01	6.10 ± 0.10
Isosilybin A	2.55 ± 0.40	1.89 ± 0.03	5.85 ± 0.52
Isosilybin B	2.69 ± 0.27	1.94 ± 0.07	5.70 ± 0.35

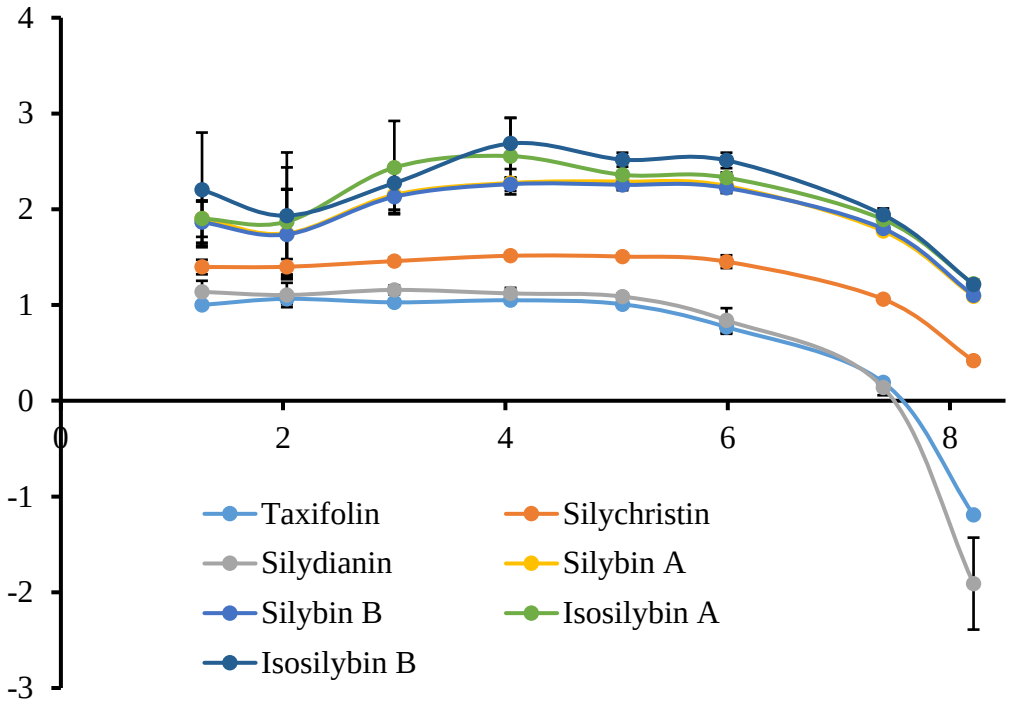

Figure 2. The Log D vs pH of silymarin constituents. Each point represents mean ± SD of triplicate values.

3.3 Phase Solubility

The phase solubility curve (Figure 3) of silymarin prepared by both methods (conventional and heating) depicts a linear increase in solubility of silymarin constituents as a function of increase in concentration of SBE-β-CD, indicating an A_N type curve (47). The affinity (stability) constants ($K_{1:1}$) and complexation efficiencies (CE) of SBE-β-CD–silymarin constituents were calculated from slope and intercept of phase solubility curve.

Equation 1. Stability constant

$$\boldsymbol{K_{1:1} = \frac{m}{S_0(1-m)}}$$

Equation 2. Complexation efficiency

$$\boldsymbol{CE = \frac{m}{(1-m)}}$$

where *m* is the slope of the curve obtained by plotting the drug solubility versus cyclodextrin concentration, determined by linear regression. The *CE* and $K_{1:1}$ of the SBE-β-CD–silymarin complex are presented in Table 5. The *CE* and $K_{1:1}$ of silymarin constituents were calculated considering the intrinsic solubility of silymarin constituents in water. The increase in the solubility of silymarin constituents was higher, when heating method was used compared to conventional method. The formation of cyclodextrin–drug inclusion complex depends on their steric arrangement and thermodynamic factors. The complexation process involves dislodging of water molecule from the hydrophobic cavity and formation of hydrogen bond interactions between cyclodextrin and drug molecule (72). In heat method, on increasing the temperature to 75 °C of the cyclodextrin–silymarin mixture, the process of water molecule removal from hydrophilic cavity of cyclodextrin is accelerated and favors the accommodation of drug moiety into the cavity. The conventional method requires longer duration for cyclodextrin to attain equilibrium with drug molecule, this could be 3 to 7 days differ from molecule to molecule. In case of heating method, the time taken is only 60 minutes and can be used for molecules which are stable at 75 °C, this method can be easily adopted for scaleup process in industries.

The solubility of TX, SC, SD, SA, SB, ISA and ISB in 100 mM of SBE-β-CD prepared using heating method was found to be increased by 12.2, 36.2, 138, 650, 400, 377 and 522 folds compared to their intrinsic solubility, respectively (Figure 4). The solubility of TX, SC, SD, SA, SB, ISA and ISB in 100 mM of SBE-β-CD prepared using conventional method was found to be increased by 9.57, 33.3, 124, 262, 231, 316 and 442 folds compared to their intrinsic solubility, respectively (Figure 5). The $K_{1:1}$ of SBE-β-CD–silymarin constituents complex were in the order of ISB > ISA > SA > SB > SD > SC > TX and ISB > SA > SB > ISA > SD > SC > TX for complexes prepared by conventional and heating method, respectively (Table 5). The stability

constant of silymarin constituent complexes prepared by both methods are directly proportional to Log P of silymarin, this indicates increase in lipophilicity of molecule have higher affinity to cyclodextrin cavity (Table 4 and 5).

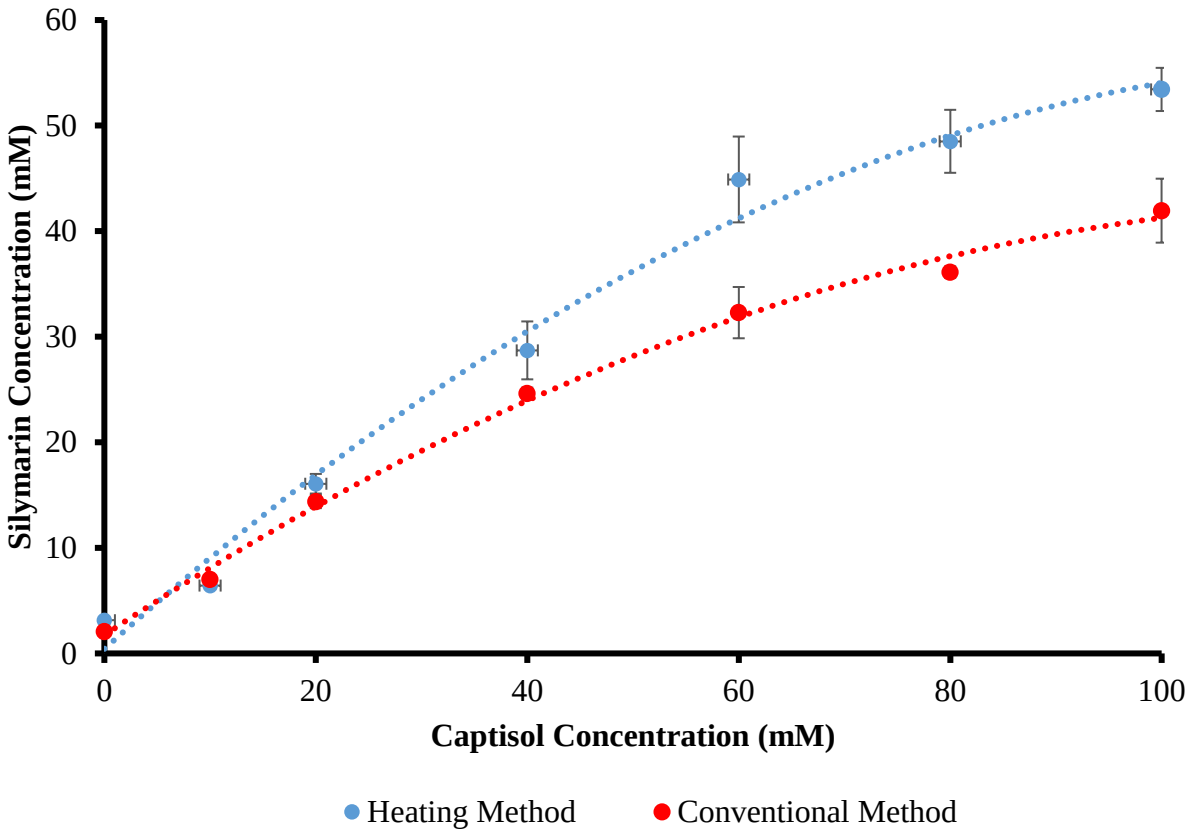

Figure 3. Phase solubility profile of Silymarin in SBE-β-CD by heating and conventional method. Each point represents mean ± SD of triplicate values.

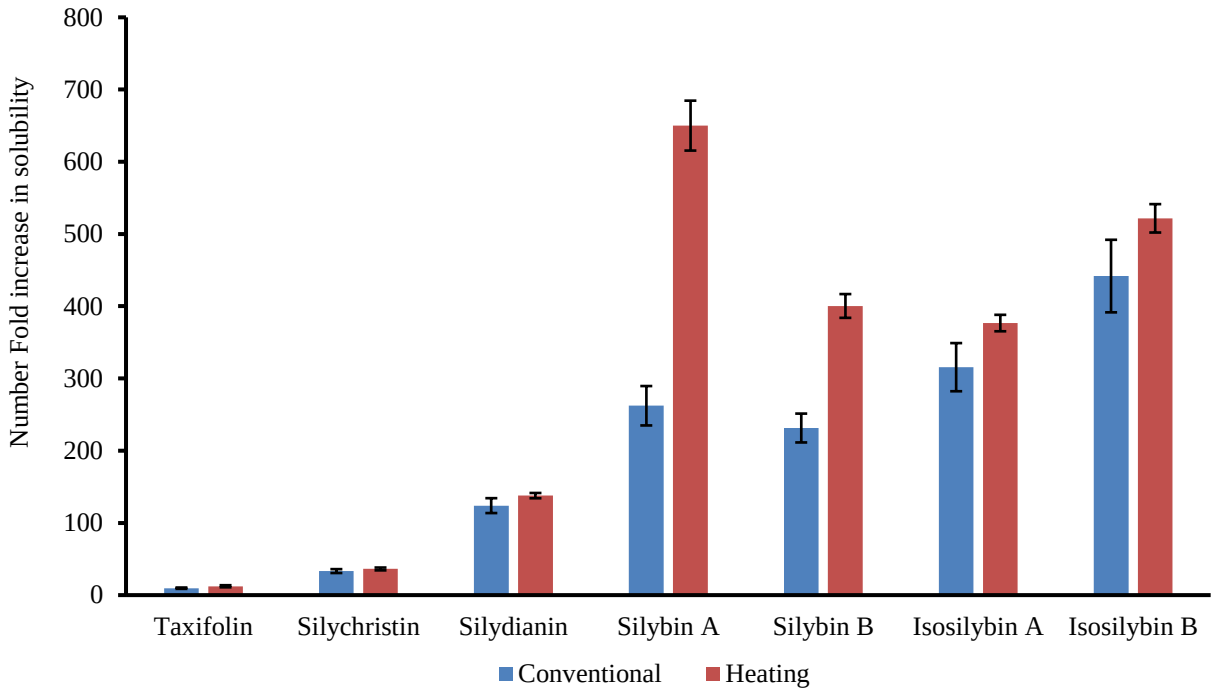

Figure 4. Number fold increase in **s**olubility of silymarin constituents by SBE-β-CD prepared using heating and conventional method. Each point represents mean ± SD of triplicate values.

Table 5. Solubility of silymarin constituents in 100 mM SBE-β-CD, complexation efficiency (CE) and stability constant ($K_{1:1}$) of silymarin constituents in SBE-β-CD prepared using heating and conventional method. Each point represents mean ± SD of triplicate values.

Silymarin Constituents	**Heating**			**Conventional**		
	(mM ± S.D.)	**CE**	**$K_{1:1}$**	**(mM ± S.D.)**	**CE**	**$K_{1:1}$**
Taxifolin	5.43 ± 0.52	0.038 ± 0.006	85.4 ± 13.6	4.24 ± 0.33	0.025 ± 0.001	58.4 ± 4.16
Silychristin	10.9 ± 0.48	0.123 ± 0.009	409 ± 29.9	10.0 ± 0.65	0.106 ± 0.004	355 ± 13.4
Silydianin	16.0 ± 0.35	0.207 ± 0.011	1784 ± 93.2	14.4 ± 0.98	0.170 ± 0.007	1471 ± 63.6
Silybin A	4.65 ± 0.20	0.049 ± 0.002	6889 ± 306	1.88 ± 0.16	0.018 ± 0.001	2578 ± 130
Silybin B	9.13 ± 0.31	0.106 ± 0.006	4665 ± 247	5.28 ± 0.37	0.054 ± 0.002	2368 ± 89.0
Isosilybin A	5.70 ± 0.14	0.068 ± 0.005	4474 ± 308	4.77 ± 0.41	0.051 ± 0.003	3405 ± 167
Isosilybin B	1.64 ± 0.05	0.019 ± 0.001	6056 ± 256	1.39 ± 0.13	0.014 ± 0.001	4560 ± 308

3.4 Solubility of SBE-β-CD-silymarin complex in simulated GI fluids

The drug to get absorbed across the membrane barriers, drug has to be in their solubilized form at the site of absorption (47). To ensure the silymarin remains in their solubilized form in GI fluids on oral administration, its essential to evaluate the stability and solubility of SBE-β-CD-silymarin complex in simulated GI fluids.

There was no change in solubility of silymarin, except for SBE-β-CD-SD the solubility was decreased in FASSIF and FESSIF by 33.4 and 14.7 %, respectively. The decrease in solubility of SD could be due to contents of FESSIF and FASSIF displacing the SD from the cavity of SBE-β-CD. Previous reported studies have demonstrated sodium taurocholate and lecithin present in intestinal fluid displaces progesterone from HP-β-CD-progesterone complex (19).

Table 6. Solubility of SBE-β-CD–Silymarin complex in water and in simulated gastrointestinal fluid. Each point represents the mean ± SD of triplicate values.

Silymarin constituents	**Water (µg/mL)**	**FASSGF (%)**	**FESSGF (%)**	**FASSIF (%)**	**FESSIF (%)**
Taxifolin	292 ± 1.27	100 ± 0.73	101 ± 1.03	97.0 ± 2.06	98.1 ± 1.36
Silychristin	868 ± 2.71	100 ± 1.15	100 ± 1.58	97.1 ± 1.32	93.7 ± 1.09
Silydianin	234 ± 3.23	100 ± 1.47	101 ± 2.05	66.6 ± 3.45	85.3 ± 1.73
Silybin A	159 ± 0.52	102 ± 1.26	101 ± 0.88	100 ± 1.89	97.7 ± 0.74
Silybin B	369 ± 1.68	101 ± 0.84	101 ± 0.90	99.2 ± 1.75	98.1 ± 1.12
Isosilybin A	443 ± 2.51	101 ± 0.72	101 ± 1.22	98.2 ± 1.40	96.0 ± 1.62
Isosilybin B	124 ± 0.97	100 ± 1.30	101 ± 2.08	100 ± 1.76	95.3 ± 2.75

3.5 Stability studies

The stability of the lyophilized silymarin complex prepared by conventional method under two sets of conditions, 25 °C (60% RH) and 40 °C (75% RH), was ≥ 94.4 and ≥ 90.1% for periods 12 months, respectively (Figure 5). The stability of the lyophilized silymarin complex prepared by heating method under two sets of conditions, 25 °C (60% RH) and 40 °C (75% RH), was ≥ 92.2 and ≥ 94.2% for periods 12 months, respectively (Figure 5).

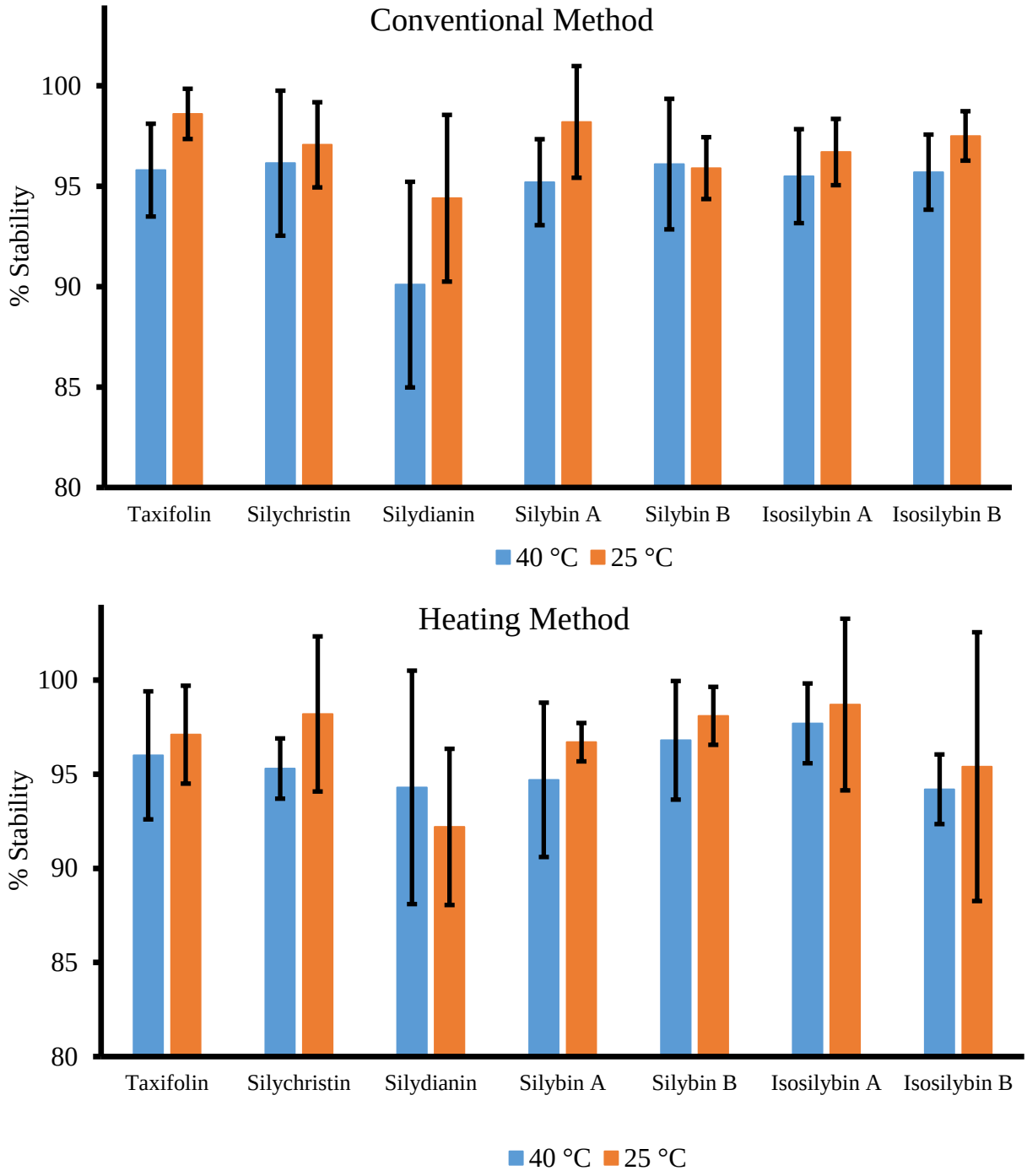

Figure 5. Stability of the lyophilized SBE-β-CD–silymarin complex prepared by heating and conventional methods at 25 °C (60% RH) and 40 °C (75% RH) for periods of 12 months. Each point represents the mean ± SD of triplicate values.

3.6 *Ex vivo* porcine intestinal permeation studies

The *ex vivo* porcine intestinal permeation study results shown in Figure 6 demonstrates that the SBE-β-CD–silymarin constituents complex have higher permeability compared to silymarin constituents dissolved in PBS containing 0.5% of Brij S20. The silymarin was dissolved in PBS containing 0.5% of Brij S20, as they are not soluble in aqueous media Brij S20 was used to facilitate the solubilization. The intestinal apparent permeability coefficient P_{app} of silymarin was in following order for TX > SD > SC > SA ≥ SB ≥ ISA ≥ ISB and ISB > SA > SB > ISA > SC > TX ≥ SD, respectively. The lag phase for silymarin constituents dissolved in Brij S20 for TX, SC were 2 h and for SD, SA, SB, ISA and ISB were 4 h, In case of SBE-β-CD–silymarin complex there was no lag phase observed.

The intestinal apparent permeability coefficient P_{app} of TX, SC, SD, SA, SB, ISA and ISB from SBE-β-CD–silymarin constituents complex was 4.80, 20.5, 10.2, 67.1, 77.7, 40.9 and 117 fold higher compared to silymarin constituents dissolved in PBS containing 0.5% of Brij S20, respectively. The permeation across barrier was directly proportional to partition coefficient and concentration gradient of a compound across the barrier (Table 4, 5 and 7, Figure 6). The *ex vivo* intestinal permeability study results indicate SBE-β-CD used in the formulation increased permeation of silymarin across the intestinal barrier. The enhancement of permeation was due to increasing in concentration gradient across the barrier and SBE-β-CD's permeation enhancing effect on barrier.

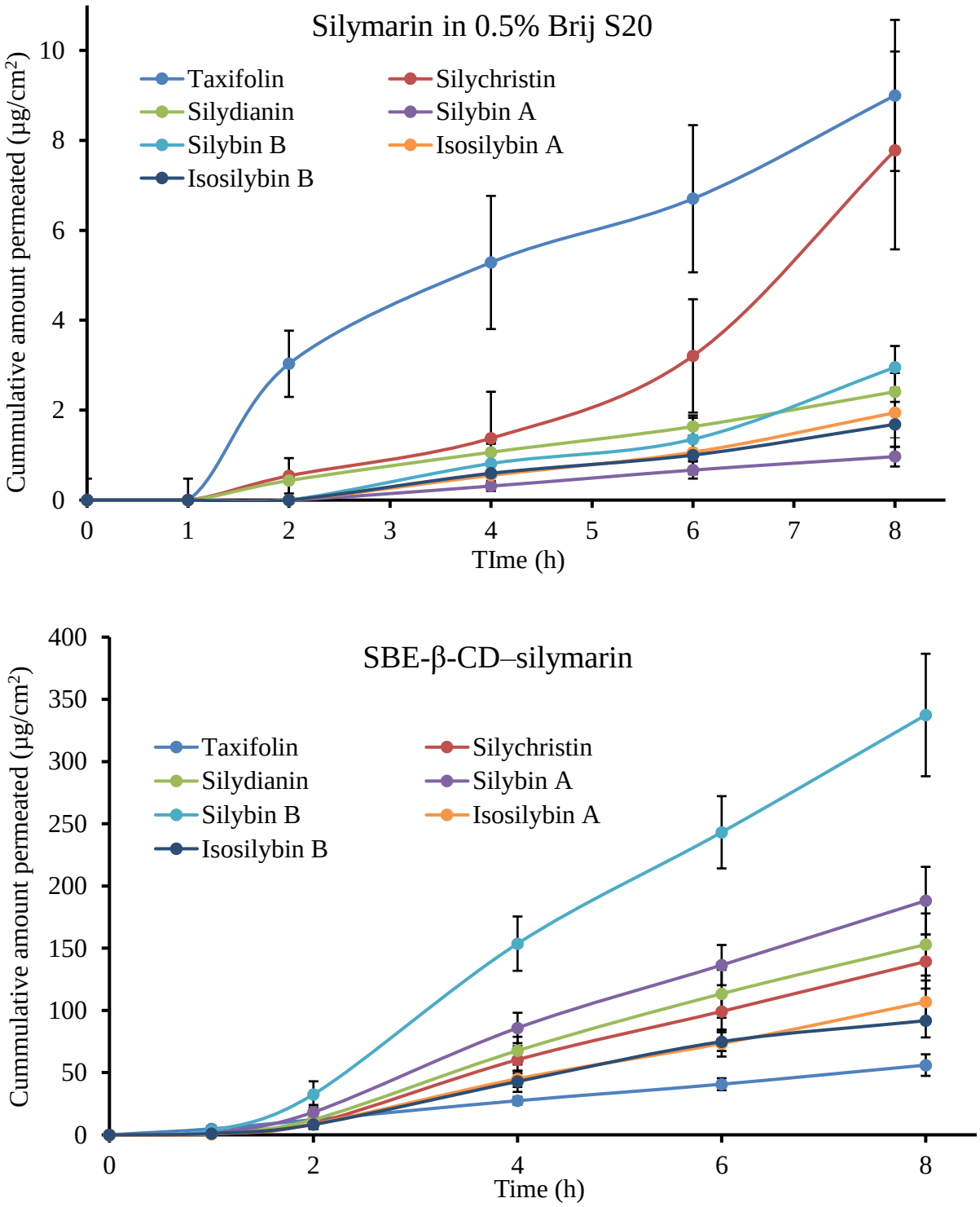

Figure 6. Permeation of silymarin across rat intestine: Silymarin in 0.5% of Brij S20 and SBE-β-CD–silymarin complex in water. Each point represents the mean ± SD of sextuplicate values.

Table 7. Apparent intestinal permeability (P_{app}) of silymarin: SBE-β-CD–silymarin complex in water and silymarin in 0.5% of Brij S20. Each point represents the mean ± SD of sextuplicate values.

Silymarin Constituents	SBE-β-CD–silymarin complex	Silymarin in 0.5% of Brij S20
Taxifolin	4.51 ± 0.72	0.94 ± 0.22
Silychristin	5.94 ± 0.87	0.29 ± 0.18
Silydianin	4.47 ± 0.71	0.44 ± 0.08
Silybin A	18.8 ± 2.47	0.28 ± 0.07
Silybin B	17.1 ± 2.27	0.22 ± 0.10
Isosilybin A	8.59 ± 1.27	0.21 ± 0.06
Isosilybin B	26.8 ± 3.39	0.23 ± 0.07

3.7 Recovery

The simple protein precipitation method was employed for extraction of Silymarin constituents from plasma and tissue homogenate. As silymarin constituents have good solubility in acetonitrile and methanol. The extraction trials were performed with acidified and alkalinized acetonitrile and methanol for enhancing the recovery of analytes from biological samples and to precipitate proteins. At different concentration level (LQC and HQC) of each analyte the recovery was evaluated, and peak area ratio was considered for the calculations. The results (Table 8) demonstrated the recovery of TX, SD, SC, SA, SB, ISA and ISB from different matrices were concentration independent and reproducible with the use of acetonitrile (without acidification nor alkalinization).

Table 8. The percentage recovery of Silymarin constituents in rat plasma and tissue homogenate.

Silymarin			Matrix (n=3) mean ± SD							
	QC levels	Conc. (ng/mL)	Plasma	Liver	Spleen	Brain	Lungs	Heart	Kidney	Ocular
Taxifolin	LQC	91.2	84.1 ± 7.59	89.5 ± 1.90	95.7 ± 3.03	93.8 ± 10.3	103 ± 3.22	96.5 ± 4.59	99.3 ± 7.22	95.5 ± 6.02
	HQC	3162	79.9 ± 1.39	97.9 ± 8.14	93.0 ± 2.95	101 ± 3.86	103 ± 3.49	91.9 ± 1.89	100 ± 3.61	89.5 ± 7.65
	MQC	4864	77.9 ± 5.57	93.5 ± 6.55	109 ± 3.49	106 ± 2.51	101 ± 6.98	99.5 ± 1.94	106 ± 4.15	88.5 ± 4.96
Silychrsitin	LQC	145	95.3 ± 3.90	90.1 ± 7.21	92.9 ± 7.17	104 ± 2.00	85.8 ± 2.57	101 ± 5.82	99.1 ± 9.26	87.0 ± 3.48
	HQC	5017	103 ± 2.40	90.9 ± 4.08	93.9 ± 1.46	91.9 ± 4.57	97.3 ± 2.65	90.0 ± 0.86	87.9 ± 2.14	85.3 ± 6.62
	MQC	7719	100 ± 8.01	94.7 ± 5.05	94.3 ± 2.48	92.6 ± 5.02	96.3 ± 4.11	92.8 ± 0.21	90.3 ± 3.71	85.5 ± 4.05
Silydianin	LQC	145	96.2 ± 7.37	96.8 ± 9.05	91.1 ± 4.63	99.2 ± 12.3	97.9 ± 9.27	93.0 ± 4.66	101 ± 6.47	86.5 ± 6.69
	HQC	5017	101 ± 5.75	94.9 ± 6.03	108 ± 1.92	94.5 ± 2.09	105 ± 15.00	104 ± 0.09	98.8 ± 1.35	93.9 ± 9.03
	MQC	7719	92.0 ± 2.72	96.2 ± 2.55	96.6 ± 3.15	87.1 ± 2.04	102 ± 5.65	97.1 ± 0.23	96.5 ± 3.90	85.4 ± 4.61
Silybin A	LQC	72.4	94.3 ± 6.76	86.7 ± 1.76	102 ± 7.31	103 ± 3.98	99.5 ± 4.57	97.5 ± 5.09	86.7 ± 1.37	74.0 ± 4.09
	HQC	2509	105 ± 2.01	91.1 ± 3.83	94.6 ± 2.10	91.3 ± 4.99	96.8 ± 1.65	89.2 ± 1.72	87.9 ± 1.34	83.1 ± 6.54
	MQC	3860	102 ± 8.27	99.9 ± 5.32	94.3 ± 2.16	97.3 ± 1.66	94.1 ± 5.52	91.6 ± 0.39	89.3 ± 3.73	81.5 ± 4.84
Silybin B	LQC	72.4	90.1 ± 5.36	96.6 ± 9.54	96.5 ± 7.66	103 ±12.3	96.7 ± 7.75	93.4 ± 4.21	102 ± 10.7	86.7 ± 5.64
	HQC	2509	103 ± 3.56	92.0 ± 3.71	93.5 ± 1.79	91.9 ± 5.09	97.5 ± 3.21	89.7 ± 0.34	88.4 ± 1.73	85.3 ± 7.03
	MQC	3860	99.9 ± 8.86	99.1 ± 5.44	94.4 ± 1.85	96.4 ± 1.91	95.3 ± 4.53	92.5 ± 0.16	87.5 ± 0.60	82.8 ± 2.57
Isosilybin A	LQC	109	104 ± 3.36	97.4 ± 1.91	98.2 ± 4.46	99.1 ± 2.85	99.0 ± 2.68	82.4 ± 4.36	95.3 ± 7.73	71.7 ± 1.73
	HQC	3763	103 ± 4.07	92.0 ± 2.55	94.0 ± 1.62	90.2 ± 5.89	96.5 ± 2.60	88.4 ± 1.94	88.1 ± 1.49	84.0 ± 6.56
	MQC	5789	98.7 ± 9.74	99.6 ± 5.17	94.3 ± 1.96	96.3 ± 2.07	95.4 ± 4.57	92.1 ± 0.60	89.9 ± 3.66	84.7 ± 2.76
Isosilybin B	LQC	36.2	100 ± 5.17	97.0 ± 15.2	86.4 ± 8.49	98.6 ± 4.32	102 ± 4.97	104 ± 7.76	94.1 ± 4.12	76.0 ± 2.28
	HQC	1254	103 ± 3.62	93.0 ± 3.79	95.3 ± 1.98	91.3 ± 4.57	96.4 ± 3.14	88.7 ± 0.05	86.9 ± 1.40	83.4 ± 6.20
	MQC	1930	99.1 ± 9.27	99.3 ± 5.53	95.6 ± 1.83	95.9 ± 1.76	95.0 ± 5.03	93.0 ± 0.73	89.2 ± 3.73	86.8 ± 4.65

3.8 *In vivo* pharmacokinetic studies

As the silymarin is most extensively used herbal supplement and clinically studied for various pharmacological activities, it is essential to the study pharmacokinetics of all seven constituents of silymarin in preclinical models prior to testing on human subjects. The plasma profile of silymarin oral bioavailability depicts AUC of silymarin are higher in group of animals administered with SBE-β-CD–silymarin complex compared to group administered with silymarin suspension. The Figure 7 demonstrates, absorption of silymarin was faster and higher in SBE-β-CD–silymarin complex group compared to silymarin suspension group. The AUC considered for determining the relative oral bioavailability of TX, SC, SD, SA, SB, ISA and ISB was 0 to 60, 0 to 60, 0 to 30, 0 to 120 min, 0 to 120 min, 0 to 120 min and 0 to 90 min, respectively (Figure 7 and Table 9). The relative oral bioavailability of TX, SC, SA, SB, ISA and ISB in SBE-β-CD–silymarin complex group was found to be increased by 1.31, 2.37, 3.51, 2.82, 6.64 and 5.71 compared to silymarin suspension group, respectively (Table 9). This study demonstrates SBE-β-CD–silymarin complex would be better formulation for enhancing the oral bioavailability of TX, SC, SA, SB, ISA and ISB.

The relative bioavailability of SD was same in both groups SBE-β-CD–silymarin complex and silymarin suspension group, there was no influence of SBE-β-CD. Previous reported studies have demonstrated, bile salt in intestinal fluid replaces drug from cyclodextrin cavity leading to precipitating the drug in intestinal lumen and thus decreasing the drug absorption (19,41,42). The above studies demonstrate, the decrease in bioavailability of SD could be due to their lower log P and displacement of SD from SBE-β-CD–SD complex by GI contents of FASSIF and FESSIF by 33.3 and 14.7%, respectively.

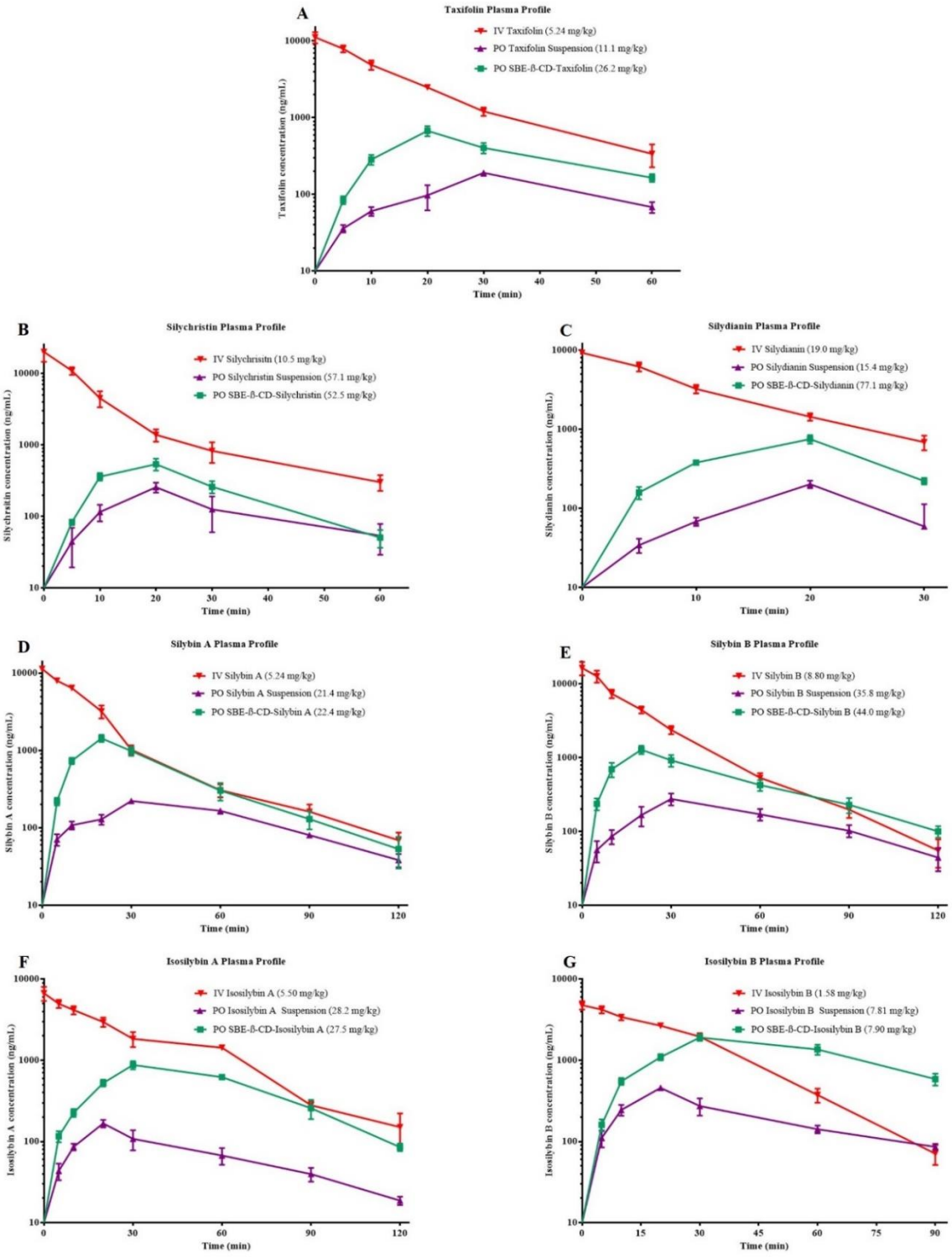

Figure 7. Plasma profile of taxifolin(A), silychrsitin(B), silydianin(C), silybin A(D), silybin B(E), isosilybin A(F) and isosilybin B(G) upon oral administration of SBE-β-CD–silymarin complex, silymarin suspension, and IV administered SBE-β-CD–silymarin complex. Each point represents the mean ± SD of quadruplicate values.

Table 9. The silymarin dose administered to animals and pharmacokinetic parameters of silymarin in rats on oral administration of silymarin suspension and SBE-β-CD–silymarin complex, and intravenous administration of SBE-β-CD–silymarin complex. Each point represents the mean ± SD of quadruplicate values.

Parameters	Oral silymarin suspension						
	Taxifolin	Silychristin	Silydianin	Silybin A	Silybin B	Isosilybin A	Isosilybin B
Dose (mg/kg/BW)	11.1	57.1	19.0	21.4	35.8	28.2	7.81
$AUC_{0-2\,h}$ (ng.h/mL)	107 ± 14.2	116 ± 30.7	50.0 ± 8.90	248 ± 11.0	283 ± 35.5	136 ± 9.25	300 ± 24.5
Tmax (min)	30	20	20	30	30	20	20
Cmax (ng/mL)	191 ± 34.6	256 ± 65	202 ± 54.4	223 ± 19.1	276 ± 50.4	167 ± 30.3	458 ± 65.3
$T_{1/2}$	NA	NA	NA	204 ± 23.1	70.1 ± 9.31	79.7 ± 21.0	88.2 ± 14.8
% F_{abs}	1.93 ± 0.29	0.71 ± 0.22	2.55 ± 0.52	1.98 ± 0.10	1.52 ± 0.22	1.01 ± 0.08	2.66 ± 0.25
Oral SBE-β-CD–Silymarin complex							
Dose (mg/kg/BW)	26.2	52.5	77.1	22.4	44.0	27.5	7.9
$AUC_{0-2\,h}$ (ng.h/mL)	391 ± 44.3	241 ± 30.2	204 ± 15.9	907 ± 89.4	982 ± 146	878 ± 22.4	1729 ± 141
Tmax (min)	20	20	20	20	20	30	30
Cmax (ng/mL)	673 ± 101	538 ± 102	752 ± 91.6	1438 ± 153	1260 ± 173	876 ± 102	1911 ± 180
$T_{1/2}$ (min)	58.3 ± 4.05	NA	NA	57.6 ± 18.6	66.3 ± 2.39	48.5 ± 4.38	40.7 ± 2.58
% F_{abs}	2.52 ± 0.34	1.68 ± 0.24	2.56 ± 0.23	6.94 ± 0.79	4.28 ± 0.73	6.64 ± 0.20	15.2 ± 1.42
Intravenous SBE-β-CD–silymarin complex							
Dose (mg/kg/BW)	5.24	10.5	15.4	5.24	8.80	5.50	1.58
$AUC_{0-2\,h}$ (ng.h/mL)	2625 ± 158	2862 ± 420	1601 ± 45.8	3061 ± 210	4584 ± 404	2886 ± 111	2279 ± 117
C_0 (ng/mL)	11147 ± 1878	19962 ± 5483	9241 ± 588	11316 ± 759	16418 ± 3393	6700 ± 1330	4765 ± 456
C_{max} (ng/mL)	7907 ± 816	10839 ± 1321	6183 ± 797	7950 ± 318	12737 ± 2356	4973 ± 564	4213 ± 349
$T_{1/2}$	54.7 ± 6.43	43.0 ± 13.4	44.7 ± 5.57	27.3 ± 1.21	42.5 ± 0.83	60.7 ± 13.5	60.8 ± 5.70
Cl (ml)	28.5 ± 1.30	58.2 ± 7.39	135 ± 3.79	27.6 ± 1.62	28.8 ± 2.30	18.3 ± 2.06	9.17 ± 0.91
Vd (L/kg)	2.26 ± 0.35	3.25 ± 0.66	8.67 ± 0.96	1.09 ± 0.10	1.76 ± 0.11	1.57 ± 0.16	0.80 ± 0.07

Note: NA: Due levels were below limit of quantitation in plasma samples elimination phase was not able to capture to calculate $T_{1/2}$

3.9 Estimation of silymarin metabolites in oral pharmacokinetic plasma samples

Although aqueous solubility and *ex vivo* intestinal permeation of silymarin was increased by several folds by SBE-β-CD and no displacement of TX, SD, SA, SB, ISA and ISB from SBE-β-CD cavity in GI fluids, the oral bioavailability increase of SBE-β-CD–silymarin was approximately 1.31- 6.64 folds. The decrease in oral bioavailability could be due to extensive first pass metabolism and elimination of silymarin (62,73). In present study, the oral plasma samples were treated with glucuronidase and sulfatase enzyme to estimate the unconjugated, glucuronide conjugate, sulfate conjugate and total (free and conjugated) silymarin. The concentration of total silymarin in oral plasma samples would suggest the extent of silymarin absorption on oral administration. The AUC of unconjugated, conjugated and total silymarin on oral administration of silymarin suspension and SBE-β-CD–silymarin are depicted in Figure 8A and B, respectively.

The Tmax of glucuronide and sulfate conjugate TX, SC, SD, SA, SB, ISA and ISB was same as Tmax of unconjugated/free silymarin on oral administration. The AUC of total TX, SC, SD, SA, SB, ISA and ISB was increased by 10.5, 28.0, 16.8, 22.9, 15.0, 14.0 and 10.5 fold compared to unconjugated/free silymarin on oral administration of silymarin suspension, respectively. The AUC of total TX, SC, SD, SA, SB, ISA and ISB was increased by 12.6, 35.4, 22.1, 39.2, 22.7, 21.3 and 17.7 fold compared to unconjugated/free silymarin on oral administration of SBE-β-CD–silymarin, respectively. The results demonstrate 64.4 and 27.8% of silymarin are present as glucuronide and sulfate conjugate on oral administration of silymarin suspension, respectively and 68.7 and 27.2% of silymarin are present as glucuronide and sulfate conjugate on oral administration of silymarin suspension. This study indicates the extent of absorption was increased on oral administration of SBE-β-CD–silymarin complex compared to silymarin suspension and the percentage of metabolite formed was same in both groups.

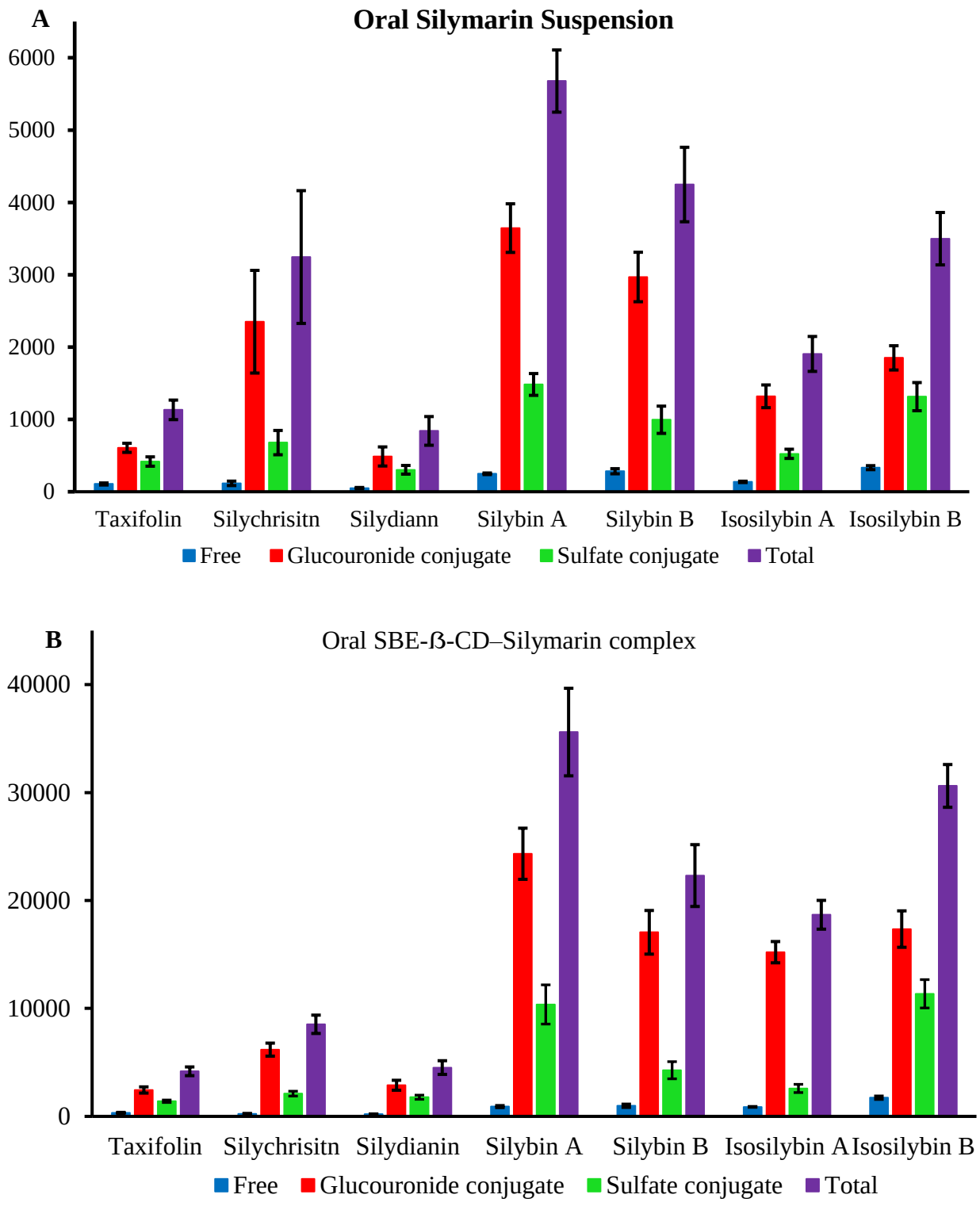

Figure 8. The AUC_{0-t} of free silymarin, glucouronide silymarin conjugate, sulphate silymarin conjugate and total silymarin in rat plasma on oral administration of silymarin suspension(A) and SBE-β-CD–silymarin complex(B) in rat plasma. Each point represents the mean ± SD of quadruplicate values.

3.10 Silymarin tissue distribution

Over 30 clinical studies have carried out to evaluate the potential therapeutic effects of silymarin extract or silibinin or used as an adjunct drug along with other therapeutic agents in management and treatment of various disorders like diabetic nephropathy, hepatitis, tuberculosis, leukemia, nonalcoholic fatty liver disease, prostate cancer, upper gastrointestinal adenocarcinoma, liver toxicants, metastatic colorectal cancer, galactagogues effect, Beta-Thalassemia major and steatosis. These clinical studies have been carried out by administering Legalon®, Silymarin phytosome and silymarin extract, most of the studies have shown inconsistent study results attributed to its low and variable oral bioavailability (<10% in humans) (74). Hence, it is important to evaluate the amount of silymarin distributed to its target organ in preclinical species prior to evaluating the therapeutic effect of silymarin in humans.

The concentration of silymarin in different tissue are presented in Figure 9. On oral administration of silymarin formulations, silymarin constituents TX, SC, SD, SA, SB, ISA and ISB levels were found in lungs, kidney and liver. All constituents were found in spleen except SD and ISB, whereas only SB and SC levels were found in brain and, SC, ISA, SA and SB were found in heart. The total amount of silymarin present in liver, brain, spleen, lungs, kidney and heart was found to be 1172, 326, 334, 988, 535 and 260 ng/gm of tissues on oral administration of SBE-β-CD–silymarin complex. The total amount of silymarin present in liver, brain, spleen, lungs, kidney, heart and ocular was found to be 2377, 310, 739, 6804, 1141, 350 and 125 ng/gm of tissues on oral administration of SBE-β-CD–silymarin complex.

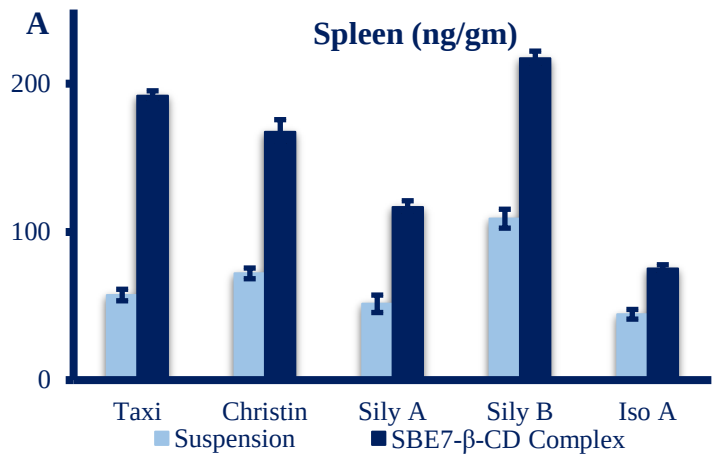
A
Spleen (ng/gm)
200
100
0
Taxi
Christin
Sily A
Sily B
Iso A
Suspension
SBE7-β-CD Complex

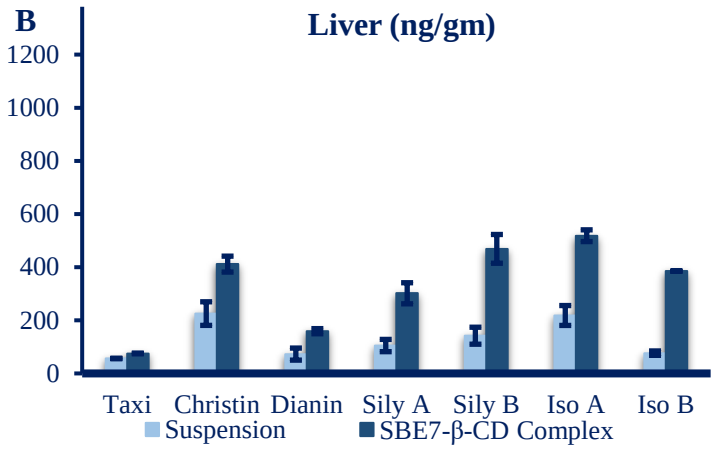
B
Liver (ng/gm)
1200
1000
800
600
400
200
0
Taxi
Christin
Dianin
Sily A
Sily B
Iso A
Iso B
Suspension
SBE7-β-CD Complex

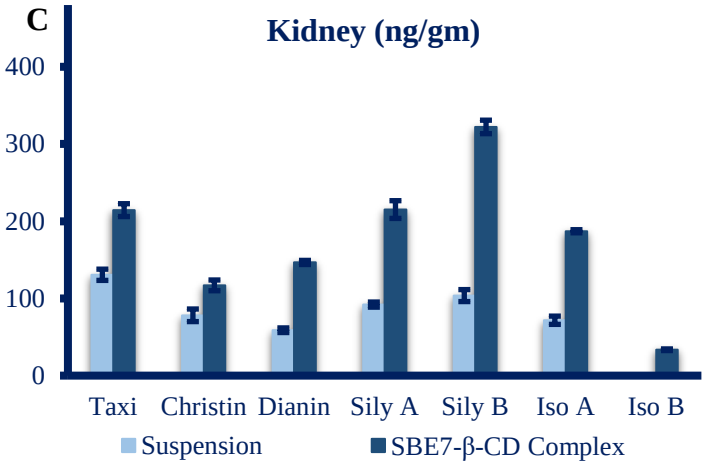
C
Kidney (ng/gm)
400
300
200
100
0
Taxi
Christin
Dianin
Sily A
Sily B
Iso A
Iso B
Suspension
SBE7-β-CD Complex

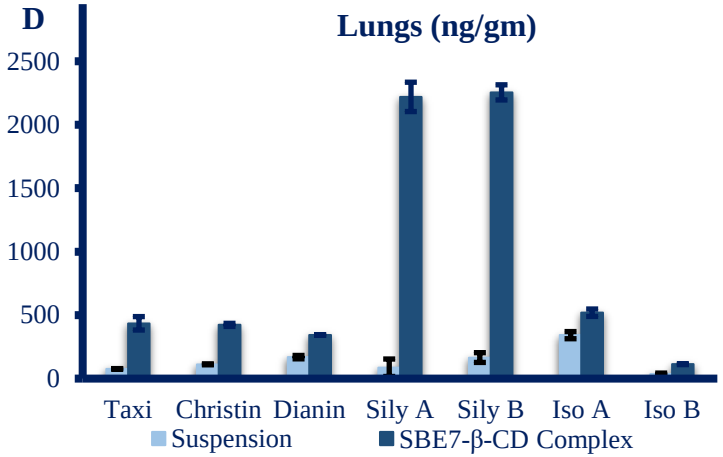
D
Lungs (ng/gm)
2500
2000
1500
1000
500
0
Taxi
Christin
Dianin
Sily A
Sily B
Iso A
Iso B
Suspension
SBE7-β-CD Complex

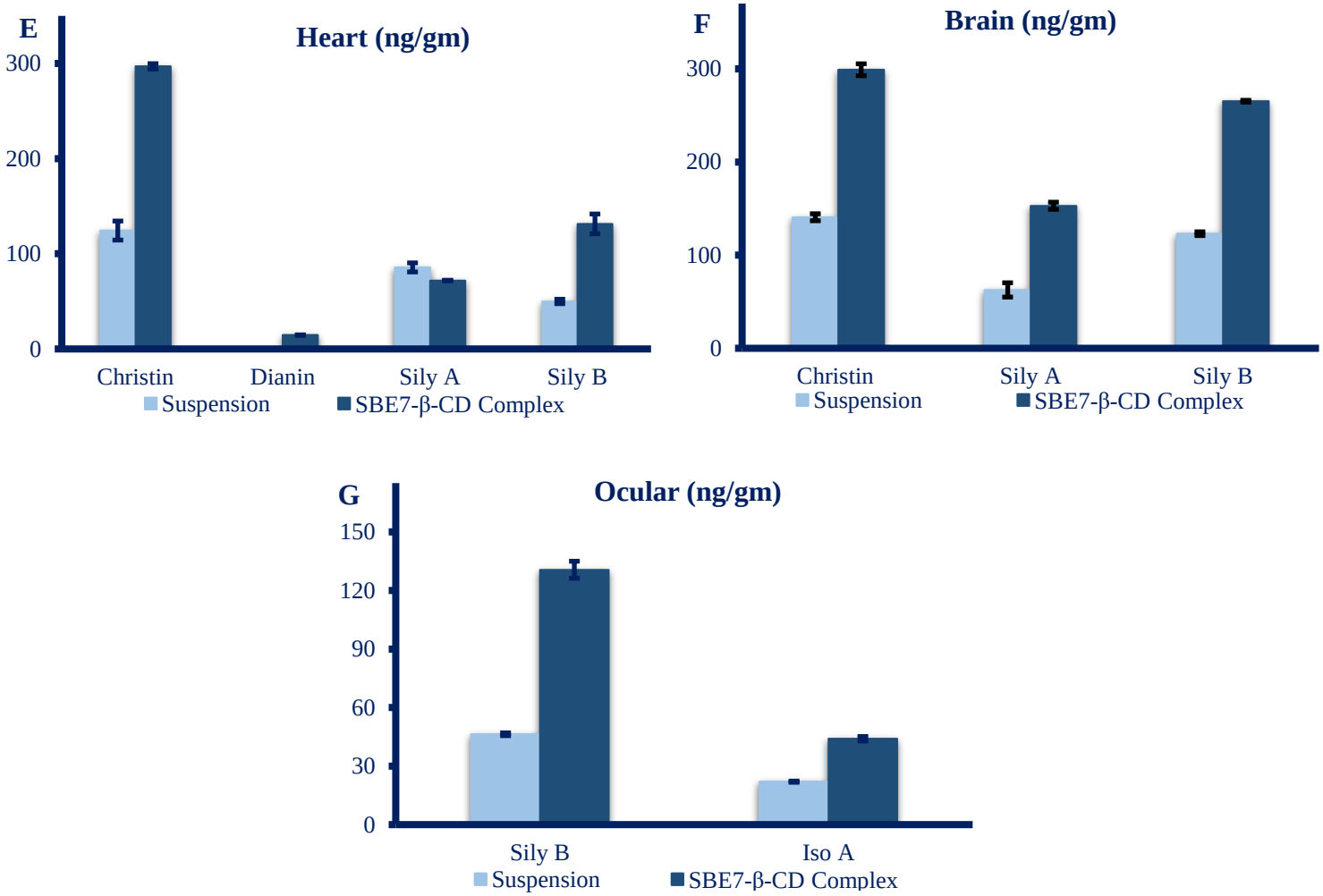

Figure 9. The concentrations of silymarin constituents TX, SC, SD, SA, SB, ISA and ISB in (A) spleen, (B) liver, (C) kidney, (D) lungs, (E) heart, (F) brain and (G) ocular on oral administration of silymarin suspension and SBE-β-CD–silymarin complex

4. Conclusion

The solubility of silymarin in water was enhanced by SBE-β-CD with an A_N type phase solubility curve and heating method was found to be more efficient with less time consuming. The solubility of SBE-β-CD–TX, SC, SA, SB, ISA and ISB complex solubility in GIF was not changed, SBE-β-CD–SD solubility was decreased in FASSIF and FESSIF. The *ex vivo* intestinal permeation of silymarin was increased on SBE-β-CD complexation. There was no effect of SBE-β-CD on oral pharmacokinetics of SD, whereas oral bioavailability of TX, SC, SA, SB, ISA and ISB were increased by 1.31 to 6.64 folds on oral administration of SBE-β-CD–silymarin complex compared to silymarin suspension. The studies indicate 92.2 and 95.9% of absorbed drug are rapidly metabolized on oral administration of silymarin suspension and SBE-β-CD–silymarin, respectively. This study demonstrates heating method can be employed to scale-up the preparation of stable SBE-β-CD–silymarin complex. The tissue distribution studies showed increased levels of silymarin constituents in plasma and tissue samples on oral dosage of SBE-β-CD–silymarin complex and compared to the group dosed with silymarin suspension. This study demonstrates the SBE-β-CD-silymarin complex would be a better alternative to enhance the tissue exposure and oral bioavailability of silymarin constituents.

CHAPTER 4

Development of SBE-β-CD-silymarin Topical Formulation

1. Introduction

Silybum marianum fruits and seeds are used for over 2000 yrs (74) for mitigation of cirrhosis, hepatitis and to protect liver from amanita toxins (56,57). The major constituents of silymarin extract comprises of taxifolin (TX), silychristin (SC), silydianin (SD), silybin A (SA), silybin B (SB), isosilybin A (ISA) and isosilybin B (ISB) (55). In recent times, the extract of Silybum marianum seeds (silymarin) is most extensively studied for variety of pharmacological activities (75). The *in vitro*, preclinical and clinical studies have demonstrated silymarin possesses a dermatological beneficial effect in treatment of UV induced erythema, melanoma, non-melanoma skin cancer, rosacea, melasma, vitiligo, psoriasis and wound healing (76).

The rate limiting step for absorption of silymarin is solubility and the systemic bioavailability of silymarin may be enhanced by increasing solubility (61). The solubility enhancement of BCS class II drug and thus its dermal bioavailability is the most challenging aspects of drug development process of topical drug delivery system. Cyclodextrin inclusion complex preparation technique is most commonly employed to improve the aqueous solubility (7). Our initial studies have demonstrated solubility of silymarin in water was enhanced by SBE-β-CD with an A_N type phase solubility curve and the increase in aqueous solubility of TX, SC, SD, SA, SB, ISA and ISB was 12.3, 36.2, 138, 650, 400, 377 and 522-fold compared to intrinsic aqueous solubility, respectively.

The objective of present study is to determine *in-vitro* dermal kinetics of silymarin constituent in human skin models and develop SBE-β-CD–silymarin topical formulation and their evaluation. The non-specific binding of silymarin to human skin and intrinsic skin clearance of silymarin in human skin model was determined. The porcine skin penetration of SBE-β-CD–silymarin was evaluated and permeation enhancers were screened to potentiate the silymarin penetration. The SBE-β-CD–silymarin topical formulation was developed by incorporation of permeation enhancers and optimized the formulation to stabilize the cream and to increase the permeation of silymarin across skin and penetration of silymarin into skin (human cadaver).

2. Materials and Methods

2.1 Chemicals and reagents

Isosilybin and silychristin was purchased from Tractus Company Limited, England. Silydianin was purchased from ChromaDex Inc. USA. Taxifolin was purchased from Enzo Life Sciences Inc. USA. Silymarin extract, silibinin (silybin), D-α-tocopheryl polyethylene glycol succinate, taurine, Tween 80, phenyl piperazine, Dimethicone and phosphate buffered saline were purchased from Sigma-Aldrich (St. Louis, MO), USA. SBE-β-CD was a gift sample obtained from Ligand Pharmaceuticals, Inc., USA. Sodium taurocholate was purchased from Alfa Aesar, USA. Euthasol® (pentobarbital sodium and phenytoin sodium) solution was procured from Virbac, USA. Methocel E15 Premium EL (hydroxypropyl methyl cellulose) was a gift sample from Dow Chemical company, USA. Polyethylene glycol 400, propylene glycol, octyldodecanol, light mineral oil, macrogol cetostearyl ether 20, cetostearyl alcohol, cremophor A 25 macrogolglycerol ricinoleate, cremophor A6, glycerol monostearate, cetostearyl alcohol 50, cetostearyl alcohol 70 and stearic acid were gift samples obtained from BASF chemicals company, USA. Transcutol was

a gift sample obtained from Gattefosse SAS, France. The HPLC grade solvents acetonitrile, methanol, dibasic potassium phosphate, dibasic sodium phosphate, glacial acetic acid, hydrochloric acid, sodium hydroxide, sodium chloride, sodium acetate, ortho-phosphoric acid and Milli Q water were of research grade used without further purification.

2.2 HPLC analysis

The HPLC system consisted of Waters system equipped with performance PLUS inline degasser along dual λ absorbance detector set at 288 nm. The chromatographic separation of silymarin constituent was achieved on a Symmetry Shield RP18 column (150 x 4.6 mm, 5 µm); which was maintained at ambient room. The binary mobile phase system consisted of reservoir A (Methanol : 10mM Ammonium acetate pH 5 [65:35 v/v]) and reservoir B (10 mM ammonium acetate pH 5) were run as per gradient program (0-1.9 min: 25% A and 75% B; 2.0-14.9 min: 80 % A and 20 % B and 15-37.9 min: 80 % A and 20% B and 38-40 min: 25 % A and 75 % B). A flow rate of 1 mL/min was used throughout the analytical run.

2.3 *In vitro* Human skin Binding

The Human skin drug protein binding of silymarin was evaluated by modified charcoal adsorption method (77). In this method, charcoal was coated with dextran by addition of 0.6 gm of charcoal to 100 mL of DPBS containing 0.06% dextran and stirred with a magnetic stirrer at room temperature. The volume of charcoal suspension required for the experiment was determined. To 15 mL centrifuge tubes 2 (A), 4 (B) and 6 (C) mL of charcoal suspensions were added and centrifuged at 4000 rpm for 30 min. After centrifugation supernatant was carefully decanted and spiked with 1 mL of 10 µM TX, SC, SD, silibinin and isosilybin to charcoal pellets

of 2, 4 and 6 mL in triplicates. These tubes were stirred and immediately centrifuged at 4000 RPM for 30 min, the supernatant was analyzed for silymarin constituents using HPLC. The tubes at which no silymarin constituents were detected was selected for human skin binding assay, as the pellets can completely adsorb unbound silymarin constituents.

Human cadaver skin was minced into smaller pieces and weighed. To 1 gm of skin 4 mL of Dulbecco's Phosphate-Buffered Saline pH 7.4 was added and homogenate using tissue homogenizer. The skin homogenate was equilibrated for 30 min with 10 μM of silymarin constituents (n=3) in triplicates and transferred to centrifuge tube containing pellet of dextran coated charcoal by continuous stirring at 37 °C. The serial samples were withdrawn from the above mixture at 0, 2, 5, 10 and 15 min and centrifuged at 4000 rpm for 10 min. The supernatant was separated and silymarin constituents from supernatant were extracted and subjected to HPLC analysis.

2.4 *In vitro* human skin clearance

2.4.1 *In vitro* human skin S9 fraction clearance

The S9 fractions is tissue homogenate containing cytochrome P450 isoforms (phase I enzymes) and phase II enzymes. The pooled mixed gender human skin S9 fraction was procured from BioIVT company, USA was used for skin clearance studies. TX, SC, SD, silibinin, isosilybin and testosterone at 10 μM was preincubated at 37 °C with human skin S9 fraction (1 mg/mL) in 66.7 mM phosphate buffer pH 7.4 for 5 min. After preincubation nicotinamide adenine dinucleotide phosphate (NADPH) and uridine diphosphate glucuronic acid (UDPGA) was added to above mixture and incubated for 0, 15, 30, 60, 90 and, 120 min. One aliquot was incubated for 120 min (without NADPH and UDPGA), to study any chemical instability or non-NADPH and

UDPGA dependent enzymatic degradation. The reaction was terminated by adding ice-cold quenching solution, and centrifuged for 15 min at 13,000rpm. The supernatant was transferred to a vial and subjected to HPLC analysis to evaluate the amount of silymarin constituents present in the incubation mixture at different time intervals.

Data analysis

Elimination rate constant (ke) is slope obtained by plotting % disappearance vs time

- **T½**= -0.693/ke
- **S9 fraction intrinsic clearance (µL/min/mg)** = (Elimination rate constant * Volume of incubation µL) / protein in incubation (mg)
- **Intrinsic clearance (µL/min/kg)** = S9 fraction intrinsic clearance * protein yield from the human skin S9 fraction

2.4.2 *In vitro* Human epidermal keratinocyte and dermal fibroblast clearance

2.4.2.1 Human epidermal keratinocyte Cell culture

The human epidermal keratinocyte cells were maintained at 37 °C in a humidified atmosphere of 5% CO2 and 90% relative humidity. The Keratinocytes-serum free growth medium with 50 ng/mL human recombinant endothelial growth factor and 2 mM L-glutamine supplemented with 10% fetal bovine serum, penicillin (100 mg/mL) and streptomycin (100 mg/mL) was used for cell growth. The medium was replaced every other day in flask and when the cells reached 80-90% confluence, cells were detached using Trypsin-ethylene diamine tetra acetic acid (EDTA). The detached cells were plated at a density of 0.5 million cells/well in 96-well culture plates.

2.4.2.2 Human dermal fibroblast Cell culture

The human dermal fibroblast cells were maintained at 37 °C in a humidified atmosphere of 5% CO2 and 90% relative humidity. The fibroblast basal medium supplemented with 10% fetal bovine serum, fibroblast growth kit-low serum, penicillin (100 mg. mL^{-1}) and streptomycin (100 mg. mL^{-1}) was used for cell growth. The medium was replaced every other day in flask and when the cells reached 80-90% confluence, cells were detached using Trypsin-EDTA. The detached cells were plated at a density of 0.5 million cells/well in 96-well culture plates.

2.4.2.3 *In vitro* human epidermal keratinocyte and dermal fibroblast clearance

On attaining cell confluence of 90–95% in 96–well plates, these plates were used for metabolic stability studies. The medium was aspirated, and human epidermal keratinocytes / dermal fibroblasts cells were treated with growth medium consisting of 10 µM of TX, SC, SD, silibinin, isosilybin and testosterone in sextuplets. The drug treated plates were incubated for 0, 6, 12, 18 and 24 h. After incubation period, the reaction was terminated by adding ice-cold acetonitrile containing 0.1% formic acid and internal standards (dapsone). The 96 well plates were centrifuged at 4000 rpm for 10 min and supernatant subjected to HPLC analysis to evaluate the amount of silymarin constituents present in the incubation mixture at different time intervals. The assay validity was assessed by use of positive control testosterone which is extensively metabolized by skin metabolic enzymes.

Data analysis

Elimination rate constant (ke) is slope obtained by plotting % disappearance vs time

- **t½**= -0.693/ke
- **V (µL/106 Cells)** = Incubation volume (µL) / Number of cells in incubation (10^6)
- **Intrinsic clearance (µL/min/million cells)** = V*0.693 / t½

2.5 *In vitro* Release, *Ex vivo* Permeation and Penetration Testing

In vitro release, *ex vivo* permeation and penetration testing of silymarin formulations were performed using Franz diffusion cells.

2.5.1 Preparation of Porcine epidermis

The freshly isolated porcine belly skin was obtained from the slaughterhouse. The skin was cut into smaller pieces and washed with phosphate buffered saline. The subcutaneous layer and hair were removed from skin. The skin was wrapped in an aluminum foil and placed in water bath for 2 min at 60 °C. Immediately the epidermis was peeled off from the skin and the epidermis was stored at 4 °C.

2.5.2 Preparation of Human cadaver skin

The human cadaver skin was obtained from New York Firefighters skin bank, NY, USA. Cryo-preserved skin was thawed at 32 °C and cut into circular sections. The thawed skin was washed with PBS pH 7.4 thoroughly and used for *ex vivo* permeation and penetration studies.

2.5.3 Methodology

Nylon membrane of pore diameter 0.2 µm was used for the *in vitro* release studies. Nylon membrane or porcine skin epidermis or human cadaver skin was sandwiched between two chambers of a Franz diffusion cell with an active diffusion area of 0.64 cm^2, and the stratum corneum surface was exposed to the donor chambers. The resistance across porcine skin epidermis and human skin cadaver was measured using a wave form generator to ensure the integrity of skin segment. Porcine skin epidermis and human cadaver skin with resistance of ≥10 $K\Omega.cm^2$ was used for permeation and penetration studies. The receiver chamber was filled with 5 mL of PBS 7.4 pH containing 0.5% of Brij, which was constantly stirred with help of magnetic stir bar at 600 rpm. The whole Franz diffusion cell assembly was maintained at 32 ± 1 °C with the help of thermostatic water circulator. The formulation was loaded onto donor chamber. At predetermined time intervals samples were withdrawn through the sampling port of Franz diffusion cells and equal volume of fresh receptor fluid was replaced. After the study, skin was removed and washed thoroughly to remove the formulation or drug from the surface of skin. The skin was weighed, minced into smaller pieces and homogenized using homogenizer. The silymarin content in the receptor fluid and homogenate was determined using HPLC.

2.6 Extraction method

A simple protein precipitation method was used for extraction of silymarin constituents from *in-vitro* and *ex-vivo* study samples. To an aliquot of 50 µL of skin homogenate / in-vitro samples, an internal standard solution (5 µL of dapsone 5 µg/mL) was added and the mixture was vortexed. To above samples 200 µL of acetonitrile was added and the mixture was vortexed. The sample was centrifuged at 4 °C for 10 min at 14,000 rpm on a Centrifuge 5430R (Eppendorf, Germany) and the supernatant was transferred to a vial for HPLC analysis. The silymarin

constituents and IS eluted at 7.90, 16.1, 19.1, 20.1, 25.3, 27.0, 32.2 and 34.1 min for IS, TX, SC, SD, SA, SB, ISA and ISB, respectively with a total run time of 40 min.

2.7 Screening of permeation enhancers

The permeation enhancers were screened to enhance the penetration of SBE-β-CD enabled silymarin in to porcine epidermis. *Ex vivo* penetration studies performed as explained in section 2.5. To the donor compartment 500 µL of 10% D-α-tocopheryl polyethylene glycol succinate (TPGS), 5% taurine, 10% tween 80, TPGS:Tween 80 (5:5%), 0.15% phenyl piperazine, 20% polyethylene glycol (PEG) 400, 20% propylene glycol (PG) and 10% transcutol in SBE-β-CD–silymarin complex and 500 µL of control silymarin dissolved in 0.5% of Brij S20 were loaded for studies. After 24 h donor chamber was emptied out and porcine epidermis was removed. Silymarin content in porcine skin homogenate and receptor fluid was determined using HPLC.

2.8 Development of SBE-β-CD-silymarin Topical Formulation

The SBE-β-CD-silymarin cream was developed by incorporating penetration enhancers. The different excipients were evaluated to stabilize the cream formulation. In oil phase emollients octyldodecanol (OD) (2 to 5%) and light mineral oil (9 to 12%); emulsifiers macrogol cetostearyl ether 20 (MCSE) (1 to 5%), cetostearyl alcohol (3 to 7.5%), cremophor A 25 macrogolglycerol ricinoleate (1.5 to 5%), cremophor A6 (1 to 3%), glycerol monostearate (GMS) (1 to 5%); viscosity enhancing agents cetostearyl alcohol 50 (CSA 50) (2 to7%), cetostearyl alcohol 70 (CSA 70) (2 to 7%) and stearic acid (2 to 5%) were screened and defoaming agent dimethicone (0.5%). In aqueous phase SBE-β-CD-silymarin (complex), penetration enhancers and glycerin as humectant was used.

2.8.1 Cream preparation

The SBE-β-CD-silymarin cream was prepared by conventional method using Silverson Homogenizer L5M-A (Silverson Machines INC, USA). The Oil phase was heated separately at 70 °C. The aqueous phase heated at 70 °C in beaker, where the temperature was controlled with a circulating water bath and stirred. The oil was added slowly with the constant stirring to the aqueous phase. Both the phases were homogenized for 120 minutes at 1000 rpm min with temperature-controlled program as depicted in Figure 1. Transcutol was added at 75th min of homogenization, when the temperature reaches below 50 °C.

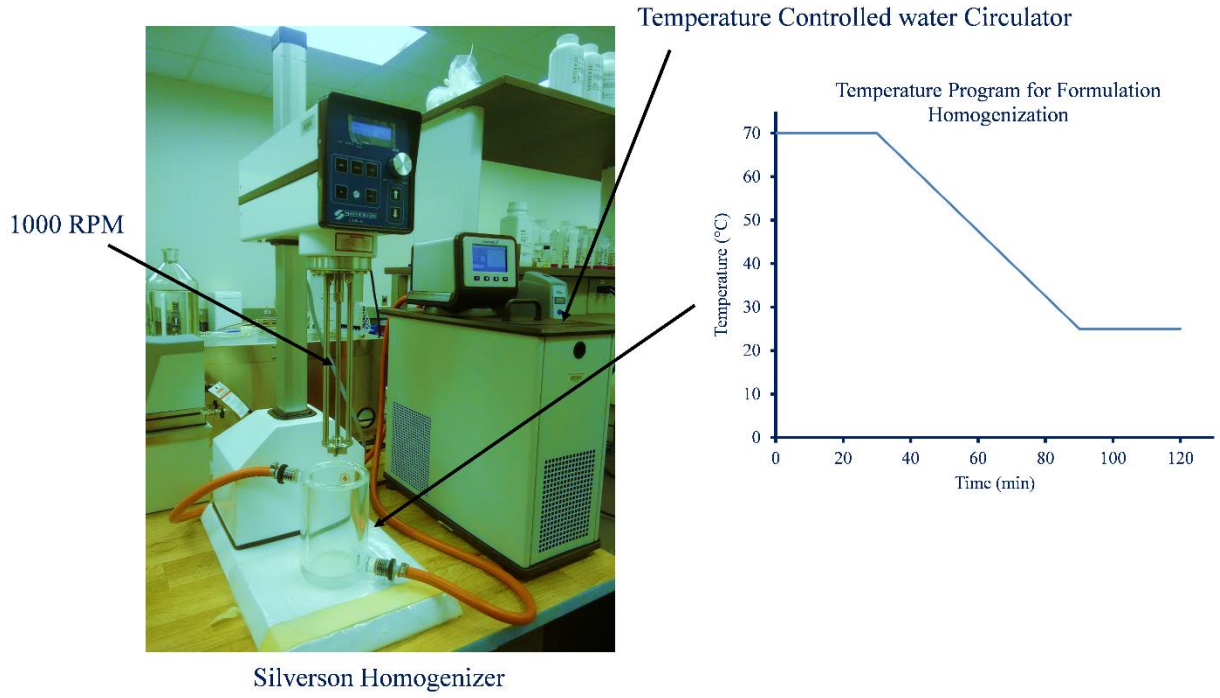

Figure 1. Silverson homogenizer and temperature program used for preparation of SBE-β-CD-silymarin cream.

2.8.2 Freeze thaw cycle testing of cream

The creams prepared were subjected to Freeze-thaw cycle testing to determine the stability of cream at extreme temperature conditions. The Freeze-thaw testing was performed by exposing cream to freezing conditions (approximately -20 °C) for 24 h and allowed to thaw at room temperature for 24 h. These creams were then placed at higher temperature (approximately 45 °C) for 24 h and then placed at room temperature again for 24 h. The sample was visualized for significant changes in consistency and stable formulations were further subjected to 2 more cycles of freeze thaw testing (78). After three cycles of freeze thaw, the consistency of creams, pH and globule size of stable formulation were evaluated and compared with formulations stored at room temperature (not exposed to freeze thaw).

2.8.3 Measurement of cream pH

The stability and solubility of drug constituents in topical drug formulation is dependent on pH of creams. The pH of creams significantly influences the ionization of drug, thus solubilization of drug in formulation and leading to changes in permeability of drug across skin (79). The pH of stable creams (fresh creams and creams subjected to Freeze thaw test) was measured using Mettler Toledo pH meter, equipped with In-Lab® Micro pH probe. The probe was placed in creams and ensured cream is in uniform contact with active surface of pH probe to record pH. After recording pH, excess cream on the probe was wiped off and washed with de-ionized water. After washing, two more readings of cream pH were recorded.

2.8.4 Globule Size

The distribution of globule size in creams influence permeation of the drug across biological barrier (80). Hence, here in this study distribution of globule size was evaluated to study the effect of freeze thaw on microstructure of creams. Approximately 10 mg of cream was directly weighed on a clean microscope glass slide and a film applicator was placed on the slide such that the clearance between applicator blade (Gardco® Microm II applicator blade, Japan) and the glass slide was set to 10 µm. The tail of applicator was slightly tilted upwards. By application of slight pressure on slide, the applicator was pulled slowly to form a uniform film. The film was immediately focused using 60X magnification under DSC mode, using Olympus microscope and pictures were captured. The diameter of 100 globules was randomly measured using Cell Sens software. The d10, d50 and d90 were extrapolated from the cumulative frequency Vs globule size plot.

2.8.5 *In vitro* release testing of SBE-β-CD–silymarin Topical Formulation

The SBE-β-CD-silymarin creams with minimal changes in pH and globule size post Freeze thaw cycle were subjected to *in vitro* release testing. *In vitro* release testing was performed as described in section 2.5, donor compartment was loaded with 300 mg of SBE-β-CD–silymarin cream covering the entire active diffusion area. The donor compartment was sealed with parafilm to simulate infinite conditions (81). The receptor fluids were withdrawn at 0, 0.5, 1, 2, 3, 4, 5 and 6 h time intervals. The concentration of drug in aliquots were analyzed using HPLC.

2.8.6 *In vitro* permeation testing of SBE-β-CD–silymarin cream

The SBE-β-CD–silymarin creams possessing good *in vitro* release characteristics were subjected to *ex vivo* permeation and penetration testing. *Ex vivo* permeation testing was performed as described in section 2.5, creams were applied at 15 mg/cm^2 on the epidermal surface of skin using a spatula. Silymarin content in skin homogenate and receptor fluid collected at 24 h was determined using HPLC.

One SBE-β-CD–silymarin creams with good *ex vivo* permeation and penetration were selected. This formulation was evaluated for *ex vivo* human cadaver skin penetration at 6, 12, 18 and 24 h time intervals and receptor fluid were collected to determine the amount permeated across the skin. The concentration of drug in receptor fluid and homogenate were analyzed using HPLC.

2.9 SBE-β-CD–silymarin topical formulation stability.

The final SBE-β-CD–silymarin cream was packed in screw capped HDPE bottles and stored in a stability chamber under two conditions, at 40 °C and 75% RH and at 25 °C and 60% RH. After period of 3 months, the stability of cream was assessed by evaluating drug content using HPLC.

3. Results and Discussion

3.1 *In vitro* Human skin Binding

The human skin drug binding is essential to determine for drugs intended for dermal or transdermal drug delivery. The non-specific drug binding effects the therapeutic efficacy of drug. Only unbound drug would permeate across the skin or penetrate skin to produce its therapeutic activity. Initial silymarin binding to dextran coated charcoal studies demonstrated, the dextran

coated charcoal pellet present in tube B (4 mL charcoal suspension) completely adsorbed the spiked silymarin constituents. The tube B was selected to further evaluate the *in vitro* human skin binding of silymarin.

The percent drug remaining in the supernatant was plotted versus time, this curve was fitted to a two-compartment model using Phoenix WinNonlin software (Version 1.5) with intravenous bolus input using a non-linear regression (77). The Cmax value at time 0 min is extent of human skin protein bound drug and percentage bound is calculated from Cmax at 0 min. The silymarin bound to human skin components was in the order of SC > TX > SB > ISA > ISB > SA > ISB and extend of drug bound is presented in Table 1. The study results demonstrate activity of ~7.63% of silymarin delivered to skin is uncertain. As, in case of skin the blood flow is low, hence maintaining equilibrium between bound and unbound drug is difficult compared to plasma protein drug binding.

Table 1. Percentage of drug bound to human skin components (n=3).

Parameters	**% Bound (mean ± SD)**
Taxifolin	10.4 ± 1.88
Silychrsitin	12.3 ± 0.49
Silydianin	7.30 ± 1.43
Silybin A	6.30 ± 1.22
Silybin B	7.77 ± 1.59
Isosilybin A	7.31 ± 1.03
Isosilybin B	2.09 ± 0.49

3.2 *In vitro* human skin clearance

Skin contains several enzymes that could potentially lead to biotransformation of drugs during permeation. The extent of biotransformation of drug in the skin should be considered as a prerequisite for development of a transdermal drug delivery system. Results from this study can be used to standardize the dose of silymarin required to be incorporated in the formulation to produce its beneficial effects on skin. Substrate depletion method was employed for determining intrinsic clearance and half-life by plotting percentage remaining against time. Testosterone was used as a control in *in-vitro* human skin clearance studies. Previously reported studies have demonstrated testosterone is extensively metabolized in skin (82).

3.2.1 In vitro human skin S9 fraction clearance

The Figure 2 depicts the percentage remaining against time curve of silymarin and testosterone. The percentage drug metabolized, half-life and intrinsic clearance of silymarin and testosterone is presented in Table 2. The half-life of silymarin was in order of SB > ISA > ISB > SC > SA > TX > SD in Human skin S9 fraction. The studies demonstrated SD was most extensively cleared and SB was least cleared in human skin S9 fraction. The 74.2% of testosterone was metabolized at 2 h in human skin S9 fraction, demonstrating the validity of assay conditions.

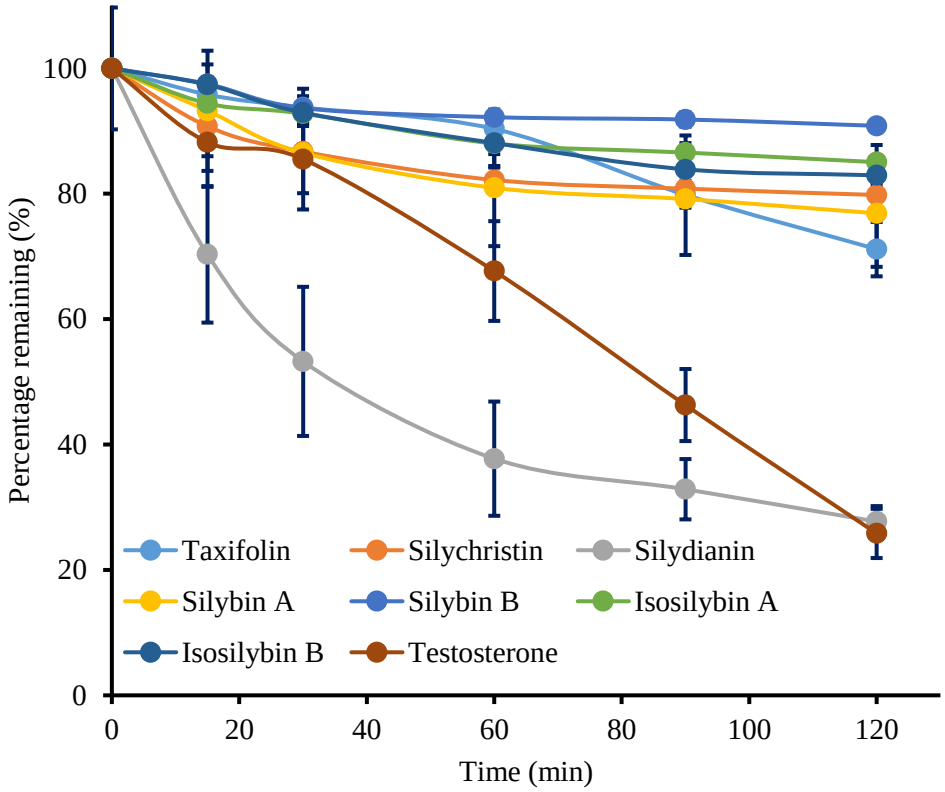

Figure 2. Testosterone (control) and silymarin percentage metabolized with time in human skin S9 fraction (n=3).

Table 2. Percentage metabolized, half-life and intrinsic clearance of testosterone (control) in presence of human skin S9 fractions (n=3).

Parameters	% Metabolized	Half life ($t_{1/2}$) min	S9 Intrinsic clearance (µL/min/mg)
Testosterone	74.2 ± 3.92	64.4 ± 21.3	10.8 ± 1.14
Taxifolin	28.8 ± 4.34	258 ± 42.3	2.73 ± 0.45
Silychrsitin	20.2 ± 2.49	417 ± 34.1	1.67 ± 0.14
Silydianin	72.3 ± 2.47	70.3 ± 2.76	9.87 ± 0.39
Silybin A	23.1 ± 8.54	397 ± 87.0	1.80 ± 0.38
Silybin B	9.17 ± 0.12	953 ± 132	0.74 ± 0.10
Isosilybin A	15.0 ± 2.74	565 ± 117	1.26 ± 0.26
Isosilybin B	17.1 ± 1.48	433 ± 84.1	1.64 ± 0.31

The human skin S9 fractions procured from BioIVT was mixed gender and pooled fraction. As per the certificate analysis of BioIVT, these fractions have demonstrated Uridine 5'-diphospho-glucuronosyltransferase (phase I) and CYP3A4 (phase II) enzyme activity.

3.2.2 In vitro Human epidermal keratinocyte and dermal fibroblast clearance

Human epidermal keratinocyte and dermal fibroblast clearance study was developed and validated to study the metabolism of drugs in human skin model and predict skin clearance. The Figure 3 depicts the percentage remaining against time curve of silymarin and testosterone. The percentage drug metabolized, half-life and intrinsic clearance of silymarin and testosterone is presented in Table 3. The half-life of silymarin was in order of SB > SC > TX > SA > ISB > SD > ISA in human epidermal keratinocyte. The studies demonstrated ISA was most extensively cleared and SB was least cleared in human skin S9 fraction. The 75.8 % of testosterone was

metabolized at 24 h in human epidermal keratinocyte, demonstrating the validity of assay conditions.

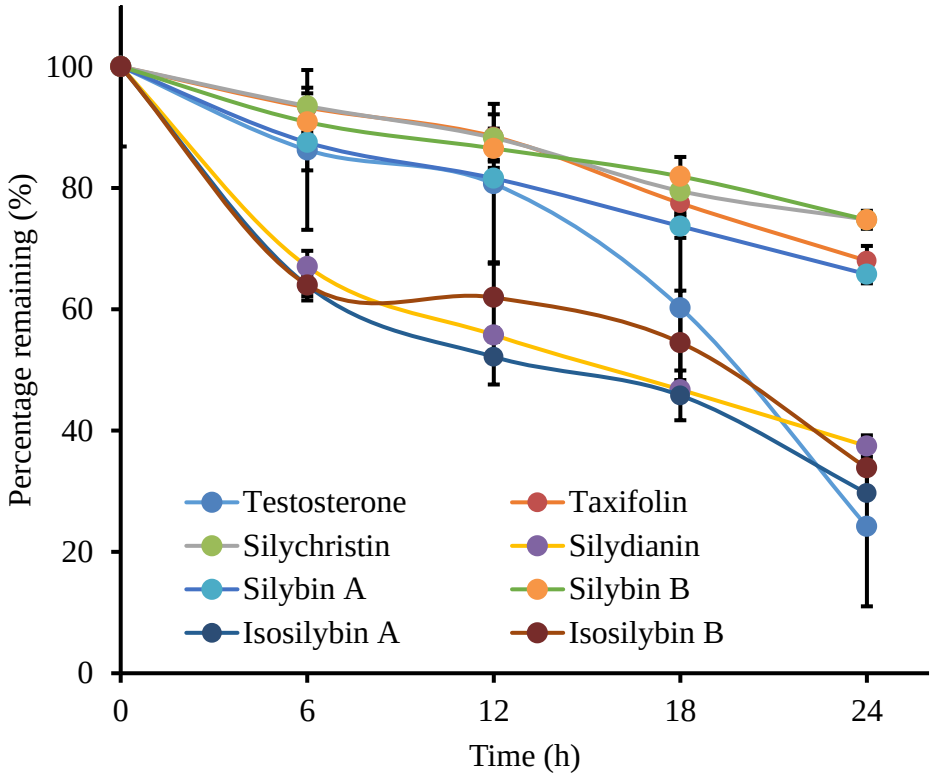

Figure 3. Testosterone (control) and silymarin percentage metabolized with time in human epidermal keratinocytes (n=4).

Table 3. Percentage metabolized, half-life and intrinsic clearance of testosterone (control) in presence of human epidermal keratinocytes (n=4).

Parameters	% Metabolized	Half life ($t_{1/2}$) h	Intrinsic clearance (µL/hr/10^6 cells)
Testosterone	75.8 ± 3.20	13.0 ± 1.19	267 ± 25.5
Taxifolin	32.0 ± 2.44	43.5 ± 3.00	79.8 ± 5.41
Silychrsitin	25.2 ± 0.60	56.0 ± 3.40	62.0 ± 3.66
Silydianin	62.6 ± 1.77	17.9 ± 0.75	194 ± 8.13
Silybin A	34.2 ± 1.50	41.3 ± 3.02	84.1 ± 6.40
Silybin B	25.3 ± 1.48	60.7 ± 3.21	57.2 ± 3.11
Isosilybin A	70.3 ± 0.63	15.1 ± 0.55	230 ± 8.67
Isosilybin B	66.2 ± 3.36	19.4 ± 1.33	179 ± 12.1

The Figure 4 depicts the percentage remaining against time curve of silymarin and testosterone. The percentage drug metabolized, half-life and intrinsic clearance of silymarin and testosterone is presented in Table 4. The half-life of silymarin was in order of ISA > SC > ISB > TX > SA > SB > SD in human dermal fibroblasts. The studies demonstrated SB was most extensively cleared and SC was least cleared in human dermal fibroblasts. The 64.5 % of testosterone was metabolized at 24 h in human dermal fibroblast, demonstrating the validity of assay conditions.

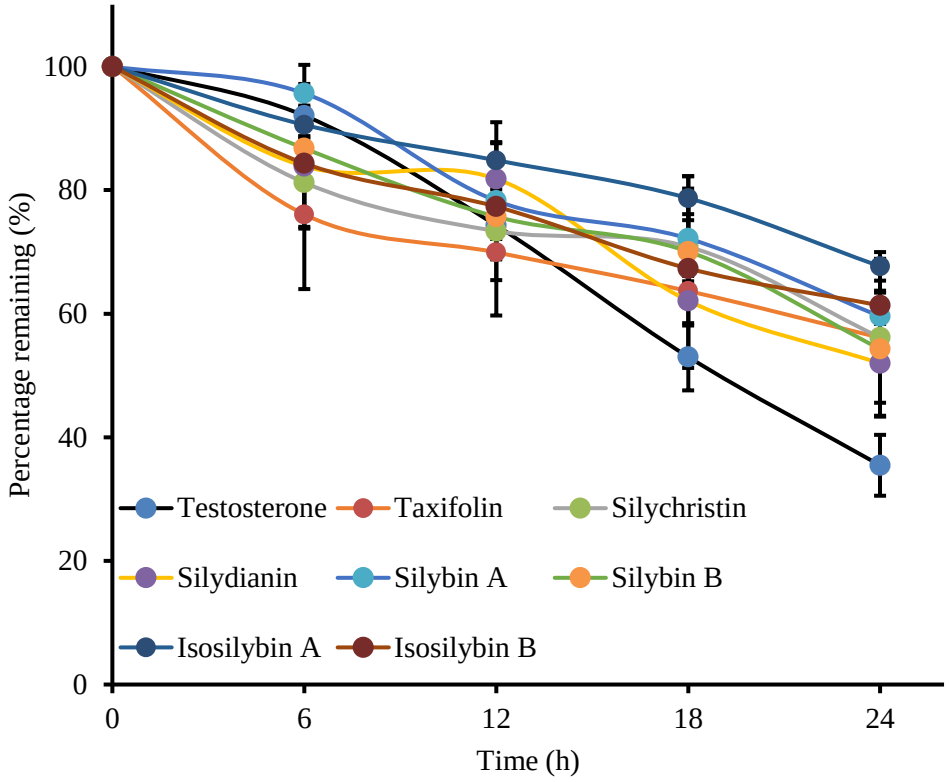

Figure 4. Testosterone (control) and silymarin constituent percentage metabolized with time in human dermal fibroblasts (n=3).

Table 4. Percentage metabolized, half-life and intrinsic clearance of testosterone (control) in presence of human dermal fibroblasts (n=3).

Parameters	% Metabolized	Half life ($t_{1/2}$) h	Intrinsic clearance (µL/hr/10^6 cells)
Testosterone	64.5 ± 4.93	15.9 ± 1.94	128 ± 62.3
Taxifolin	43.8 ± 12.7	33.2 ± 12.1	114 ± 42.5
Silychrsitin	43.8 ± 12.7	35.0 ± 15.6	70.7 ± 55.3
Silydianin	48.0 ± 6.38	25.8 ± 1.57	82.7 ± 53.3
Silybin A	40.4 ± 4.16	32.2 ± 6.80	111 ± 21.6
Silybin B	45.7 ± 2.78	29.0 ± 1.84	120 ± 7.84
Isosilybin A	32.3 ± 2.31	45.2 ± 3.35	76.9 ± 5.90
Isosilybin B	38.7 ± 2.08	34.8 ± 3.39	100 ± 10.3

The extent of silymarin metabolism in human epidermal keratinocytes and dermal fibroblast were different. This study indicates the enzyme milieu present in both cells are completely different. Hence, it's essential to evaluate the clearance of drugs intended for dermal and transdermal drug delivery in both cell lines to avail the beneficial therapeutic effects of drugs.

3.3 Screening of permeation enhancers

The drugs should permeate across the skin or penetrate skin to produce its intended therapeutic activity in dermatological disorders. The effect of different permeation enhancers on the penetration of SBE-β-CD enabled complex is presented in Table 5. The SC, SD, SA, SB and ISA penetrated from SBE-β-CD–silymarin complex, whereas no silymarin constituents were penetrated the skin from control (silymarin dissolved in 0.5% of Brij S 20). Demonstrating SBE-β-CD have intrinsic skin penetration enhancing property. Further, series of permeation enhancers

were screened to potentiate the skin penetration effect of SBE-β-CD. Among, all enhancers screened polyethylene glycol 400, propylene glycol and transcutol increased the skin penetration of all constituents TX, SC, SD, SA, SB, ISA and ISB. Propylene glycol was found to be more efficient in increasing skin penetration compared to other enhancers. In presence of 20% of propylene glycol, skin penetration of SC, SD, SA, SB and ISA was increased by 12.2, 18.8, 5.55, 9.50 and 6.89-fold compared to SBE-β-CD–silymarin complex without enhancer, respectively.

Table 5. Effect of permeation enhancer on the penetration of SBE-β-CD enabled silymarin constituents into the porcine epidermis

Enhancers used in SBE-β-CD–silymarin complex	**Silymarin constituents (ng)/ mg of epidermis after 24h (Mean ± SEM) n=6**						
	Taxifolin (n=6)	**Silychristin (n=6)**	**Silydianin (n=6)**	**Silybin A (n=6)**	**Silybin B (n=6)**	**Isosilybin A (n=6)**	**Isosilybin B (n=6)**
Control	BLQ	BLQ	BLQ	BLQ	BLQ	BLQ	BLQ
Blank	BLQ	50 ± 3.89	81.3 ± 7.41	20.4 ± 4.82	32.4 ± 6.21	31.3 ± 5.12	BLQ
TPGS (10%)	BLQ	127 ± 9.54	116 ± 9.32	69.9 ± 10.2	63.9 ± 5.87	54.2 ± 7.41	32.8 ± 4.06
Taurine (5%)	BLQ	110 ± 11.5	327 ± 76.2	48.8 ± 6.23	96.4 ± 14.8	67.6 ± 10.2	24.8 ± 4.17
Tween 80 (10%)	BLQ	56.1 ± 6.32	63.9 ± 7.61	33.0 ± 3.91	49.5 ± 7.84	27.2 ± 2.86	20.9 ± 3.67
TPGS : Tween 80 (5 : 5%)	5.22 ± 1.2	59.9 ± 4.81	78.6 ± 8.93	34.6 ± 3.47	43.2 ± 9.23	27.2 ± 5.23	22.8 ± 3.14
Phenyl piperazine (0.15%)	16.4 ± 6.83	92.6 ± 11.8	68.5 ± 5.87	36.0 ± 5.76	67.1 ± 7.95	56.9 ± 7.48	26.9 ± 1.89
PEG 400 (20%)	7.12 ± 1.75	86.3 ± 6.41	135 ± 8.89	45.6 ± 7.84	55.7 ± 6.32	69.4 ± 10.2	34.2 ± 2.32
Propylene glycol (20%)	44.8 ± 2.62	616 ± 69.1	1525 ± 182	113 ± 16.2	308 ± 45.1	216 ± 26.4	61.9 ± 3.48
Transcutol (20%)	35.8 ± 4.45	348 ± 35.7	468 ± 36.9	57.8 ± 11.9	128 ± 17.4	106 ± 17.1	26.2 ± 1.43

* Control (silymarin in 0.5% of Brij 20), Blank (SBE-β-CD–silymarin complex), BLQ: Below limit of quantitation, NA: Not applicable.

3.4 Development of SBE-β-CD–silymarin Topical Formulation

Oil in water (O/W) SBE-β-CD–silymarin cream was prepared by incorporating PG 20% and transcutol 5% as penetration enhancers. In creams, the composition of aqueous phase was SBE-β-CD–silymarin complex (57%), PG (20%), transcutol (5%) and glycerol (1%). The aqueous composition of creams was kept constant and composition of oil phase was optimized to prepare a stable cream.

Two sets of creams were prepared, 1st set of creams was prepared with oil composition of light mineral oil (9 to 12%), cremophor A 25 macrogolglycerol ricinoleate (2 to 4%), cremophor A6 (1 to 2%) and cetostearyl alcohol (3 to 8%). Decreasing the concentration of emulsifier cremophor A 25 macrogolglycerol ricinoleate <3% and viscosifying agent concentration <3% resulted in phase separation of creams. The 2nd set of creams was prepared with oil composition of OD (3 to 12%), CSA 50 (2 to 7%), CSA 70 (2 to 7%), MCSE 20 (1 to 5%) and GMS (1 to 4%). As the concentration of viscosifying agents decreased to <2% resulted in phase separation of creams.

3.4.1 Freeze thaw cycle testing of cream

Creams stable at room temperature for 7 days was exposed to freeze thaw cycle test. On subjecting to freeze thaw cycle 1st set of creams were not stable. The 1st set of creams were thick and there was formation of lumps in the cream post freeze thaw test. The 2nd set of creams containing MCSE 20, GMS and ≥3% of CSA50 or ≥3% of CSA70 were stable post freeze thaw cycle. The composition of creams stable post freeze thaw cycle test is presented in Table 6.

Table 6. The composition of stable creams post freeze thaw test.

Ingredients	Percentage (%)									
	F1	**F2**	**F3**	**F4**	**F5**	**F6**	**F7**	**F8**	**F9**	**F10**
Complex	57.0	57.0	57.0	57.0	57.0	57.0	57.0	57.0	57.0	57.0
Water	2.5	0.5	2.5	0.5	3.5	1.5	2.5	0.5	2.5	0.5
Glycerine	1.0	1.0	1.0	1.0	1.0	1.0	1.0	1.0	1.0	1.0
PG	20.0	20.0	20.0	20.0	20.0	20.0	20.0	20.0	20.0	20.0
Transcutol	5.0	5.0	5.0	5.0	5.0	5.0	5.0	5.0	5.0	5.0
OD	4.0	4.0	4.0	4.0	4.0	4.0	4.0	4.0	4.0	4.0
MCSE 20	3.0	4.0	3.0	4.0	3.0	4.0	3.0	4.0	3.0	4.0
GMS	3.0	4.0	3.0	4.0	3.0	4.0	3.0	4.0	3.0	4.0
CSA 50	4.0	4.0	3.0	3.0	0.0	0.0	0.0	0.0	2.0	2.0
CSA 70	0.0	0.0	0.0	0.0	3.0	3.0	3.0	3.0	2.0	2.0
Stearic acid	0.0	0.0	1.0	1.0	0.0	0.0	1.0	1.0	0.0	0.0
Dimethicone	0.5	0.5	0.5	0.5	0.5	0.5	0.5	0.5	0.5	0.5

3.4.2 Measurement of cream pH

The pH of fresh creams and post-freeze thaw test creams were in range of 4.72 to 5.36 and 4.61 to 5.29 (Table 7) for fresh creams and post freeze thaw subjected creams, respectively. The pH of post freeze thaw cream was slightly decreased (Table 7). However, the change in pH of the creams were negligible and hence this test demonstrates there would be no effect on the solubility of drug constituents due to pH change in cream post freeze thaw cycle.

Table 7. Cream pH of different formulations pre and post-freeze thaw test.

Formulation ID	Pre-Freeze thaw Test pH (Mean ± SD) n=3	Post-Freeze thaw Test pH (Mean ± SD) n=3	% Change in pH (Mean)
F1	4.72 ± 0.22	4.61 ± 0.10	-2.25
F2	5.30 ± 0.19	5.11 ± 0.13	-3.56
F3	5.36 ± 0.23	5.18 ± 0.09	-3.34
F4	5.36 ± 0.12	5.27 ± 0.05	-1.75
F5	5.30 ± 0.05	5.15 ± 0.04	-2.71
F6	5.19 ± 0.12	5.18 ± 0.01	-0.16
F7	5.26 ± 0.05	5.12 ± 0.08	-0.40
F8	4.74 ± 0.08	4.76 ± 0.08	-4.61
F9	5.31 ± 0.04	5.29 ± 0.04	-2.49
F10	5.28 ± 0.07	5.04 ± 0.10	-2.57

3.4.3 Globule Size determination

Increase in temperature decreases viscosity of creams leading to disruption of globules thus formation of smaller size globules and make creams more susceptible to coalescence followed by phase separation. Decrease in the temperature would lead to crystallization of components in cream and leading to changes in size of globules. However, the effect of temperature on the creams depends on nature of oil phase, solubility of drug and ratio of oil to water in O/W creams (82). The globule size of creams which were stable at freeze thaw test was measured. The d10, d50 and d90 diameter were extrapolated from the cumulative frequency Vs globule size plot. Where, d10, d50 and d90 are diameters at which 10, 50 and 90% of globules is comprised of globule with lesser diameter than d10, d50 and d90 values, respectively.

The globule size distribution of creams F3, F4, F7 and F8 was increased post freeze-thaw cycle, however there was no change in globule size distribution of creams F1, F2, F5, F6, F9 and F10 (Table 8). The d10, d50 and d90 of F3, F4, F7 and F8 were increased, this could be attributed to the presence of stearic acid in these formulations. The change in globule size of F3, F4, F7 and F8 creams demonstrates changes in the microstructure, which could adversely affect the stability of formulation and permeation of the drugs incorporated in the creams.

Table 8. The globule size distribution in O/W creams.

Formulation ID	Globule Diameter (µm)					
	Pre-Freeze thaw (µm)			Post-Freeze thaw (µm)		
	d10	d50	d90	d10	d50	d90
F1	1.41	2.37	4.33	1.27	2.9	6.01
F2	1.16	1.91	4.15	2.73	4.59	6.99
F3	1.15	1.82	4.01	1.23	2.45	6.03
F4	1.23	2.27	4.15	1.49	3.27	6.01
F5	1.37	3.07	5.57	1.32	2.98	6.53
F6	1.22	2.25	4.21	1.63	2.95	5.61
F7	1.14	1.84	4.39	1.93	3.43	6.13
F8	2.13	3.98	5.93	2.9	5.15	7.37
F9	1.31	2.36	3.43	1.33	2.62	6.17
F10	1.19	2.17	4.01	1.34	3.02	4.89

3.4.4 *In vitro* release testing of SBE-β-CD–silymarin creams

The SBE-β-CD–silymarin creams F1, F2, F5, F6, F9 and F10 with minimal changes in globule size was tested for *in vitro* release. *In vitro* release test of topical dosage forms can be used as a tool to assess the formulations potential to deliver drug consistently at the site of absorption. The *in vitro* release rate can demonstrate the collective influence of various physical and chemical properties like globule size, solubility and rheological properties of formulations (81).

In vitro release rate and profile of silymarin constituents from creams F1, F2, F5, F6, F9 and F10 are presented in Table 8 and Figure 5, respectively. The release study data demonstrates *in vitro* release rates of silymarin constituents from formulations are in order of F2 < F1 < F10 <

F9 < F5≈ F6 (Table 9). The lag phase for drug release were in order of F5=F6 < F9 < F10 < F2 < F1. The decreased *in vitro* release rate and percentage drug release from F1, F2, F9 and F10 formulations can be attributed to viscosity of formulations, previous reported studies have demonstrated CSA 50 increases the viscosity of formulations compared to CSA 70 containing formulations (83).

Table 9. *In vitro* release rates of silymarin constituents from F1, F2, F5, F6, F9 and F10 creams.

Silymarin Constituents	**In vitro Release Rate (μg/cm^2/h) Mean ± SD (n=3)**					
	F1	F2	F5	F6	F9	F10
Taxifolin	0.85 ± 0.33	0.77 ± 0.02	5.84 ± 0.48	5.79 ± 0.72	2.85 ± 0.29	2.80 ± 0.31
Silychristin	1.25 ± 0.57	0.84 ± 0.10	22.9 ± 0.81	25.1 ± 2.46	8.00± 1.58	5.90 ± 0.87
Silydianin	2.16 ± 0.48	1.88 ± 0.15	22.1 ± 0.67	23.4 ± 1.39	9.52 ± 1.69	7.60 ± 0.93
Silybin A	5.27 ± 1.57	4.61 ± 0.24	64.6 ± 2.25	59.0 ± 13.2	27.8 ± 2.70	27.2 ± 1.77
Silybin B	8.05 ± 2.28	8.14 ± 0.24	127 ± 9.60	116 ± 31.1	54.3 ± 5.13	50.9 ± 6.31
Isosilybin A	5.02 ± 3.36	2.54 ± 0.24	42.5 ± 0.36	42.2 ± 4.95	19.4 ± 6.38	12.8 ± 3.65
Isosilybin B	0.95 ± 0.07	0.61 ± 0.03	10.6 ± 0.40	11.1 ± 0.30	3.82 ± 0.28	3.35 ± 0.57

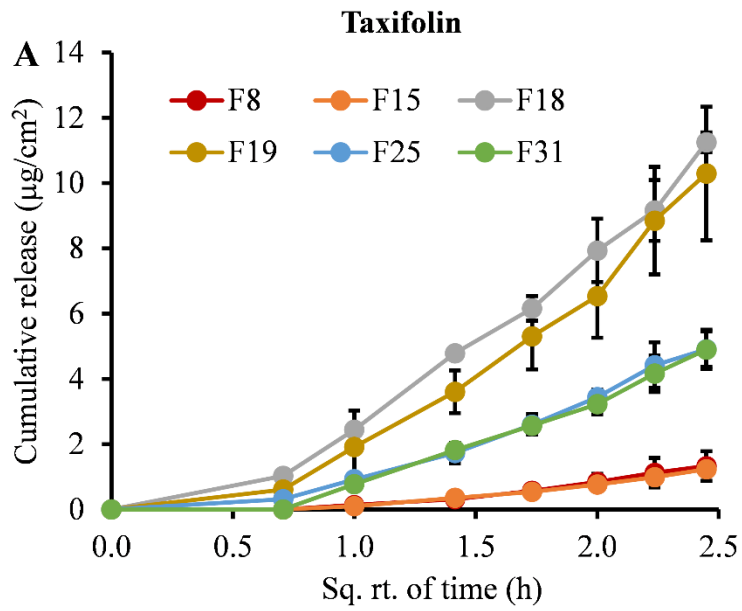
A
Taxifolin
F8
F15
F18
F19
F25
F31
Cumulative release (µg/cm²)
Sq. rt. of time (h)
0
2
4
6
8
10
12
14
0.0
0.5
1.0
1.5
2.0
2.5

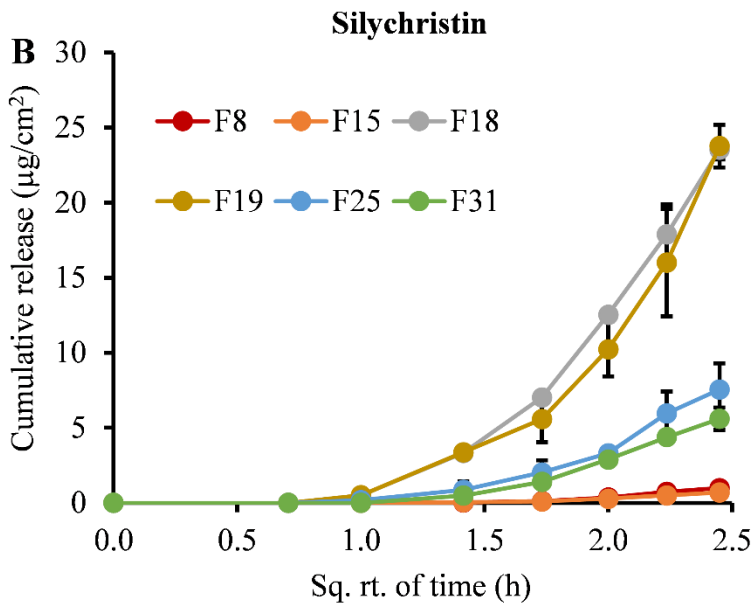
B
Silychristin
F8
F15
F18
F19
F25
F31
Cumulative release (µg/cm²)
Sq. rt. of time (h)
0
5
10
15
20
25
30
0.0
0.5
1.0
1.5
2.0
2.5

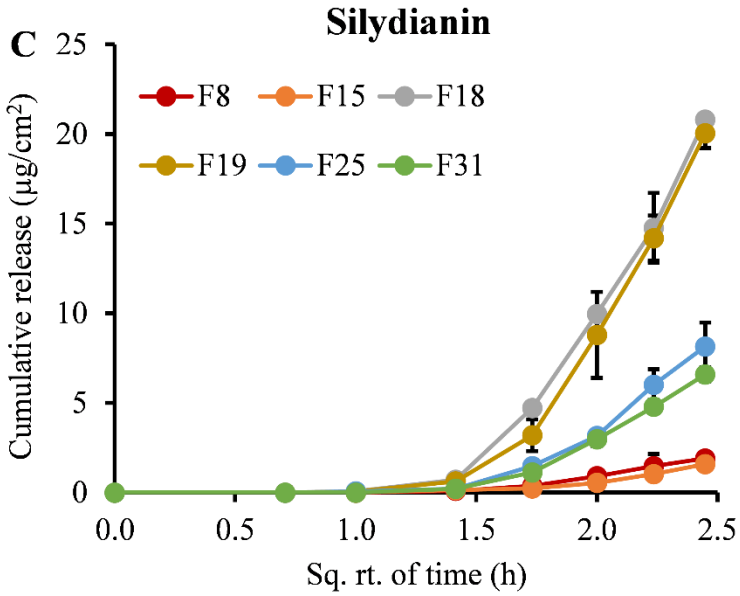
C
Silydianin
F8
F15
F18
F19
F25
F31
Cumulative release (µg/cm²)
Sq. rt. of time (h)
0
5
10
15
20
25
0.0
0.5
1.0
1.5
2.0
2.5

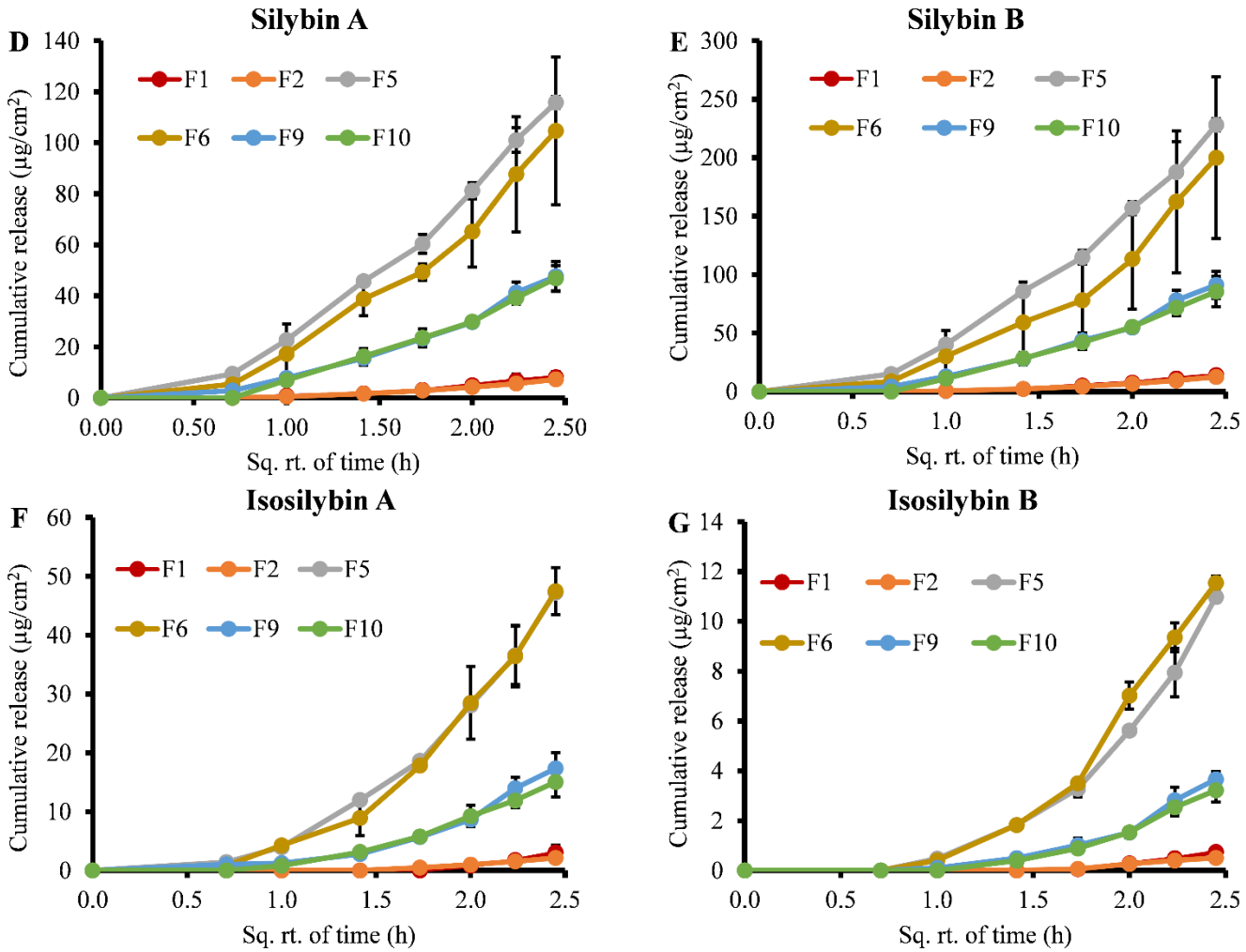

Figure 5. The *in vitro* release profile of taxifolin (A), silychristin (B), silydianin (C), silybin A (D), silybin (E), isosilybin (F) and isosilybin (D) from F1, F2, F5, F6, F9 and F10 formulations.

3.4.5 *In vitro* permeation testing of SBE-β-CD–silymarin cream

The F5 and F6 creams with good release characteristics were evaluated for *ex vivo* human cadaver skin penetration studies. The cumulative amount permeated, and amount of drug penetrated human cadaver skin presented in Figure 5 and Figure 6.

The cumulative amount of TX, SC, SD, SA, SB, ISA and ISB permeated across the human cadaver skin on application of F6 SBE-β-CD–silymarin cream was increased by 1.65, 1.78, 1.55, 1.45, 1.37, 1.39 and 1.49 compared to application of F5 SBE-β-CD-silymarin cream, respectively (Figure 6). The amount of TX, SC, SD, SA, SB, ISA and ISB penetrated human cadaver skin on application of F6 SBE-β-CD-silymarin cream was increased by 1.77, 1.16, 1.49, 1.30, 1.16, 0.91 and 1.63 compared to application of F5 SBE-β-CD-silymarin cream, respectively (Figure 5). The increase in permeation and penetration of silymarin constituents on application of F6 creams can be attributed to presence of 4% of surfactants (MCSE 20 and GMS), whereas F5 creams contains 3% of surfactants (MCSE 20 and GMS).

Based on above results the permeation and penetration of silymarin constituents on application of F6 creams were evaluated at 6, 12, 18 and 24 h in human cadaver skin. The amount of drug permeated across the skin and penetrated in to skin was increased with time (Figure 7). The order of permeation and penetration of silymarin constituents was SD < TX < SB < ISB < ISA < SB < SC and TX < SB < SD < ISB < ISA < SA at 24 h, respectively.

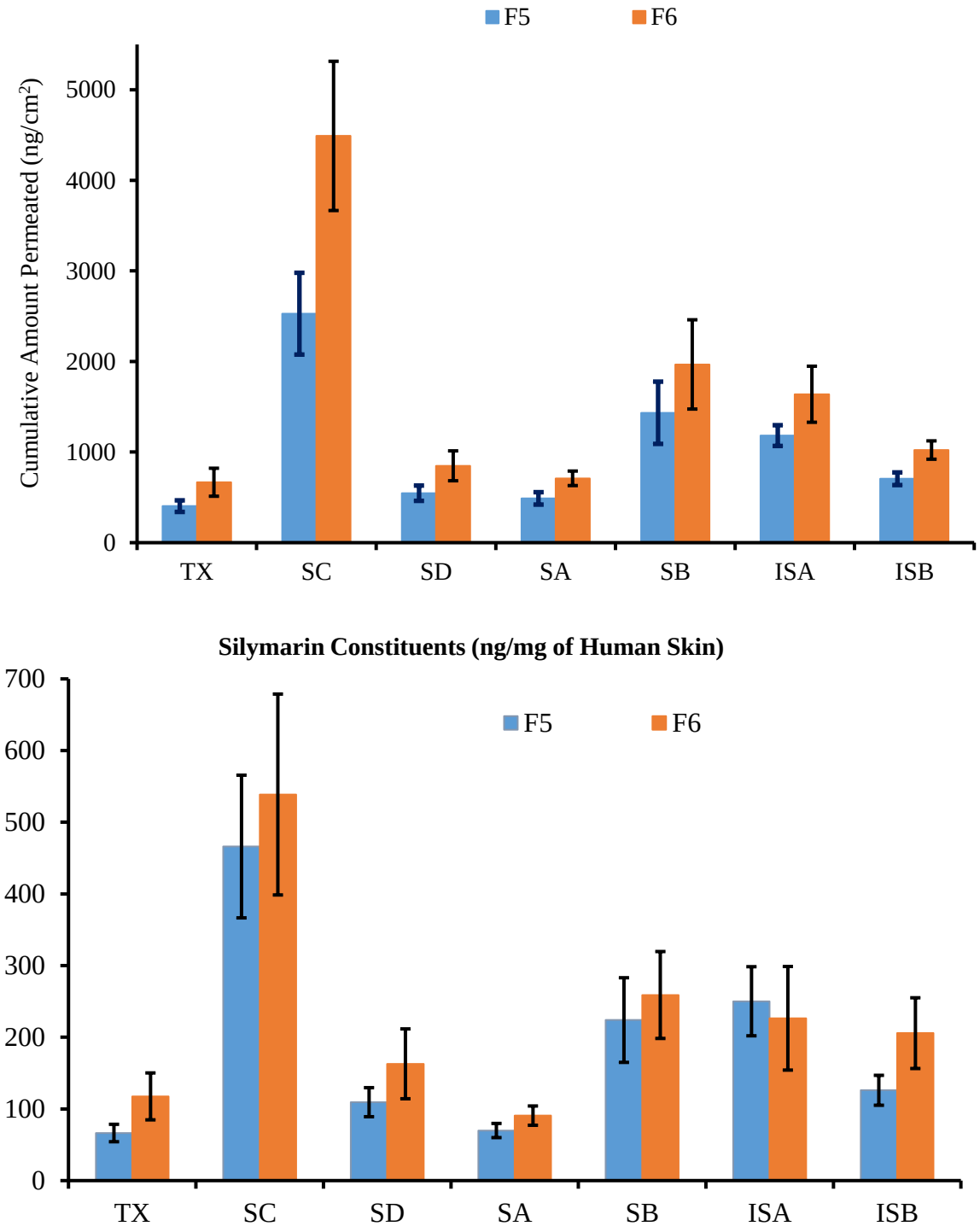

Figure 6. *Ex vivo* human skin permeation and penetration of silymarin constituents on application of F5 and F6 SBE-β-CD-silymarin topical formulation.

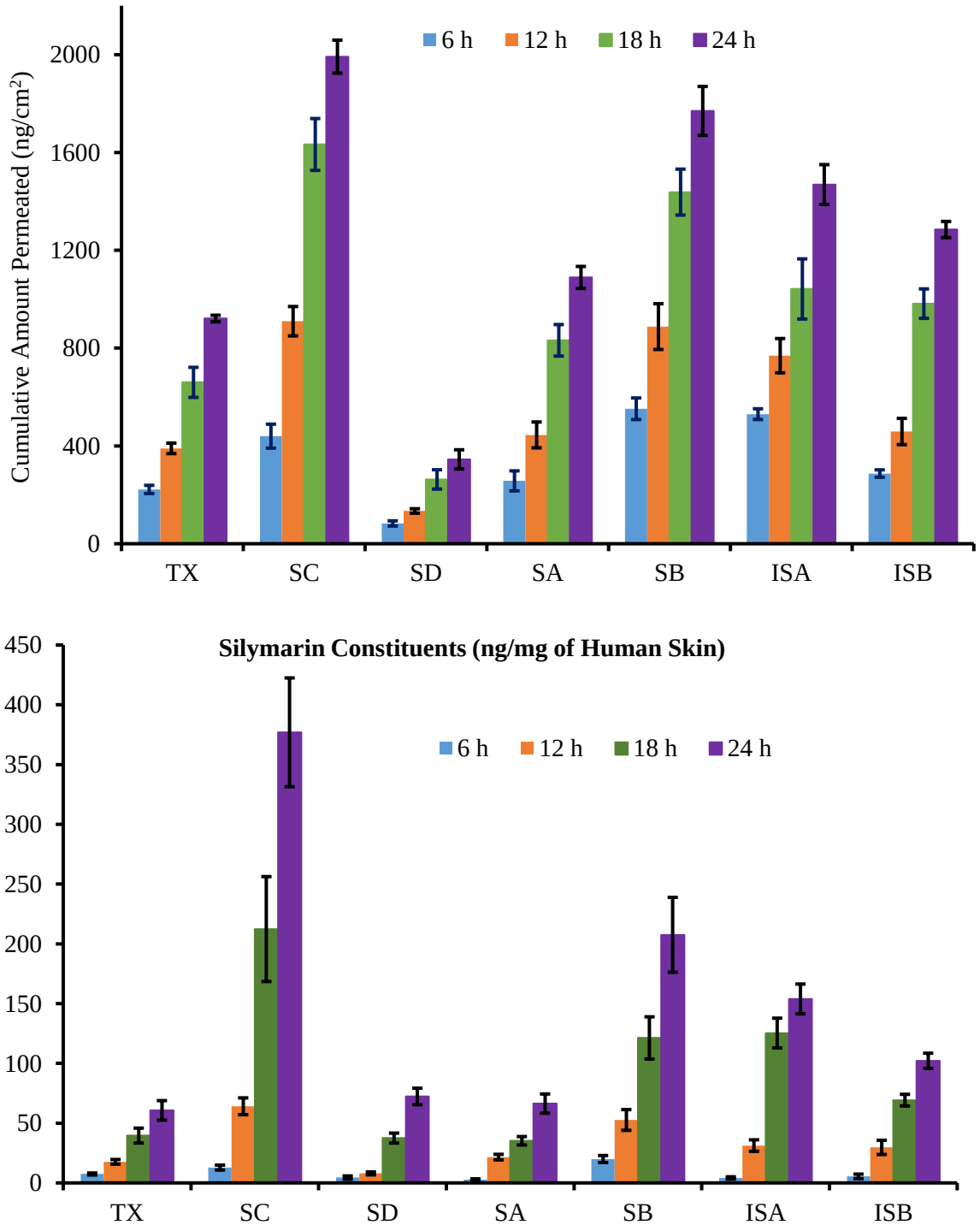

Figure 7. *Ex vivo* human skin permeation and penetration of silymarin constituents on application of SBE-β-CD-silymarin topical formulation (F6) at 6, 12, 18 and 24 h.

3.5 SBE-β-CD-silymarin topical formulation stability

The stability of silymarin constituents in SBE-β-CD–silymarin cream under two sets of conditions, 25 °C (60% RH) and 40 °C (75% RH), was ≥ 92.4 and ≥ 91.3% (Figure 8) for periods 3 months, respectively.

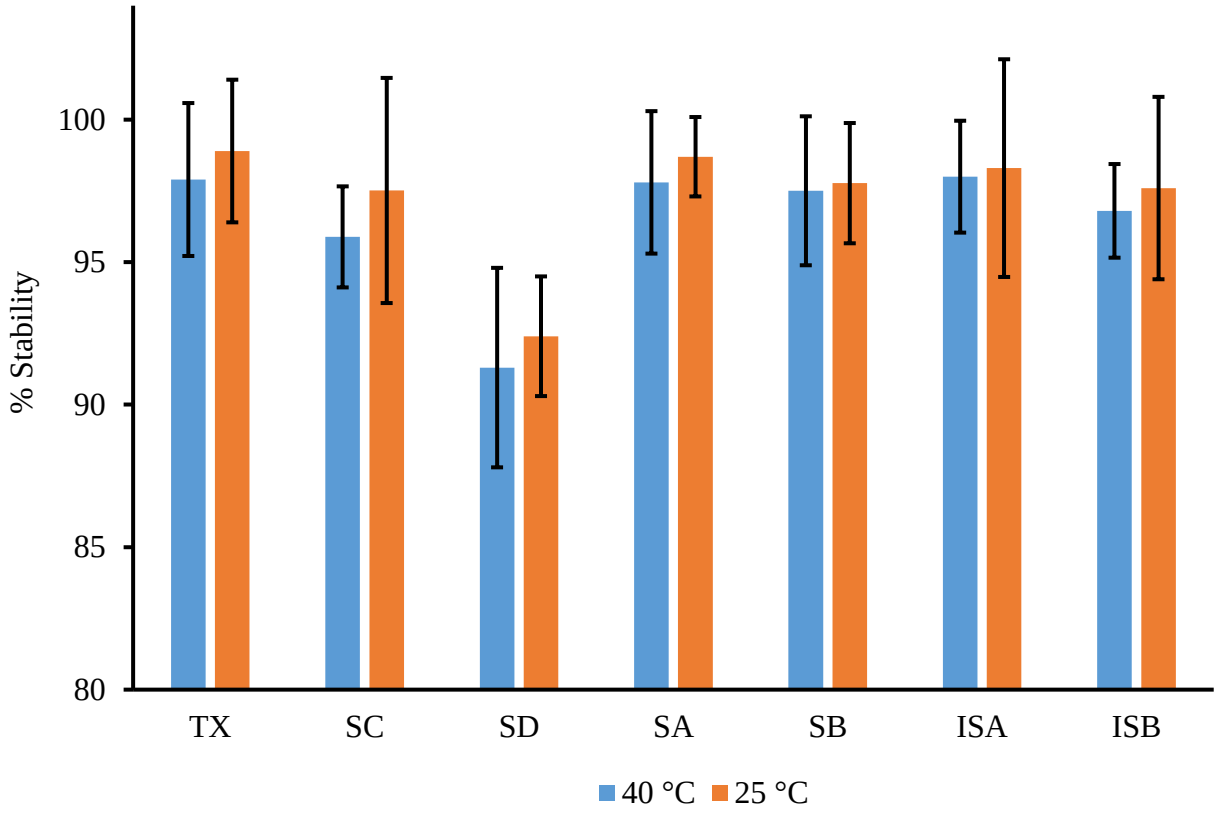

Figure 8. Stability of the silymarin constituents in SBE-β-CD–silymarin cream at 25 °C (60% RH) and 40 °C (75% RH) for periods of 3 months. Each point represents the mean ± SD of triplicate values.

4. Conclusion

The silymarin constituents have very low non-specific binding, this would have a negligible effect on the permeation, and it will not affect the therapeutic action if adequate levels of silymarin delivered. The *in-vitro* clearance study indicates that silymarin constituents have longer elimination half- life in skin except SD and thus the therapeutic effects of silymarin on skin would be prolonged on application as a topical formulation. An understanding of the capacity and impact of drug biotransformation within skin and skin binding is an important component in assessing pharmacotherapy directed to or through the cutaneous environment, which can be modulated by standardizing dose for transdermal or topical drug delivery. Ex-vivo porcine epidermis penetration studies demonstrated SBE-β-CD enhances the skin penetration of SC, SD, SA, SB and ISA. The penetration enhancer screening demonstrated propylene glycol and transcutol in SBE-β-CD–silymairn complex potentiates the skin penetration of all silymarin constituents. SBE-β-CD–silymarin cream was developed and optimized to stabilize the cream and increase the skin penetration and permeation of all silymarin constituents across the skin. The developed SBE-β-CD–silymarin cream can be used for treatment of various skin ailments.

BIBLIOGRAPHY

1. Williams HD, Trevaskis NL, Charman SA, Shanker RM, Charman WN, Pouton CW, et al. Strategies to Address Low Drug Solubility in Discovery and Development. Pharmacol Rev. 2013;65(1):315–499.
2. Kalepu S, Nekkanti V. Insoluble drug delivery strategies : review of recent advances and business prospects. Acta Pharm Sin B [Internet]. Elsevier; 2015;5(5):442–53. Available from: http://dx.doi.org/10.1016/j.apsb.2015.07.003
3. Savjani KT, Gajjar AK, Savjani JK. Drug Solubility: Importance and Enhancement Techniques. ISRN Pharm. 2012;2012(100 mL):1–10.
4. Rodde MS, Divase GT, Devkar TB, Tekade AR. Solubility and Bioavailability Enhancement of Poorly Aqueous Soluble Atorvastatin : In Vitro , Ex Vivo , and In Vivo Studies. Hindawi Publishing Corporation; 2014;2014.
5. Manuscript A. NIH Public Access. 2014;102(1):34–42.
6. Arik D, Jonathan, M. Miller Amnon H, Gregory, E. Amidon Gordon LA. The Solubility–Permeability Interplay in Using Cyclodextrins as Pharmaceutical Solubilizers: Mechanistic Modeling and Application to Progesterone. J Pharm Sci. 2010;99(6):2739–49.
7. Carrier RL, Miller LA, Ahmed I. The utility of cyclodextrins for enhancing oral bioavailability. 2007;123:78–99.
8. Valle EMM Del. Cyclodextrins and their uses : a review. 2003;
9. Stella VJ, he Q. Cyclodextrins. Toxicol Pathol. 2008;36(1):30–42.

10. European Medicines Agency. Background review for cyclodextrins used as excipients - In the context of the revision of the guideline on ‘ Excipients in the label and package leaflet of medicinal products for human use’’ (CPMP/463/00 Rev. 1).’ 2014;44(November).
11. Filicori M, Butler JP, Crowley WF. Neuroendocrine Regulation of the Corpus Luteum in the Human Evidence for Pulsatile Progesterone Secretion processed for progesterone levels . across the luteal phase with the mean LH pulse frequency. J Clin invest. 1984;73(June):1638–47.
12. Yang G, Sau C, Lai W, Cichon J, Li W. HHS Public Access. 2015;344(6188):1173–8.
13. US9011908B2.pdf.
14. Ryan N, Rosner A. Quality of life and costs associated with micronized progesterone and medroxyprogesterone acetate in hormone replacement therapy for nonhysterectomized, postmenopausal women. Clin Ther. 2001;23(7):1099–115.
15. Proprietary Name, Active Ingredient or Application Number: Progesterone. Orange Book: Approved Drug Products with Therapeutic Equivalence Evaluations.
16. ARCHER B. Depot medroxyprogesterone Management of side-effects commonly associated with its contraceptive use*1. J Nurse Midwifery. 1997;42(2):104–11.
17. Lahiani-Skiba M, Barbot C, Bounoure F, Joudieh S, Skiba M. Solubility and dissolution rate of progesterone-cyclodextrin-polymer systems. Drug Dev Ind Pharm. 2006;32(9):1043–58.
18. Zoppetti G, Puppini N, Ospitali F, Fini A. DRUG DELIVERY Solid State Characterization of Progesterone in a Freeze Dried 1 : 2 Progesterone / HPBCD Mixture. 2007;96(7):1729–36.

19. Sun L, Zhang B, Sun J. The Solubility-Permeability Trade-Off of Progesterone With Cyclodextrins Under Physiological Conditions: Experimental Observations and Computer Simulations. J Pharm Sci. Elsevier Ltd; 2018;107(1):488–94.

20. Loftsson T, Hreinsdóttir D, Másson M. The complexation efficiency. J Incl Phenom Macrocycl Chem. 2007;57(1–4):545–52.

21. Alsulays BB, Kulkarni V, Alshehri SM, Almutairy BK, Ashour E a., Morott JT, et al. Preparation and evaluation of enteric coated tablets of hot-melt extruded lansoprazole. Drug Dev Ind Pharm. 2017;43:789–96.

22. Yokota T, Tonozuka T, Shimura Y, Ichikawa K, Kamitori S, Sakano Y. Structures of Thermoactinomyces vulgaris R-47 α-Amylase II Complexed with Substrate Analogues [Internet]. Bioscience, Biotechnology, and Biochemistry. 2001. p. 619–26. Available from: http://www.tandfonline.com/doi/full/10.1271/bbb.65.619

23. Jain AS, Date A a., Pissurlenkar RRS, Coutinho EC, Nagarsenker MS. Sulfobutyl Ether7 β-Cyclodextrin (SBE7 β-CD) Carbamazepine Complex: Preparation, Characterization, Molecular Modeling, and Evaluation of In Vivo Anti-epileptic Activity [Internet]. AAPS PharmSciTech. 2011. p. 1163–75. Available from: http://www.springerlink.com/index/10.1208/s12249-011-9685-z

24. Mohammed NN, Pandey P, Khan NS, Elokely KM, Liu H, Doerksen RJ, et al. Clotrimazole–cyclodextrin based approach for the management and treatment of Candidiasis – A formulation and chemistry-based evaluation. Pharm Dev Technol. 2016;21(5):619–29.

25. MacroModel. New York (NY): Schrödinger, LLC; 2016.

26. Maestro. New York (NY): Schrödinger, LLC; 2016.

27. LigPrep. New York (NY): Schrödinger, LLC; 2016.

28. Friesner RA, Banks JL, Murphy RB, Halgren TA, Klicic JJ, Mainz DT, et al. Glide: A New Approach for Rapid, Accurate Docking and Scoring. 1. Method and Assessment of Docking Accuracy. J Med Chem. 2004;47(7):1739–49.

29. Sherman W, Day T, Jacobson MP, Friesner RA, Farid R. Novel procedure for modeling ligand/receptor induced fit effects. J Med Chem. 2006;49(2):534–53.

30. D. E. Shaw. Desmond Molecular Dynamics System. New York (NY): Schrödinger Release; 2017.

31. Maestro-Desmond Interoperability Tools. New York (NY): Schrödinger, LLC; 2017.

32. Mark P, Nilsson L. Structure and dynamics of the TIP3P, SPC, and SPC/E water models at 298 K. J Phys Chem A. 2001;105(43):9954–60.

33. D.Quigley MIJP. Constant pressure Langevin dynamics: theory and application. Comput Phys Commun [Internet]. 2005;169(1–3):322–5. Available from: https://www-sciencedirect-com.umiss.idm.oclc.org/science/article/pii/S0010465505001694

34. Jantratid E, Janssen N, Reppas C, Dressman JB. Dissolution media simulating conditions in the proximal human gastrointestinal tract: An update. Pharm Res. 2008;25(7):1663–76.

35. Khan A, Iqbal Z, Shah Y, Ahmad L, Ullah Z. Enhancement of dissolution rate of class II drugs (Hydrochlorothiazide); a comparative study of the two novel approaches; solid dispersion and liqui-solid techniques. Saudi Pharm J. King Saud University; 2015;23(6):650–7.

36. Loftsson T, Hreinsdóttir D, Másson M. Evaluation of cyclodextrin solubilization of drugs. Int J Pharm. 2005;302(1–2):18–28.

37. Ribeiro A, Figueiras A, Santos D, Veiga F. Preparation and Solid-State Characterization of Inclusion Complexes Formed Between Miconazole and Methyl-β-Cyclodextrin. AAPS PharmSciTech. 2008;9(4):1102–9.

38. Sharma A, Jain CP. Carvedilol-β-cyclodextrin Systems Preparation, Characterization and in vitro Evaluation.pdf.

39. Hamed R, Awadallah A, Sunoqrot S, Tarawneh O, Nazzal S, AlBaraghthi T, et al. pH-Dependent Solubility and Dissolution Behavior of Carvedilol—Case Example of a Weakly Basic BCS Class II Drug. AAPS PharmSciTech. 2016;17(2):418–26.

40. Fagerberg JH, Al-Tikriti Y, Ragnarsson G, Bergström CAS. Ethanol effects on apparent solubility of poorly soluble drugs in simulated intestinal fluid. Mol Pharm. 2012;9(7):1942–52.

41. Stappaerts J, Augustijns P. Displacement of itraconazole from cyclodextrin complexes in biorelevant media: In vitro evaluation of supersaturation and precipitation behavior. Int J Pharm. Elsevier B.V.; 2016;511(1):680–7.

42. Stella VJ, Rao VM, Zannou EA, Zia V. Mechanisms of drug release from cyclodextrin complexes. Adv Drug Deliv Rev. 1999. p. 3–16.

43. Determination of stability constants of tauro- and glyco-conjugated bile salts with the negatively charged sulfobutylether-β-cyclodextrin.pdf.

44. Meyerhoffer SM, McGown LB. Critical Micelle Concentration Behavior of Sodium Taurocholate in Water. Langmuir. 1990;6(1):187–91.

45. Thongngam M, McClements DJ. Influence of pH, ionic strength, and temperature on self-association and interactions of sodium dodecyl sulfate in the absence and presence of chitosan. Langmuir. 2005;21(1):79–86.

46. Olesen NE, Westh P, Holm R. Displacement of Drugs From Cyclodextrin Complexes by Bile Salts: A Suggestion of an Intestinal Drug-Solubilizing Capacity From an In Vitro Model. J Pharm Sci. 2016;105(9):2640–7.

47. Uekama K, Hirayama F, Irie T. Cyclodextrin Drug Carrier Systems. Chem Rev. 1998;98(81):2045–2076 ST–Cyclodextrin Drug Carrier Systems.

48. Rao VM, Stella VJ. When can cyclodextrins be considered for solubilization purposes? J Pharm Sci. 2003;92(5):927–32.

49. Loftsson T. Drug permeation through biomembranes: Cyclodextrins and the unstirred water layer. Pharmazie. 2012;67(5):363–70.

50. Zuo Z, Kwon G, Stevenson B, Diakur J, Wiebe LI. Flutamide-hydroxypropy-beta-chiyclodextrin complex: formulation, physical characterization, and absorption studies using the Caco-2 in vitro model. J Pharm Pharm Sci. 2000;3(2):220–7.

51. Olesen NE, Westh P, Holm R. A heuristic model to quantify the impact of excess cyclodextrin on oral drug absorption from aqueous solution. Eur J Pharm Biopharm. Elsevier B.V.; 2016;102:142–51.

52. Wilson CC, Weitschies W, Butler J. Gastrointestinal Transit and Drug Absorption. Oral Drug Absorpt - Predict Assess. 2010;25(February):41–65.

53. Bartle D. Women and men. N Z Health Hospital. 1996;41(5):18-19; discussion 20-21.

54. Camilleri M, Colemont LJ, Phillips SF, Brown ML, Thomforde GM, Chapman N, et al. Human gastric emptying and colonic filling of solids characterized by a new method. Am J Physiol Gastrointest Liver Physiol. 1989;257(2):G284–90.

55. Zhu H, Brinda BJ, Chavin KD, Bernstein HJ, Patrick KS, Markowitz JS, et al. An Assessment of Pharmacokinetics and Antioxidant Activity of Free Silymarin Flavonolignans in Healthy Volunteers : A Dose Escalation Study. 2013;di(September):1679–85.

56. Manuscript A. NIH Public Access. 2009;269(2):352–62.

57. Garcia J, Costa VM, Carvalho A, Baptista P, De PG, Lourdes M De, et al. Amanita phalloides poisoning : Mechanisms of toxicity and treatment. 2015;86:41–55.

58. Christodoulou E, Kechagia I, Tzimas S, Balafas E, Kostomitsopoulos N, Archontaki H, et al. Serum and tissue pharmacokinetics of silibinin after per os and i . v . administration to mice as a HP- ᴺʟ -CD lyophilized product. Int J Pharm [Internet]. Elsevier B.V.; 2015;493(1–2):366–73. Available from: http://dx.doi.org/10.1016/j.ijpharm.2015.07.060

59. Post-white J, Ladas EJ, Kelly KM. Advances in the Use of Milk Thistle (Silybum marianum). 2007;6(2):104–9.

60. Mcdonell E, Green J, Kalisch A. Milk thistle (Silybum marianum) Abstract and key points What is it ? Does it work ? Is it safe ? Evidence tables References Document history Ingredients / Components. 2019;

61. Theodosiou E, Stamatis H, Kolisis F. Bioavailability of silymarin flavonolignans : drug formulations and biotransformation. 2014;1–18.

62. Wen Z, Dumas TE, Schrieber SJ, Hawke RL, Fried MW, Smith PC. Pharmacokinetics and Metabolic Profile of Free , Conjugated , and Total Silymarin Flavonolignans in Human Plasma after Oral Administration of Milk Thistle Extract ABSTRACT : 2008;36(1):65–72.

63. Kumar N, Rai A, Reddy ND, Raj PV, Jain P, Deshpande P, et al. Pharmacological Reports Silymarin liposomes improves oral bioavailability of silybin besides targeting hepatocytes , and immune cells. Pharmacol Reports [Internet]. Institute of Pharmacology, Polish Academy of Sciences; 2014;66(5):788–98. Available from: http://dx.doi.org/10.1016/j.pharep.2014.04.007

64. Siliphos C. A Review of the Bioavailability and Clinical Efficacy of Milk Thistle Phytosome : 2005;10(3).

65. Li X, Yuan Q, Huang Y, Zhou Y, Liu Y. Development of Silymarin Self-Microemulsifying Drug Delivery System with Enhanced Oral Bioavailability. 2010;11(2):672–8.

66. Das G. Preparation and Evaluation of Gastroretentive Floating Tablets of. 2009;57(June):545–9.

67. Journal AI, Ahmad U, Akhtar J, Singh SP, Ahmad J, Siddiqui S. Silymarin nanoemulsion against human hepatocellular carcinoma : development and optimization. Artif Cells, Nanomedicine, Biotechnol [Internet]. Informa UK Limited, trading as Taylor & Francis Group; 2018;0(0):231–41. Available from: https://doi.org/10.1080/21691401.2017.1324465

68. Gaertn L. Silymarin-solid dispersions : Characterization and influence of preparation methods on dissolution. 2010;60:427–43.

69. Kellici TF, Ntountaniotis D, Leonis G, Chatziathanasiadou M, Chatzikonstantinou A V, Becker-baldus J, et al. Investigation of the Interactions of Silibinin with 2 - Hydroxypropyl-β -cyclodextrin through Biophysical Techniques and Computational Methods. 2015;

70. Chemistry P. Cyclodextrins 1. 2008;(1):30–42.

71. Chiang P, Hu Y. Simultaneous Determination of LogD , LogP , and pKa of Drugs by Using a Reverse Phase HPLC Coupled with a 96-Well Plate Auto Injector Simultaneous Determination of LogD , LogP , and pK a of Drugs by Using a Reverse Phase HPLC Coupled with a 96-Well Plate Auto Injector. 2015;(April).

72. Gidwani B, Vyas A. A Comprehensive Review on Cyclodextrin-Based Carriers for Delivery of Chemotherapeutic Cytotoxic Anticancer Drugs. 2015;2015.

73. Calani L, Brighenti F, Bruni R, Rio D Del. Phytomedicine Absorption and metabolism of milk thistle flavanolignans in humans. Eur J Integr Med [Internet]. Elsevier GmbH.; 2012;20(1):40–6. Available from: http://dx.doi.org/10.1016/j.phymed.2012.09.004

74. Hlangothia D, Abdel-rahman F, Nguyen T, Anthony K, Saleh MA. Distribution of Silymarin in the Fruit of Silybum marianum L . Pharmaceutica Analytica Acta. 2016;7(11).

75. Karimi G, Vahabzadeh M, Lari P, Rashedinia M, Moshiri M. " Silymarin ", a Promising Pharmacological Agent for Treatment of Diseases. 2011;14(4):308–17.

76. Mehraban S, Feily A. Journal of Pigmentary Disorders Silymarin in Dermatology : A Brief Review. 2014;1(4):1–3.

77. Khurana M, Paliwal JK, Kamboj VP, Gupta RC. Binding of centchroman with human serum as determined by charcoal adsorption method. 1999;192:109–14.

78. US DHHS, FDA and CVM. Guidance for Industry: Drug Stability Guidelines. US Department of Health and Human Services, Food and Drug Administration. Center for Veterinary Medicine 2008.

79. Li N, Wu X, Jia W, Zhang MC, Tan F, Zhang J. Effect of ionization and vehicle on skin absorption and penetration of azelaic acid. Drug Development and Industrial Pharmacy. 2012;38:985–94.

80. Shinde U, Pokharkar S, Modani S. Design and Evaluation of Microemulsion Gel System of Nadifloxacin. Indian Journal of Pharmaceutical Sciences.2012:237–47.

81. US DHHS, FDA and CDER. Guidance for Industry: Non Sterile Semisolid Dosage Forms. Scale-Up and Postapproval Changes: Chemistry, Manufacturing, and Controls; In Vitro Release Testing and In Vivo Bioequivalence Documentation. US Department of Health and Human Services, Food and Drug Administration. Center for Drug Evaluation and Research 1997.

82. Tadros TF. Emulsion Formation , Stability , and Rheology. Wiley. 2013.

83. Bhide S. Functionality And Role Of Different Fatty Alcohols In Topical O / W Cream Formulation. 2018.

VITA

Vijay Kumar Shankar
PhD Candidate at University of Mississippi
svijaykumarmhadeek@yahoo.com
www.linkedin.com/in/vijay-kumar-shankar-DMPK
Contact no. +1 662-202-8837

Summary

- PhD research focused on evaluating effect of sulfobutyl ether β-cyclodextrins on oral and dermal pharmacokinetics of drugs.
- Expertise in designing *in-vitro* ADME assays, preclinical formulation development and pharmacokinetic studies of new chemical entities (NCE's) to facilitate lead candidate selection and optimization.
- Proficient in bioanalytical method development and validation for quantification of NCE's and generic compounds.

Academic Credentials

PhD in Pharmaceutical sciences GPA 3.80 (scale of 4)	University of Mississippi, Department of Pharmaceutics and Drug delivery, Mississippi, US	**2015 – 2019**
Master of pharmacy (Pharmacology)	Government college of Pharmacy (RGUHS) Bangalore, India	**2009** – **2011**
Bachelor of pharmacy	JSS college of pharmacy (RGUHS) Mysore, India	**2005** – **2008**

Research experience

- **Research assistant** at The University of Mississippi, Mississippi, US. **Since 2015**
  - Development and characterization of Captisol-Enabled™ silymarin topical formulation.
  - Development of UV induced erythema model for screening of novel topical formulations to evaluate its potential in treatment of UV induced erythema and it's UV protective effect.
  - Assay development and validation to evaluate *in-vitro* skin intrinsic clearance of drugs using human skin models.

- Dermatokinetics of silymarin constituents.
-
- Optimization of sulfobutyl-ether-β-cyclodextrin levels in oral formulations to enhance progesterone bioavailability.
- Oral bioavailability enhancement of silymarin using Captisol®
- Exploring effect of cyclodextrin on drug plasma protein binding kinetics.
- LC-MS/MS bioanalytical method development and validation of benzalkonium chloride and its application for dermal toxicity assessment.

➢ **Master of Pharmacy** (Pharmacology) **June 2010** – **May 2011**

- Dissertation topic "Studies on influence of losartan on pharmacodynamics and pharmacokinetics of glibenclamide in rats and rabbits"

Professional experience

➢ **Deputy Head for Analytical Department,** Jubilant Biosys Ltd. India **Oct 2014** – **Jan 2015**

- Led team in setting up of analytical GLP lab facility.
- Bioanalytical and analytical method validation in accordance with OECD test guidelines and the principles of GLP.

➢ **Research Associate** in DMPK at Jubilant Biosys Ltd. India **July 2011** – **Sep 2015**

- Led integrated project team for performing DMPK studies and presented data at cross-functional and client meetings.
- Developed proficiency in designing and executing *in-vitro* ADME assays
  - Microsomal, S9, cytosol and hepatocyte stability
  - CYP 450 inhibition: IC50, K_i and K_{inact} determination
  - CYP phenotyping using recombinant and microsomal enzymes
  - Protein binding assays (EQD)
  - Caco2 and MDR1-MDCK bidirectional permeability assay
- Expertise in rationalized selection of potential molecules for *in-vivo* studies based on ADME data and executed preclinical pharmacokinetics, tissue distribution and mass balance studies.
- Proficient in designing *in-vitro* ADME assays to predict Human drug clearance.
- New assays validated
  - High throughput Dried DMSO solubility assay
  - High throughput method for simultaneous determination of Log P, Log D and pKa
  - Dried Blood Spot analysis
  - Evaluation of P-gp efflux liability *in-vivo*
  - Developed and validated *ex-vivo and in-vivo* studies for decreasing the variability in estimation of biomarkers.

Awards and Recognitions

- Recipient of **Graduate Achievement Award 2019** by the Graduate School, The University of Mississippi.
- Recipient of **Dissertation Fellowship Award** for Spring 2019 semester by the Graduate School, The University of Mississippi.
- Recipient of **Publons Peer Review Awards 2018** for placing in the **top 1% of reviewers in Pharmacology and Toxicology** on Publons' global reviewer database, determined by the number of peer review reports performed during the 2017-2018 Award year.
- Published research article "Water Activity and its Significance in Topical Dosage Forms" was selected as featured article by Journal of Pharmaceutical Sciences as it contains **"Most Original and Most Significant Findings"**
- Recipient of Graduate Student Council Research Grant for 2017 funded by the **Graduate Student Council of The University of Mississippi** for project entitled "*In-vitro Skin Metabolic Stability and Keratin Binding of Silymarin*"
- Initiated as an active member of Chi chapter at University of Mississippi in 2017 for "**Rho Chi Honor Society**" with outstanding academic excellence.
- Received student travel award for attending the NISBRE meeting (Washington, DC) funded by an **IDeA from the NIGMS of the NIH, USA** for presenting iposter "*Metabolic Stability of ∆9-Tetrahydrocannabinol in Human Skin Model*"
- Awarded Best oral presentation by **67th Indian Pharmaceutical Congress 2015, India** for presentation on "*In-vitro Metabolism of Tetrahydrocannabinol in Human Epidermal Keratinocytes*"
- Recipient of 2014-2015 Center of Research Excellence in Natural Products Neuroscience (CORE-NPN) Assistantship Award funded by the **National Institutes of Health** for project entitled "*In-vitro Metabolism of Tetrahydrocannabinol and Cannabidiol in Human Skin Model*"
- Recognized and awarded as "**Best Team Player-2012**" by Jubilant Biosys, In appreciation for commitment to delivery as a member of the DMPK department.
- Recognized and awarded as "**Best Team Player-2012**" by Jubilant Biosys, In appreciation for commitment for DMPK deliverables as an ABB001 project team member.
- Recognized and awarded as "**Best Team Player-2011**" by Jubilant Biosys for contribution as a member of the EN3356-Team for the year 2011 and for displaying commendable team spirit and camaraderie towards accomplishment of the objectives.
- Recognized and awarded as "**Best Trainee Research Associate-2011**" by Jubilant Biosys for the significant contribution and execution of *in-vitro* ADME assays.

Technical Skills

- Proficient in operating and troubleshooting of instruments
  - LC-MS/MS (Waters Xevo TQD, API-4000, API-5500, Q-Trap and Thermo)
  - HPLC (Shimadzu), Waters alliance 2996 and Waters Acuity UPLC
- *In-vitro* passive and active (iontophoresis) skin permeation test using horizontal, vertical and flow through Franz diffusion cells.
- Expertise in handling hepatocytes, Caco2, MDR1-MDCK, human epidermal keratinocytes, dermal fibroblasts and HACAT cell lines.
- Expertise in executing *in-vitro* drug transporter studies in different cell lines.
- Development of chemical induced peripheral neuropathic pain model.
- Oral, intravenous, intraperitoneal and subcutaneous dosing in rodents and non-rodent models.
- Intranasal, sublingual and rectal dosing in rats.
- Serial sampling of CSF in rats from cisterna magna.
- Acquainted with handling of Dissolution apparatus, Differential scanning calorimeter and FTIR instruments.

Software Proficiency

Microsoft Office Word, Excel, Power Point, GraphPad Prism, Analyst, Empower, Lab solutions, TSQ, Masslynx, WinNonlin and Phoenix software.

Publications

- Rahul Lalge, Priyanka Thipsay, **Vijay kumar Shankar**, Abhijeet Maurya, Manjeet Pimparade, Suresh Bandari, Feng Zhang, S. Narasimha Murthy, Michael A. Repka. Preparation and evaluation of cefuroxime axetil gastro-retentive floating drug delivery system for improved delivery via hot melt extrusion technology. International Journal of Pharmaceutics 2019; 566: 520-531.
- Haley McFall, Sandeep Sarabu, **Vijay kumar Shankar**, Suresh Bandari, S. Narasimha Murthy, Karl Kolter, Nigel Langley, Dong Wuk Kim, Michael A. Repka. Formulation of aripiprazole-loaded pH-modulated solid dispersions via hot-melt extrusion technology: In vitro and In vivo studies. International Journal of Pharmaceutics 2019; 554: 302-11.
- Muralikrishnan Angamuthu, **Vijay kumar Shankar**, S. Narasimha Murthy. Water activity and its significance in Topical dosage forms. Journal of Pharmaceutical Sciences 2018; 107(6): 1656-66.
- Anitha Police, **Vijay Kumar Shankar**, S. Narasimha Murthy. RP-HPLC Method for Simultaneous Estimation of Vigabatrin, Gamma-Aminobutyric Acid and Taurine in Biological Samples. Journal of Chromatography B 2018; 1076: 44-53.

- Patil Akash, Bhide Supriya, Bookwala Mustafa, Soneta Bhavik, **Shankar Vijay**, Almotairy Ahmed, Almutairi Mashan, Narasimha Murthy S. Stability of Organoleptic Agents in Pharmaceuticals and Cosmetics. AAPS PharmSciTech 2018; 19(1): 36-47.
- **Vijay Kumar S**, Vinay Dhiman, Kalpesh Kumar Giri, Kuldeep Sharma, Mohd Zainuddin, Ramesh Mullangi. Development and validation of a RP-HPLC method for the quantitation of tofacitinib in rat plasma and its application to a pharmacokinetic study. Biomedical chromatography 2015; 29(9):1325-9.
- Suresh P. S, **S.Vijay Kumar**, Avinash Kumar, Ramesh Mullangi. Development of an LC-MS/MS method for determination of bicalutamide on dried blood spots: application to pharmacokinetic study in mice. Biomedical chromatography 2015; 29(2):254-60.
- Kumar A, **Vijay Kumar S**, Gurav S, Zainuddin M, Dewang P, Kethiri RR, Rajagopal S, Mullangi R. Development and validation of an RP-HPLC method for the quantitation of Orteronel (TAK-700), a CYP17A1 enzyme inhibitor, in rat plasma and its application to a pharmacokinetic study. Biomedical chromatography 2013; 27(12):1590-4.
- **Kumar SV**, Rudresha G, Gurav S, Zainuddin M, Dewang P, Kethiri RR, Rajagopal S, Mullangi R. Validated RP-HPLC/UV method for the quantitation of abiraterone in rat plasma and its application to a pharmacokinetic study in rats. Biomedical chromatography 2013; 27(2):203-7.
- C.M.Sultanpur, **S.V.Kumar**, K.Deepa. Vaccines for hypertension disorder: Beneficial or detrimental. Singapore journal of scientific research 2011; 1(1):13-22.
- Chandrashekhar M Sultanpur, S. Satyanarayana, **S.Vijay Kumar**. Drug to drug interaction between gliclazide and gemfibrozil in animal model. African journal of pharmaceutical sciences and pharmacy 2011; 2(1):58-74.
- Chandrashekar M Sultanpur, Deepa K, **S.Vijay Kumar**. Comprehensive review on HbA1c in diagnosis of diabetes mellitus. International Journal of Pharmaceutical Sciences Review and Research 2010; 3(2):119-122.

Publication under Communication

- **Vijay Kumar Shankar**, Anitha Police, Pankaj Pandey, Zachary Cuny, Robert J. Doerksen, S. Narasimha Murthy. Optimization of Sulfobutyl-Eher- β-Cyclodextrins Levels in Oral Formulation to Enhance Progesterone Bioavailability.
- **Vijay Kumar Shankar**, Anitha Police, Pankaj Pandey, Zachary Cuny, Robert J. Doerksen, S. Narasimha Murthy. Oral bioavailability enhancement of silymarin constituents using SBE-β-CD.
- Anitha Police, **Vijay Kumar Shankar,** S. Narasimha Murthy. Role of Taurine Transporter in Retinal Uptake of Vigabatrin.
- Anitha Police, **Vijay Kumar Shankar,** S. Narasimha Murthy. Cellular Mechanism of Vigabatrin induced Retinal Neuronal and Epithelial Toxicity.

Poster Presentations at Scientific Conferences

- PharmSci 360 Annual meeting 2018, Washington, DC.
  - *In-vitro* Dermatokinetic of Silymarin in Human Skin Models.
  - Influence of Sulfobutylether-β-Cyclodextrin on Intravenous Pharmacokinetics of Silymarin.
  - Optimization of Sulfobutyl-Ether- β-Cyclodextrin Levels in Oral Formulation to Increase Bioavailability of Progesterone.
- AAPS Annual Convention and Meeting 2017, San Deigo, CA.
  - Development of Captisol-Enabled™ Silymarin Topical Formulation.
  - Effect of Cyclodextrin on Drug Plasma Protein Binding Kinetics.
  - Method Development and Validation of Benzalkonium Chloride using LC-MS/MS.
  - Tissue Distribution of Silymarin Constituents and their Metabolites in Rats on Oral Administration of Silymarin Formulations.
- AAPS Annual Convention and Meeting 2016, Denver, CO.
  - *In-vitro* Intestinal Permeability and Pharmacokinetic Studies of Captisol® Enabled Silymarin Constituents.
- Metabolic Stability of Δ9-Tetrahydrocannabinol in Human Skin Model (iposter). NISBRE meeting (Washington, DC) 2016 funded by an IDeA from the NIGMS of the NIH, USA.
- Progesterone (BCS Class II Model Drug) Solubility Enhancement by Modified β-Cyclodextrins complexation. AAPS Annual Convention and Meeting 2015, Orlando, FL.
- Influence of Gemfibrozil on the Pharmacokinetics and Pharmacodynamics of Gliclazide in Rats and Rabbits. 61st Indian Pharmaceutical Congress 2009, India.

Volunteer Experience

- Reviewer for Drug Development and Industrial Pharmacy Journal **Sep 2017** – **present**
- Reviewer for AAPS PharmSciTech Journal **Sep 2018** – **present**
- Abstract screener for American Association of Pharmaceutical Scientists (AAPS) **June 2017 – present.**
- **Graduate Teaching Assistant** for Basic pharmaceutics at The University of Mississippi, Department of Pharmaceutics and Drug delivery **Jan** – **May 2017**